2014-02-28

Characterization of the Visceral Endoderm Components in Early Post-Implantation Mouse Embryo Development: A Dissertation

Tingting Huang
University of Massachusetts Medical School Worcester

CHARACTERIZATION OF THE VISCERAL ENDODERM COMPONENTS IN EARLY POST-IMPLANTATION MOUSE EMBRYO DEVELOPMENT

A Dissertation Presented

By

Tingting Huang

Submitted to the Faculty of the

University of Massachusetts Graduate School of Biomedical Sciences, Worcester

in partial fulfillment of the requirements for the degree of

DOCTOR OF PHILOSOPHY

February 28th, 2014

Department of Cell and Developmental Biology

CHARACTERIZATION OF THE VISCERAL ENDODERM COMPONENTS IN EARLY POST-IMPLANTATION MOUSE EMBRYO DEVELOPMENT

A Dissertation Presented
By
Tingting Huang

The signatures of the Dissertation Defense Committee signify completion and approval as to style and content of the Dissertation

Jaime Rivera Perez, Thesis Advisor

Lewis Brian, Member of Committee

Hong Zhang, Member of Committee

James Li, Member of Committee

M. Isabel Dominguez, Member of Committee

The signature of the Chair of the Committee signifies that the written dissertation meets the requirements of the Dissertation Committee

Gregory Pazour, Chair of Committee

The signature of the Dean of the Graduate School of Biomedical Sciences signifies that the student has met all graduation requirements of the school.

Anthony Carruthers, Ph.D.,
Dean of the Graduate School of Biomedical Sciences
Department of Cell and Developmental Biology

February 28th, 2014

DEDICATION

This dissertation is dedicated to my mom and my husband, who have always been supporting me. It is also dedicated to my father (*in memorian*), who always loved me.

ACKNOLEDGEMENTS

First and foremost I like to express my sincere gratitude to Dr. Jaime Rivera for training me as professionals and always being very supportive.

Special thanks go to Yeonsoo Yoon and Giovane Tortelote for being very good friends and that we had gone through our graduate school life together.

I also want to thank the true friends I made here, who became my family abroad (Zhiqing (Julie) Zhu, Xiaochu Chen, Yuanfei Wu, Yuqing Hou, Yahui Kong) and my old friends who always manifested themselves with the words of support.

I would like to thank my lab current and previous labmates Matthew Curran, Joy Riley, Kristina Gonzalez and Sakthi Balaji for their friendship.

I would like to show my gratitude to the members of my TRAC, Greg Pazour, Brian Lewis, Hong Zhang and James Li for their guidance and valuable suggestions over the years and also to Isabel Dominguez for contributing her time and share her knowledge with me.

I wish to thank Yahui Kong and Hang Cui for their help with the immunostaining experiments. I also wish to thank Jeffery Nickerson and Jean Underwood for teaching me how to use the confocal microscope. I also want to thank Alexandre Quaresma for always being nice and kind as a friend to talk. Special thanks go to CDB lunch group (Paul Odgren, Deborah Cochran, Hanna Witwicka, Karen Imbalzano and etc.) for making my study life much more fun. I

would also show my sincere gratitude to Dr. Anthony Imbalzano and Dr. Mary Ellen Lane for being very supportive whenever I needed. Special thanks go to all the staff in GSBS and ISO office for all these years' warm-hearted assistance.

At last but mostly important, I would like to thank all my family and my relatives for their unconditional support and love, especially my parents who sacrificed themselves to provide me with good education and also my husband for always being very supportive and for sharing his life with me.

ABSTRACT

Early post-implantation vertebrate embryos are shaped by complex cellular and molecular mechanisms. In mice, the visceral endoderm, an extra-embryonic cell lineage that appears before gastrulation, provides several important functions such as nutrition and mechanical protection. My thesis research focused on the role of the visceral endoderm in embryo patterning, a newly discovered function for this tissue. My results showed that an interplay between two subpopulations of visceral endoderm the anterior and posterior visceral endoderm, located on the opposite sides of the developing conceptus, are critical for the establishment of the anteroposterior body axis of the embryo. I also found that senescence-associated β-galactosidase activity delineates the visceral endoderm marking apical vacuole, a lysosomal-like organelle. This however indicates the nutritional function of visceral endoderm cells rather than a senescent population. My studies highlight the fundamental role of extra-embryonic tissues in patterning mammalian embryos as opposed to housekeeping roles. They also reveal important difference when conducting studies at the organismal level rather than in cells in culture.

TABLE OF CONTENTS

LIST OF FIGURES

CHAPTER I

CHAPTER II

Figure A2.2. Whole mount *in situ* hybridization analysis of the expression of *Tbx4* and *Tbx20*

LIST OF THIRD PARTY COPYRIGHTED MATERIAL

Parts of this dissertation have appeared in the following publications:

Huang T, Rivera-Perez JA. Senescence-associated β-galactosidase activity marks the visceral endoderm of mouse embryos but is not indicative of senescence. *Genesis.* (In Press)

CHAPTER I:

GENERAL INTRODUCTION

The understanding of early embryonic development remains a source of fascination for scientists and lay people alike, presumably stemming from the human desire to know one's own origins. Within mammals, the mouse is the best model for understanding human development due to the following reasons: reproductive capacity, close taxonomic distance to man, relatively easy manipulation and ethical considerations compared to other mammalian models (Slack, 1991).

One fundamental question of mammalian development is how a zygote becomes a unique animal with diverse appearance and complex internal organ organization. The answer to this question lies at the early stages of development when crucial developmental decisions take place. The mouse gestation period is about 3 weeks long, however, not many people appreciate that the fundamental body plan of the embryo becomes evident within one week after fertilization (Beddington and Robertson, 1999) and soon after, a miniature individual, consisting of a central nervous system, notochord, somites, pharyngeal arches, and other tissues develops from a homogeneous group of cells, the inner cell mass of the blastocyst (Slack, 1991; Wolpert, 2002). All of these compartments, which contain specific cell types, must lie in the proper position relative to each other, which is determined by the anterior-posterior (AP), dorsal-verntral (DV) and left-right (LR) embryonic axes.

In later development, there is a fast increase in embryo size and

differentiation of specific organs (Slack, 1991; Wolpert, 2002). All this develops on the framework of the basic body plans that is laid down during gastrulation, a period of embryonic development in which the cells undergo complex morphological movements to generate the three primary germ layers (ectoderm, mesoderm and endoderm), from which the whole fetus develops later. (Snow and Bennett, 1978; Skreb et al., 1991; Tam et al., 2006; Tam and Loebel, 2007; Solnica-Krezel and Sepich, 2012)

The term gastrulation is derived from the Greek word “gaster” meaning belly or stomach, first coined by the German embryologist Ernst Haeckel in his 1872 work “The biology of calcareous sponges” (Stern, 2004). The process of gastrulation is widely studied in a variety of animal models, and it is basic for our understanding of birth defects, such as spinal bifida and LR asymmetry abnormalities (*situs inversus*, right and left Isomerism). The study of gastrulation also provides an excellent model to understand the molecular mechanisms that regulate tumor growth and metastasis, especially cell differentiation, cell migration and epithelial to mesenchymal transition (EMT). In addition, the study of gastrulation also benefits the regenerative medicine field with parallels between the mechanisms of regeneration and those that govern gastrulation (Solnica-Krezel and Sepich, 2012).

Unlike other vertebrates such as frogs and fish, the mouse embryo contains elaborate extra-embryonic tissues (Beddington and Robertson, 1999; Solnica-Krezel and Sepich, 2012). One of these extra-embryonic cell lineages,

the visceral endoderm, the subject of this work, performs critical functions to regulate gastrulation in the mammalian embryo development.

Early mouse development

The course of normal mouse development up to the implantation stage is shown in Figure. 1.1 (Hogan, 1994; Tam and Behringer, 1997; Beddington and Robertson, 1999). The first few cleavage stages after fertilization are very slow, taking approximately 48 hours to reach the 8-cell stage. Soon after, the whole embryo acquires a nearly spherical shape in a process called compaction. The compacted morula then begins the process of cavitation that results in the generation of the blastocoele. Around three days after fertilization, the embryo moves from the oviduct to the uterus. The blastocoele cavity enlarges and transforms the morula into a blastocyst, which is composed of two distinct tissues: an outer cell layer called the trophectoderm (TE) and a clump of cells attached to the interior, the inner cell mass (ICM) (Johnson and Ziomek, 1981; Slack, 1991).

The course of mouse development up to early post implantation stage is shown in Figure.1.2 (Hogan, 1994; Tam and Behringer, 1997; Beddington and Robertson, 1999). At around embryonic day 4.5 (E4.5), the ICM generates a layer named primitive endoderm (PE) on the blastocoelic surface. The PE will generate the extra-embryonic parietal and visceral endoderm (Gardner, 1983). The rest of the ICM, now called epiblast, will give rise to the fetus, including the

Figure 1.1

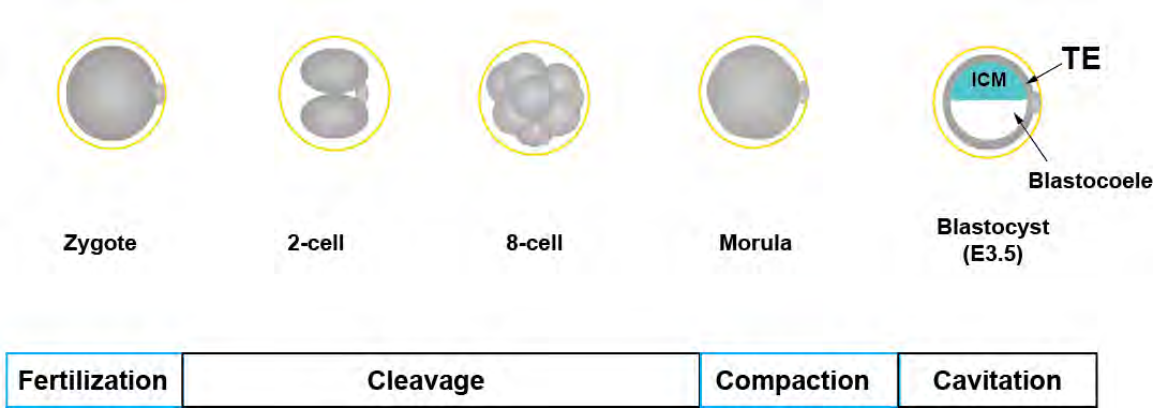
TE
ICM
Blastocoele
Zygote
2-cell
8-cell
Morula
Blastocyst
(E3.5)
Fertilization
Cleavage
Compaction
Cavitation

Figure 1.1. Schematic representation of early mouse embryogenesis up to implantation stage. Cartoon depicts E0 to E 3.5 embryo development. The fertilized egg undergoes several cell divisions to form a compacted morula. Fluid fills blastoceole and two different cell lineages begins to form - trophectoderm and inner cell mass. ICM: inner cell mass; TE, trophectoderm. This figure is adapted from the Figure. I in the paper (Rivera-Perez, 2007).

Figure 1.2

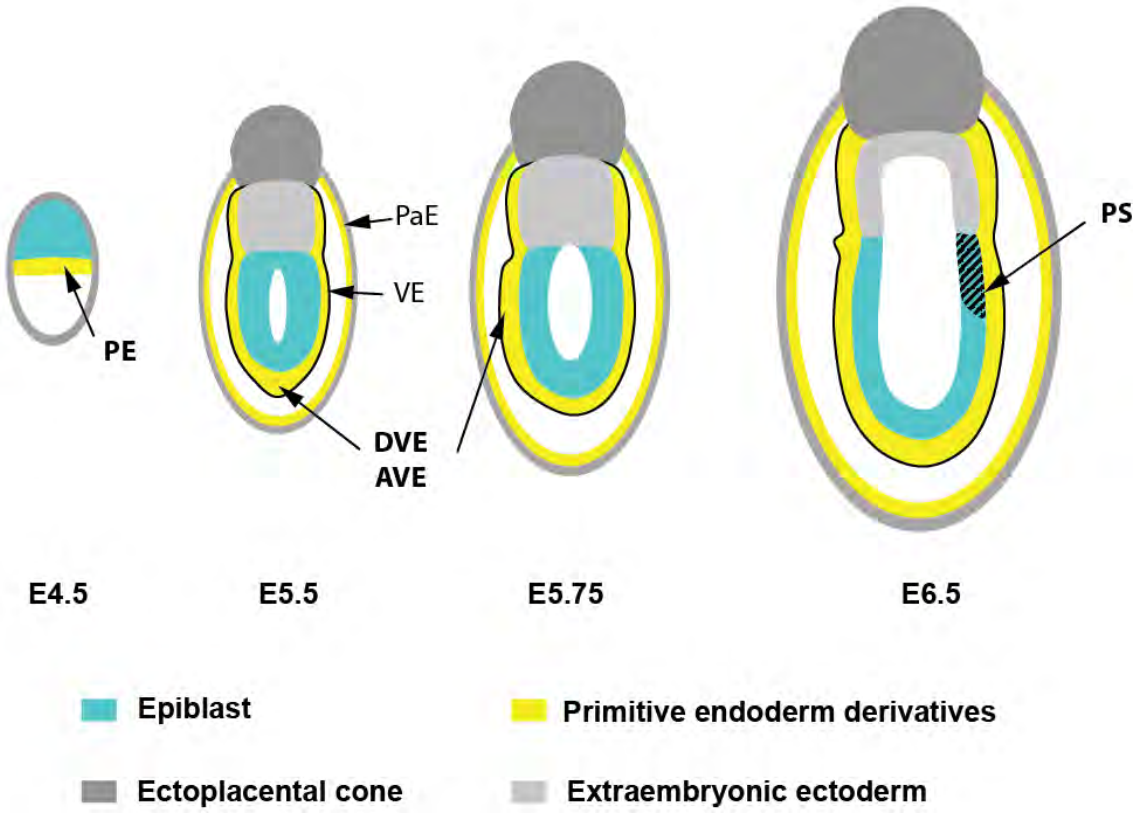
PE
PaE
VE
DVE
AVE
PS
E4.5
E5.5
E5.75
E6.5
Epiblast
Primitive endoderm derivatives
Ectoplacental cone
Extraembryonic ectoderm

Figure 1.2. Schematic representation of early post-implantation stages at peri-gastrulation stages. Cartoon illustrates two days of early post-implantation development of mouse embryogenesis (E4.5 – E6.5). The inner cell mass cells sits on top of blastoceole differentiate into primitive endoderm, and continues to form visceral endoderm, surrounding both ectoderm and epiblast at around E5. At E5.5, the visceral endoderm cells locating in the distal tip of the egg cylinder become specified and shift to the future anterior side around E5.75. Around E6.5, the primitive streak develops on the posterior side. The emergence of primitive streak is the first morphological landmark of gastrulation. The different colors (red, yellow, light grey and dark grey) represent different cell types with specific fate commitments.Primitive endoderm PE: primitive endoderm; PS, primitive streak; DVE, distal visceral endoderm; AVE anterior visceral endoderm. This figure is adapted from the Figure. I. in the paper (Rivera-Perez, 2007).

three germ layers and the extra-embryonic mesoderm (Beddington and Robertson, 1999; Stern, 2004).

The TE cells overlying the ICM, continue to divide, generating extra-embryonic ectoderm (ExE), which pushes the epiblast and surrounding visceral endoderm distally towards the blastocoele (Beddington and Robertson, 1999). The embryo thus acquires the shape of a cup made up of two cell layers, the inner epiblast and the outer visceral endoderm (VE). Recent studies suggest that the visceral endoderm overlaying the epiblast also contributes to the embryo (Kwon et al., 2008).

At around E5.5, a cavity is formed in the center of the epiblast. This proamniotic cavity is generated by a mixture of apoptotic and survival signals emanating from the visceral endoderm (Coucouvanis and Martin, 1995). During the immediate post-implantation period (E5.0 to E6.5), the mouse embryo changes dramatically in size due to the rapid proliferation of epiblast and extra-embryonic ectoderm (Tam and Behringer, 1997). Around 6.5 days after fertilization, morphological signs of embryonic anterior posterior pattern become evident with the formation of the primitive streak at one edge of the embryonic ectoderm (Slack, 1991; Beddington and Robertson, 1999). At this time, the epiblast cells, adjacent to the posterior visceral endoderm, first a homogeneous epithelium, undergo an epithelial to mesenchymal transformation and form the primitive streak. The primitive streak marks the posterior end of the future embryonic axis, which will extend across the ectoderm from the rim of the cup

(proximal) to its distal tip during the next 12–24 hr (Figure.1.3). The primitive streak is also a conduit for the generation of mesoderm and endoderm, also known as mesoendoderm. At E6.5, the posterior amniotic fold, an outgrowth of the ectoderm and extra-embryonic mesoderm, forms at the junction of the primitive streak and extra-embryonic ectoderm (Pereira et al., 2011). The posterior amniotic fold cavitates and enlarges, pushing the extra-embryonic ectoderm proximally and eventually fusing with the opposite side to the embryo. The side of the fold closer to the epiblast becomes the amnion, the innermost extraemrbyonic membrane that surrounds the fetus and thus provides protection for the embryo (Schmidt, 1992). The side nearer the ectoplacental cone becomes the chorion, a layer that surrounds the embryo and other membranes, and allows transfer of nutrients from maternal blood to fetal blood (Pereira et al., 2011).

At the anterior end of the streak, a specialized structure forms, known as the node (Figure.1.3). Axial mesendoderm derived from the node, comprises that mesoderm which will populate the midline of the embryo (prechordal plate and notochord) and the gut endoderm. The posterior end of the streak gives rise to extra-embryonic mesoderm, while lateral plate mesoderm and paraxial mesoderm emerge from the middle levels of the streak.

The appearance of the primitive streak heralds the process of gastrulation, a series cell movements and rearrangements that transform a bilayered embryo into one containing the three germ layers; ectoderm, mesoderm and endoderm. The purpose of gastrulation is to generate a body plan that serves as a blueprint

Figure 1.3

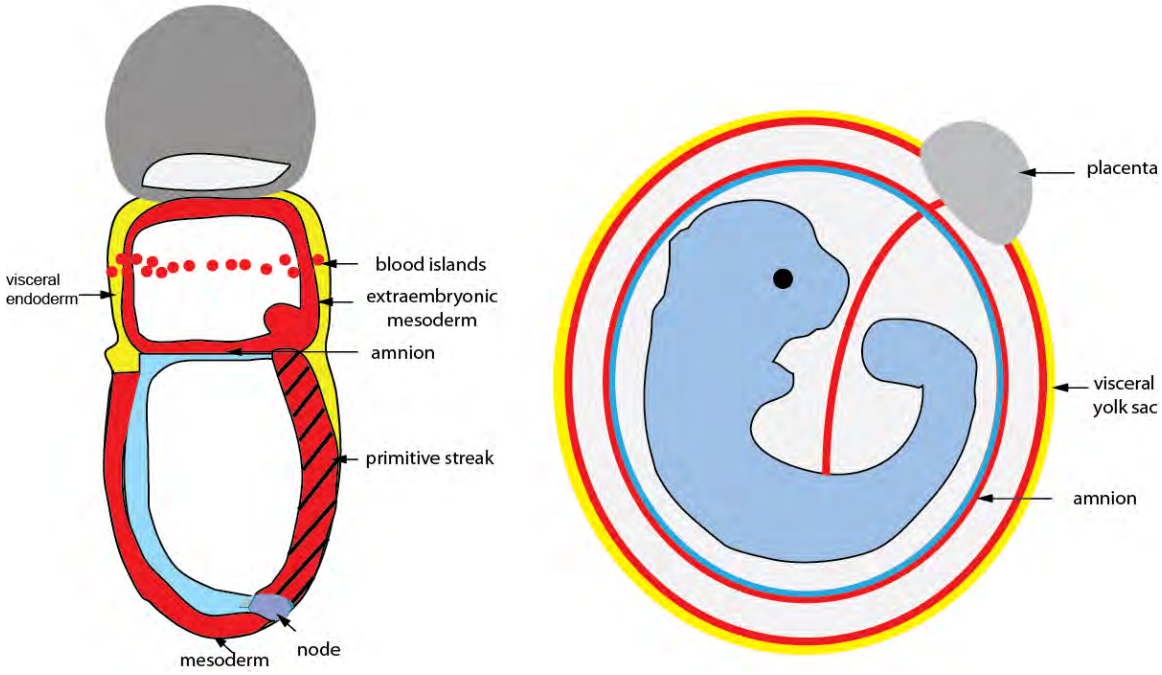
visceral
endoderm
blood islands
extraembryonic
mesoderm
amnion
primitive streak
mesoderm
node
placenta
visceral
yolk sac
amnion

Figure 1.3. Schematic representation of an E7.5 and E9.5 stage embryo. At E7.5 embryo, the amniotic folds develop at the junction of primitive streak and extraembryonic ectoderm and continues to grow to attach to the chorion; The blood islands, appear as a circle under the proximal yolk sac near the ectoplacental cone; The node is formed at the most anterior of the primitive streak and axial mesoderm come firstly out of the it. At E9.5 emrbyos, after turning, the embryo is well wraped under aminion and visceral yolk sac, and connected through the ambilicol cord to placental. eem, extraembryonic ectoderm; ps, primitive streak; mes, mesoderm; bl, blood islands; pl, placenta; vys, visceral yolk sac; am, amnion.

for the subsequent morphogenesis of the embryo (Tam and Behringer, 1997). Because of its outsized role in gastrulation, the origin of the primitive streak is critical because it defines the anteroposterior axis of the embryo.

The dorsoventral axis is determined by how the embryo is implanted in the uterus at the blastocyst stage and the orientation of the LR axis is dependent on the orientation of the DV and AP axes. Thus, the LR pattern also ultimately relies on where the streak forms. Not surprisingly, this morphological sequence of events suggests that pattern formation in the mammalian embryo could be explained once the cues for positioning the primitive streak are understood.

The visceral endoderm

The visceral endoderm, a cell layer that appears before gastrulation, is derived from the primitive endoderm, a transient cell layer that appears on the blastocoelic surface of the blastocyst between days 4 and 5 of development (Gardner, 1983; Rossant, 1986; Hogan, 1994) (Figure.1.2). The primitive endoderm generates two extra-embryonic cell types, the parietal endoderm and the visceral endoderm (Gardner, 1983). The parietal endoderm is formed when primitive endoderm cells migrate over the surface of the trophectoderm that surrounds the blastocoelic cavity. The parietal endoderm synthesizes type IV collagen and laminins and together with trophectoderm, produces the parietal yolk sac, also known as Reichert's membrane. The parietal yolk sac surrounds the embryo and filters nutrients (Gardner, 1983; Freeman, 1990; Bielinska et al.,

1999).

The visceral endoderm is derived from primitive endoderm cells that remain in contact with ICM cells. Visceral endoderm cells have microvilli on the apical surface and contain numerous endocytotic vesicles, which actively internalize various molecules, including transferrin, immunoglobulins (Ig), lipoproteins and albumins (Huxham and Beck, 1985; Ichimura et al., 1994; Assemat et al., 2005). All these features ensure that maternal nutrients are efficiently absorbed, digested and transferred to the adjacent epiblast and extra-embryonic ectoderm (Morrisey et al., 1998; Barbacci et al., 1999; Bielinska et al., 1999).

At the egg cylinder stages of development, a layer of visceral endoderm cells covers the epiblast and extra-embryonic ectoderm (Figure.1.2), however, cells in this endoderm layer are not uniform in morphology or molecular characteristics (Bielinska et al., 1999). Visceral endoderm cells overlying the epiblast, also known as embryonic visceral endoderm, are a group of monolayer cells with columnar morphology, while those covering the extra-embryonic ectocerm, known as extra-embryonic visceral endoderm, are cuboidal (Gardner, 1983; Rivera-Perez et al., 2003). These morphological features are accompanied by regional differences in gene expression, as illustrated by the marker α-fetoprotein (*Afp*) and the thyroid hormone transport protein Transthyretin (*Ttr*). Before gastrulation, *Afp* and *Ttr* are expressed only in the visceral endoderm covering the epiblast. At E 7.5, *Afp* and *Ttr* expression are relocated to visceral

endoderm covering the extra-embryonic ectoderm and proximal epiblast (Dziadek, 1978; Dziadek and Adamson, 1978; Dziadek and Andrews, 1983; Kwon and Hadjantonakis, 2009). Therefore, regional differences in gene expression may reflect different interactions between visceral endoderm and underlying ectoderm (Bielinska et al., 1999).

At around the time of gastrulation, visceral endoderm cells overlying the epiblast are gradually displaced by definitive endoderm cells derived from the epiblast. Transplantation and dye injection experiments indicate that visceral endoderm cells located anterior to the primitive streak are displaced anteriorly and laterally (Lawson and Pedersen, 1987). The displaced visceral endoderm cells, form a crescent that overlays the anterior half of the epiblast and eventually are destined to the visceral yolk sac (Figure.1.3 & Figure.1.4).

The consensus among mammalian developmental biologists was that definitive endoderm eventually extrudes the vast majority of embryonic visceral endoderm cells from the invaginating foregut endoderm and the remainder of the embryo (Tam and Behringer, 1997; Thomas et al., 1998). However, a recent analysis of the fate of the visceral endoderm using fluorescent reporters has shown that visceral endoderm cells overlying the epiblast get incorporated into the definitive endoderm layer of the embryo (Kwon et al., 2008). This study suggests the visceral endoderm, derived from an extraembryonic cell lineage may contribute to the embryonic fetus, which contradicts with the prevailing view that only three germ layers give rise to the whole embryo proper.

Figure 1.4

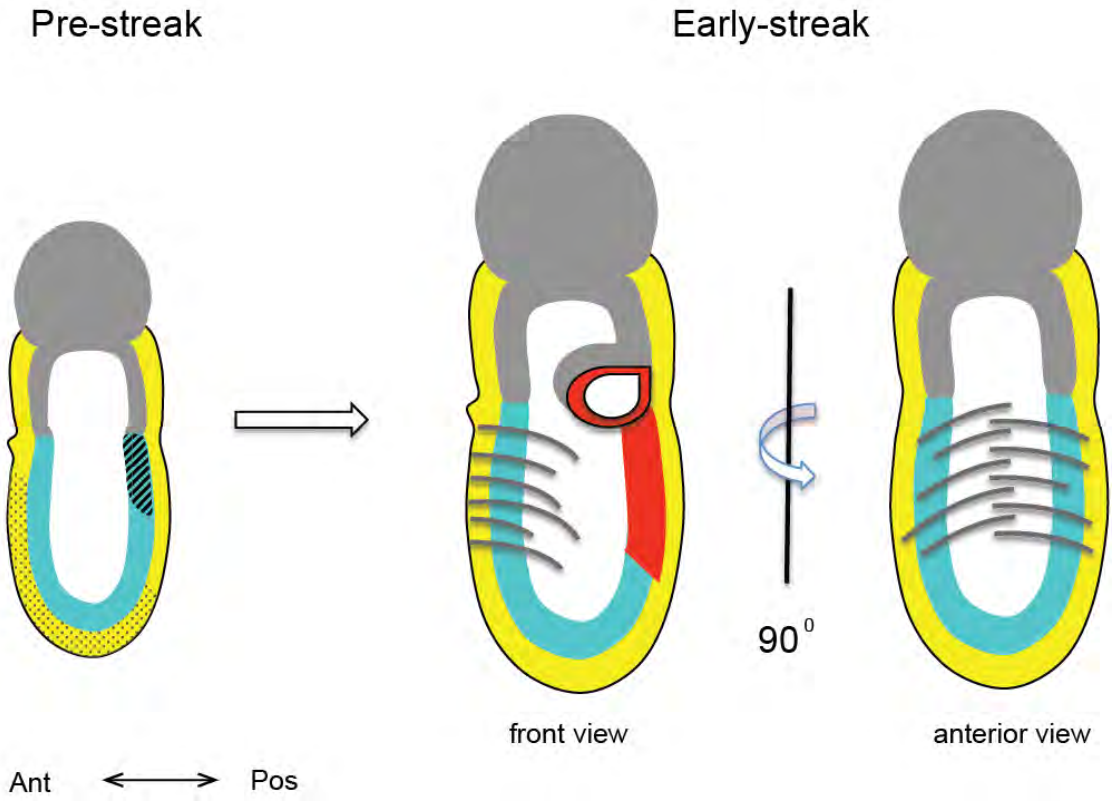
Pre-streak
Early-streak
90 0
front view
anterior view
Ant
Pos

Figure 1.4. Schematic drawing of visceral endoderm cells movements during gastrulation. The anterior and distal visceral endoderm cells (dotted) at pre-streak embryos are displaced to form a crescent that overlays the anterior half of the epiblast at early-streak embryos (strips). Ant, anterior; Pos, posterior. The different colors represent different cell types with specific fate commitments.

Besides the traditional role in gas exchange and nutrient uptake, the visceral endoderm also performs critical functions during gastrulation and provides cues for later hematopoiesis and organogenesis. Explant experiments have shown that the visceral endoderm is required for the generation of cardiomyocytes (Arai et al., 1997). In chick and in *Xenopus* experiments, *Dkk1* and *Cerberus,* which have a restricted expression pattern in visceral endoderm during early development, are known to induce cardiogenesis in a non-cell autonomous manner (Marvin et al., 2001; Schneider and Mercola, 2001; Foley et al., 2007). In addition, chimeric analysis for the homeobox gene *Otx2* showed that the visceral endoderm also plays an important role in induction of the forebrain and midbrain (Rhinn et al., 1998).

The importance of the VE in peri-impantation nutrition is evidenced by Neural tube defects (NTDs), which arise from failure to close the neural tube completely during development, an event that occurs before establishment of the placenta, representing some of the most common congenital malformations in humans (Zohn and Sarkar, 2010).

The distal and anterior visceral endoderm

One day before the emergence of the primitive streak, a group of morphological and molecularly distinct visceral endoderm cells form at the distal tip of the epiblast (Figure.1.2 & Figure.1.5). These distal visceral endoderm (DVE) cells shift in a polarized manner to the region overlying the future anterior aspect

Figure 1.5

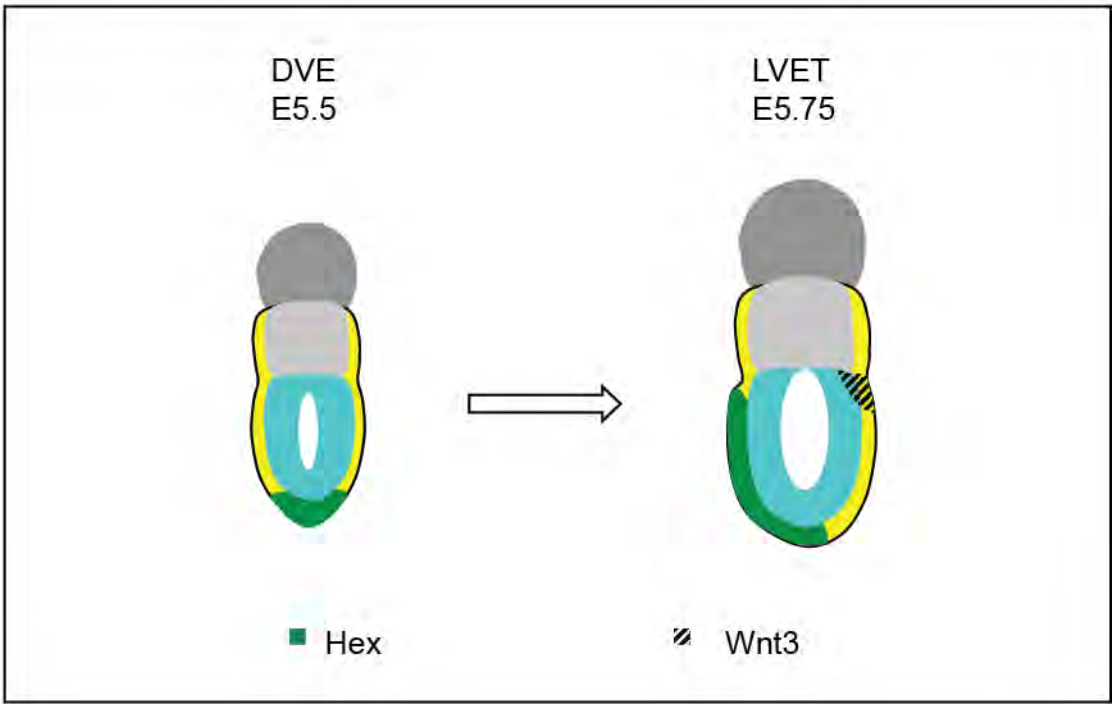

Figure 1.5. Schematic drawing of anterior visceral endoderm movements. At E5.5, distal visceral endoderm cells (green) located at distal tip of the egg cylinder shift to the future anterior side that overlays the anterior epiblast in 7 hours. Starting from E 5.5, *Wnt3* is emanating from posterior visceral endoderm (shown in strip).

of the embryo to become anterior visceral endoderm (AVE) (Thomas et al., 1998; Rivera-Perez et al., 2003; Srinivas et al., 2004). The unidirectional change in the location of distal visceral endoderm cells, has been well documented in lineage experiments using DiI (Thomas et al., 1998), iontophoresis (Rivera-Perez et al., 2003) and time-lapse imaging (Srinivas et al., 2004). However, the mechanisms behind this movement remain unknown. Differential growth rates have been proposed as a possible explanation (Thomas et al., 1998; Yamamoto et al., 2004), however, evidence is accumulating that suggest that active cell migration drives the conversion of DVE into AVE (Rivera-Perez and Hadjantonakis, 2013). There is also evidence that the canonical Wnt signaling pathway and its antagonists might also provide a mechanism in guiding the movement of DVE cells (Kimura-Yoshida et al., 2005).

The DVE/AVE is characterized by the expression of multiple genes that include *Hex* and several repressors of Nodal and Wnt signaling such as *Cer1*, *Lefty1*, *Dkk1*, *Sfrp5* and *Sfrp1* (Beddington and Robertson, 1998; Biben et al., 1998; Oulad-Abdelghani et al., 1998; Mukhopadhyay et al., 2001; Perea-Gomez et al., 2001; Pfister et al., 2007). Emerging evidence suggests that these events provide important developmental cues for anterior and posterior axial patterning (Thomas and Beddington, 1996; Bally-Cuif and Boncinelli, 1997; Tam and Behringer, 1997; Beddington and Robertson, 1998).

The posterior visceral endoderm

The posterior visceral endoderm (PVE) is a recently identified region of embryonic visceral endoderm located opposite to the AVE (Rivera-Perez et al., 2003) (Figure.1.2). . This region of visceral endoderm is characterized by the expression of *Wnt3* (Liu et al., 1999; Rivera-Perez and Magnuson, 2005) and *Mixl1* (Pearce and Evans, 1999; Robb et al., 2000). The PVE, as defined by the expression of *Wnt3*, is first discernible at around E5.5 as a small area of visceral endoderm overlying the posterior epiblast at the junction between the epiblast and extra-embryonic ectoderm. As development proceeds this area expands distally and circumferentially such that by E6.5 it spans half the length of the epiblast and tapers around the circumference of the egg cylinder (Rivera-Perez and Magnuson, 2005).

Unlike the AVE, the PVE cells do not change position and appear to have minimal mixing (Kwon et al., 2008). These cells remain in place through the process of gastrulation and get incorporated into the embryo (Kwon et al., 2008). Recent studies showed the posterior visceral endoderm plays an important role in the establishment of anteriorposterior axis (Tortelote et al., 2013). More detailed infomation regarding on posterior visceral endoderm signaling center will be shown in the following chapters.

The extra-embryonic visceral endoderm

Visceral endoderm cells overlying the extra-embryonic ectoderm become the outer layer of the visceral yolk sac (Figure.1.3). The inner lining of the

visceral yolk sac is covered by extra-embryonic mesodermal cells derived from the primitive streak. The extra-embryonic visceral endoderm lines the outside of visceral yolk sac and coordinates blood cell differentiation and vessel formation in the adjoining extra-embryonic mesoderm (Boucher and Pedersen, 1996; Belaoussoff et al., 1998; Bielinska et al., 1999). Blood islands (Figure.1.3), consisting of hematopoietic progenitors surrounded by endothelial cells, appear as a complete band in the proximal yolk sac, near the site of maternal attachment and away from the distally located embryo (Dzierzak and Medvinsky, 1995; Zon, 1995; Ferkowicz and Yoder, 2005).

Chick explant experiments also suggest that the removal of the endoderm layer disrupts erythropoiesis and blood island formation (Bielinska et al., 1999). The visceral yolk sac continues to expand in the next few days of development and after embryo turning it forms a sac that surrounds the embryo (Bielinska et al., 1999).

Vertebrate gastrulation

All vertebrates develop based on a very similar body plan (Figure 1.6). Along the anterior-posterior (A-P) axis they form head, trunk, and tail, and in the dorsal-ventral (D-V) axis they form backbone and gut. During development, the ectoderm gives rise to the central nervous system (CNS), epidermis and its derivatives. The mesoderm differentiates into prechordal plate and notochord, somites (muscle, bone), kidney, etc. The endoderm develops into the

gastrointestinal and respiratory tracts, pancreas, liver, thymus, thyroid, etc. The molecular mechanisms that govern these cell fate decisions and tissue differentiation in the embryo between different species also show striking similarities.

Amphibians

A considerable amount of work has been contributed to early embryo patterning from studying the early development of the frog *Xenopus laevis*. There are mainly two reasons for this: frog embryos are externaly fertilized and relatively big (1-2mm in diameter), so they are easily visualized, manipulated and cultured. *Xenopus* embryos also undergo very rapid cell cycles during early development – 90 minutes for the first cell cycle and 20 – 30 minutes with no gap in the next consecutive eleven cell cycles. The zygotic genome transcription commences at the end of the twelfth cell cycle and the dorsal lip of the blastopore (Speman-Mangold Organizer) forms at the fifteenth cycle, which is followed by the gastrulation movements to form all the three layers and eastablish the DV and AP axes (Gilbert, 2000; Wolpert, 2002).

Xenopus embryo patterning is lay down at the time when the sperm enters the animal hemisphere (Wolpert, 2002). The sperm entry starts cytoskeleton rearrangements and later a phenomenon known as cortical rotation, in which the egg cortex rotates 30° counterclockwise relative to the interior components of the egg and leads to the prospective dorsal side opposite to the sperm entry site

(Slack, 2013). In Xenopus embryos, an organizer, called Speman-Mangold organizer (SMO), forms in an equatorial sector at the early gastrula stage and establishes the initial patterning of the embryo (Harland and Gerhart, 1997; De Robertis et al., 2000). Experiments in which the vegetal side of the zygote was irradiated with UV light showed that the embryo did not develop dorsal tissues, leaving only a ventralized (belly) piece, suggesting the existence of dorsal determinants in the vegetal side in oocytes. This phenotype could be rescued by injection of β-catenin mRNAs (De Robertis et al., 2000). Maternal β-catenin mRNAs are enriched in the nuclei of dorsal cells during cleavages and blastula stages (De Robertis et al., 2000), suggesting the initiation of canonical Wnt signaling (Heasman, 2006). When a “morpholino” oligo complementary to Frizzled-7 Wnt receptor mRNA is injected into oocytes, it abolishes the Frizzled-7 receptor in early gastrula and leads to a ventralized phebotype (Sumanas et al., 2000). The origin of the SMO can be traced back to the Nieuwkoop center, which is an area of the dorsal-vegetal region of dorsal endoderm of the blastula, inducing the organizer in a non-cell autonomous manner (Harland and Gerhart, 1997). In explants experiments done first by Pieter Nieuwkoop, the dorsal-vegetal cells from mid-blastula embryos, were recombined with animal cap cells. The cells from the animal cap are destined to a neurectoderm fate during normal development, however, after recombination, they became mesendoderm cells. Therefore, the dorsal-vegetal cells of mid-blastula embryos have the capacity to induce the SMO. This group of cells is now known as the Nieuwkoop center

(Harland and Gerhart, 1997; Gerhart, 1999)

In experiments conducted by Pieter Nieuwkoop, the Nieuwkoop center was shown to secrete a dorsalizing signal that induces the formation of the SMO. Later it was shown that this process requires maternal Wnt activity (Vonica and Gumbiner, 2007). Recently it was proposed that maternal Wnt11 is the initial signal required for establishing axis formation in *Xenopus* embryos, acting through the Canonical Wnt Signaling Pathway (Tao et al., 2005).

Birds

The chick is one of the favorite model organism animals by embryologists because the chick embryos can be cultured ouside the egg and convenient for surgical manipulation. Also most of the organs are formed in chick in an similar way to the mammals (Wolpert, 2002; Stern, 2004).

The fertilized egg undergoes a few cleavages in the chick's oviduct to form a disc of cells, named blastoderm, lying on a huge amount of yolk. It takes the fertilized egg 20 hour to pass through the oviduct and get laid. At that time, the egg has a basic structure, which is composed of the blastoderm (60,000 cells), the egg white, shell membrane and the shell (Wolpert, 2002). After that, the cleavages go deeper and thus completely separate the cells to form cleavage furrow. The periphery cells in blastdoderm get thicker while the cells in the central region become a thin layer, which surround a cavity (the epiblast lies on the top, while the hypoblast lies on the bottom). Chick gastrulation starts with the emergence of primitive streak, visible as a dense strip which develops from the

posterior marginal zone, located at the junction between the area opaca and area pellucida at the posterior of the embryo (Wolpert, 2002).

The specification of the primary axes in chick embryos occurs during the cleavage stage. The chick embryo always develops perpendicularly to the long axis of the egg (Wolpert, 2002).The anterior-posterior axis is already established at the time when the hen lays the egg. Moreover, this axial polarity cannot be changed after that, which suggest the basic body plan is determined when the egg is in the hen intra-uterus course (Kochav and Eyal-Giladi, 1971). Gravity is considered the driving force that determines the anterior-posteior axis. As the egg passes through the uterine tract, the egg rotates around its long axis in the uterus (10-15 revolutions per hour) and this rotation separates components inside the embryo (the yolk moves under the blastoderm); one end of the blastoderm is raised up and becomes the future posterior end, where the primitive streak appears (Gilbert, 2000; Stern, 2004)

Transplant experiments show that the posterior marginal zone (PMZ) of the chick embryo can induce a complete primitive streak without contributing to the induced streak (Skromne and Stern, 2001). Among all the Wnts, only Wnt8C is expressed in the marginal zone, in a gradient decreasing from posterior to anterior. This indicates a fundamental role of Wnt signaling in inducing the chick anterior-posterior axis. Wnt activity seems to require cVg1 in chick embryos. Misexpression of Wnt1 in the area pellucida enables this region to form a primitive streak in response to cVg1. The Wnt antagonists Crescent and Dkk-1

block the primitive streak-inducing ability of cVg1 in the marginal zone. These findings suggest that Wnt activity defines the marginal zone and allows cVg1 to induce an axis.

Mouse

Unlike frog and chick embryos, the mouse embryo takes a relatively long time to reach gastrulation stages (about one third of the total gestation time). This is most likely due to viviparity (Beddington and Robertson, 1999). Before acquiring a definitive body plan, the murine embryo consumes lots of time and energy to generate complicated extraembryonic tissues. This is likely due to throphic reasons.

The Nieuwkoop center in amphibians is defined as an area of the dorsal–vegetal region of the blastula that can induce an organizer without contributing cells to the induced axial structures (Harland and Gerhart, 1997). In the mouse, the Wnt signaling pathway emanating from the posterior visceral endoderm has been proposed to be equivalent to the Nieuwkoop center for the following reasons: *Wnt3* has the right temporal and spatial expression profile (Rivera-Perez and Magnuson, 2005). In early post-implantation embryos, *Wnt3* expression is first observed in the posterior visceral endoderm of embryos dissected at E 5.5. This is likely the first symmetry breaking event, even earlier than AVE movement (Rivera-Perez and Magnuson, 2005). Belaoussoff and co-workers showed using tissue recombination experiments that a diffusible signal

from the posterior visceral endoderm has the capacity to respecify anterior ectoderm into a posterior mesodermal fate (Belaoussoff et al., 1998). In addition, visceral endoderm is traditionally thought not to contribute to the embryo (Bielinska et al., 1999). Morever, the activate form of β-catenin, an indication of canonical Wnt pathway, is present in the posterior epiblast and overlying posterior visceral endoderm (Mohamed et al., 2004). Interestingly, chicken *Wnt8c*, can induce an ectopic primitive streak in mice (Popperl et al., 1997). These data suggest that Wnt3 is the key player in the posterior visceral endoderm – Nieuwkoop center analogue- in the anterior-posterior axis establishing process.

Figure 1.6

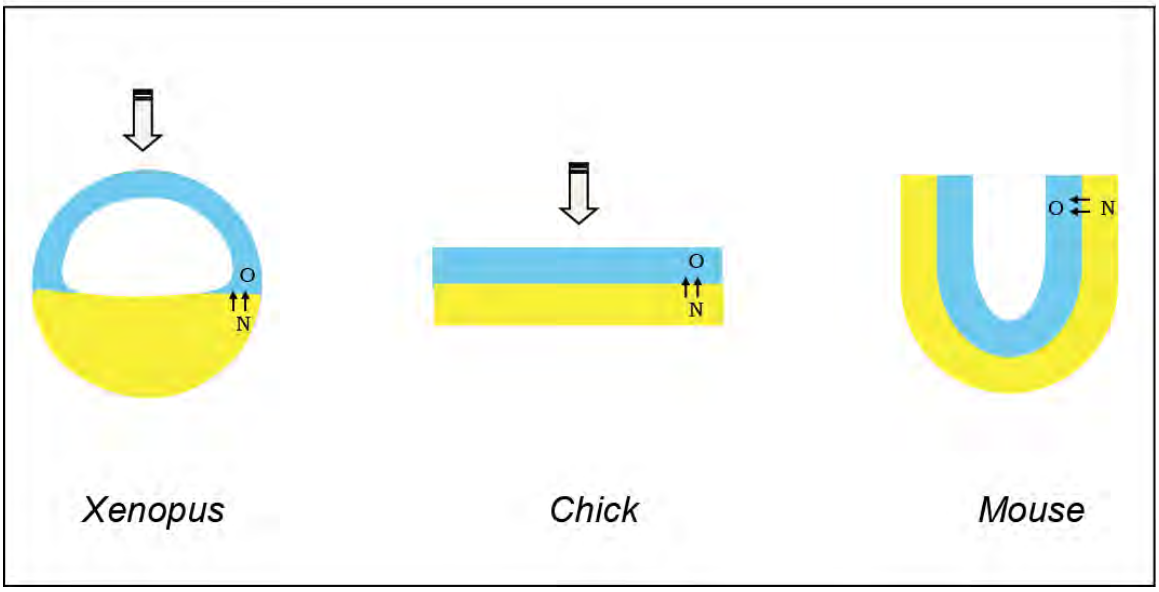

Figure 1.6. The predicted location of Nieuwkcoop center and organizer in vertebrates before gastrulation. In a *Xenopus* blastula, the blastoderm is on the outside, sitting on top of a large amount of yolk with blastocoel in between. Pushing down to flatten the frog blastoderm and also decrease the amount of hypoblast produce the equivalent of chick blastoderm. Continuing to push down to bend the chick blastoderm creates the equivalent of mouse egg cylinder. The predicted nieuwkcoop center and organizer location are as marked in different vertebrate embryos.

Signaling networks in axial specification

In mice, the induction of the primitive streak is the initial step of mesoendoderm induction. In amphibians, the induction of the spemann organizer, which releases a cocktail of factors to form the three germ layers is conducted by the Niewukoop Center (Harland and Gerhart, 1997). Maternal Wnt11 has been shown to be the initial signal to activate the canonical Wnt signaling pathway required for axis formation (Tao et al., 2005). In Chick, the equivalent to the Nieuwkoop center is considered to be the posterior marginal zone (PMZ), where *Wnt8c* is expressed in a gradient high in posterior, low in anterior parts of the blastodisc (Skromne and Stern, 2001). Therefore, the "Nieuwkoop center" in mouse should have the following features if evolutionarily conserved with other vertebrates: The mouse "Nieuwkoop center" should stay in close proximity with the primitive streak. It should stem from an extraembryonic cell lineage. The mouse "Nieuwkoop center" should be able to induce the primitive streak without contributing to it. The initial signal inside the "Nieuwkoop" center develops earlier than the formation of organizer (the primitive streak). The canonical Wnt signaling pathway should be present both in the primitive streak and the mouse "Nieuwkoop" center.

Four main types of signaling pathways are implicated in the formation of meso-endoderm and anterior-posterior patterning in mice, including signaling by bone morphogenetic proteins (BMPs), fibroblast growth factor (FGF), the transforming growth factor-beta (TGF-β) superfamily and the Wnt molecules.

Wnt Signaling

The first Wnt gene, mouse *Wnt-1*/*Int-1*, was discovered as an oncogene caused by a retroviral integration of mouse mammary tumor virus (MMTV) in mammary tumors (Nusse and Varmus, 1982). It was later recognized that *Drosophila wingless* (*Wg*) is the ortholog of the vertebrate *int-1/Wnt-1* gene (Rijsewijk et al., 1987). It is now known that Wnts are conserved in the animal kingdom, from hydra to human. Nineteen Wnt family glycoproteins have been indentified in human and mouse (Kemp, 2007).

The Wnt signal can be transduced between cells in canonical (β-catenin dependent) or noncanonical (β-catenin independent) pathways. A simple outline of canonical Wnt signaling transduction is presented in Figure.1.7. (Harland and Gerhart, 1997; Wodarz and Nusse, 1998). In the absence of Wnt ligands, the cytoplasm β - catenin is sequestered by the β-catenin degradation complex, GSK-3β/Axin/APC (glycogen synthase kinase-3/Axin/Adenomatous Polyposis Coli). In the presence of Wnt signals, the signals are transduced into the nucleus through a series of events. First, Wnts are secreted after post-translational modification, and binding to the Frizzled (Fz)/low density lipoprotein (LDL) receptor-related protein (LRP) complex on the targeted cell surface. The Wnt signal is transduced to the intracellular protein Dishevelled (Dsh), which further recruits Axin to destroy the β-catenin degradation complex. Once the degradation pathway for β-catenin is inhibited, β-catenin accumulates in the cytoplasm and

Figure 1.7

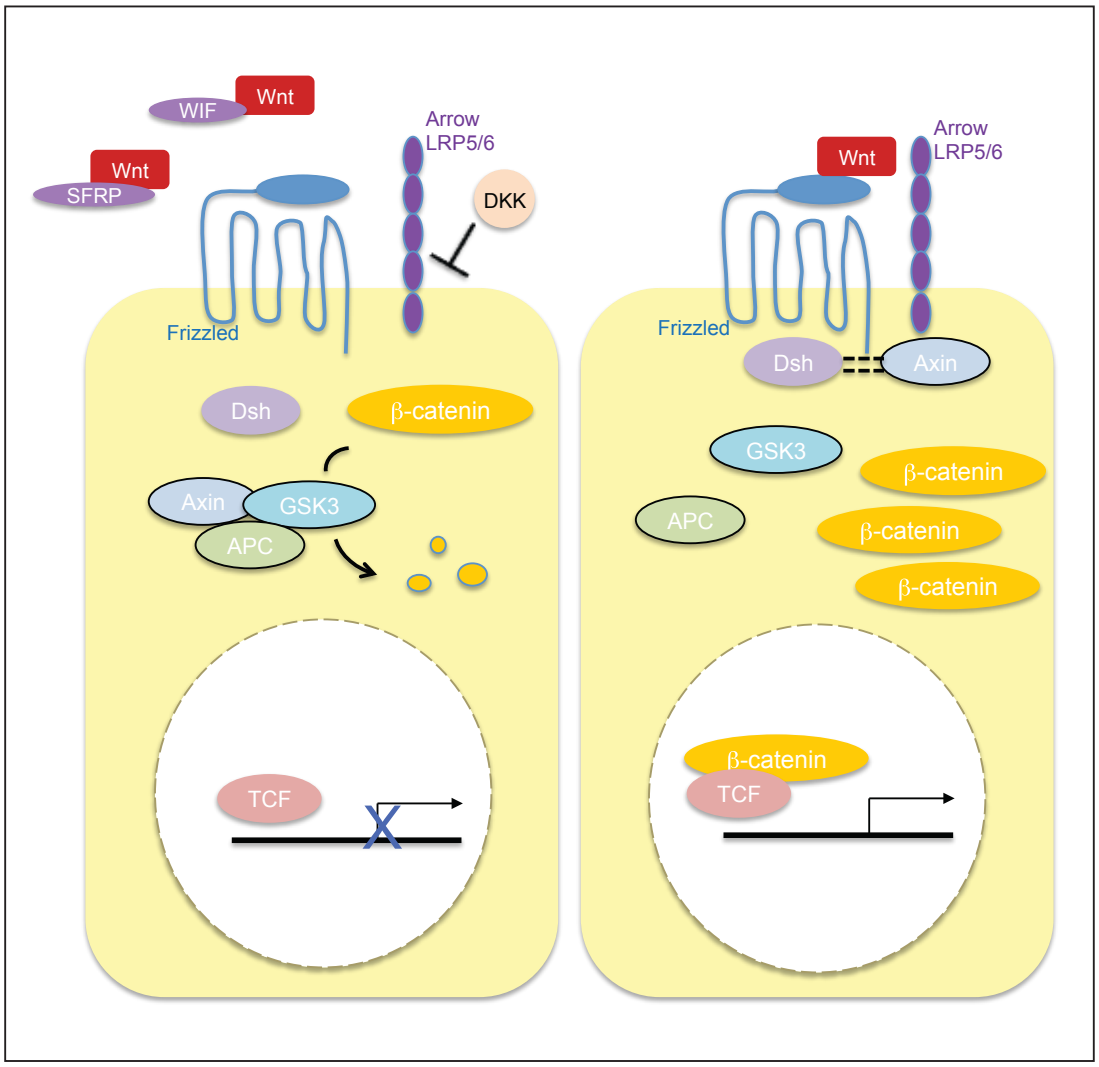
WIF
Wnt
Wnt
SFRP
Arrow
LRP5/6
DKK
Frizzled
Dsh
β-catenin
Axin
GSK3
APC
TCF
Wnt
Arrow
LRP5/6
Frizzled
Dsh
Axin
GSK3
β-catenin
APC
β-catenin
β-catenin
β-catenin
TCF

Figure 1.7. Schematic representation of canonical Wnt signaling and anatagonists. In cells (*left panel)*, in which the presence of Wnt anantagonists (SFRPs and WIFs) inhibits the binding of Wnts to Frizzled receptors, the concentration of cytoplasmal β-catenin is low since it is degraded by the Axin/GSK3/APC complex. When Wnt proteins (*right panel)* present on the cell surface by interacting with Frizzled/LRP receptor complex, this leads to the recruiments of Dishevelled (*Dsh),* which may further interacts with Axin, causing the degradation of Axin/GSK3/APC complex. This facilitate the β-catenin is accumulated in the nucleus, and interacts with TCF to regulate transcription. This figure is adapted from the Figure. 1. In the paper (Logan and Nusse, 2004).

nucleus. Finally, the enriched nuclear β-catenin interacts with transcription activators LEF/TCF (lymophoid enhancer-binding factor 1 / T cell-specific transcription factor) to control target transcription. When the Wnts are not present on the target cell surface, β-catenin is degraded by the GSK-3β/Axin/APC complex in the cytoplasm, and consequently cannot enter the nucleus to activate target gene transcription (Wodarz and Nusse, 1998; Logan and Nusse, 2004). The developmental role of Wnts in mice, has been mainly obtained through knockout studies (van Amerongen and Berns, 2006). The Wnt proteins play central roles in controlling many aspects of embryonic development (Chien et al., 2009).

Non-canonical Wnt signaling converges on two main pathways: the Wnt/Ca^{2+} and Wnt/planar cell polarity (PCP) pathways. The Wnt/Ca^{2+} pathway has been shown to regulate *Xenopus* gastrulation and the PCP pathway has been shown (Kuhl, 2002) to regulate the convergent extension movements during gastrualtion (Barrow, 2006).

Wnt signaling regulates many aspects in early mammalian development. Many Wnts, are present as early as blastocyst stage, however, no evidence shows the activation of Wnt signaling (Kemp et al., 2005). At E5.5, active β-catenin is present in the extra-embryonic visceral endoderm and posterior visceral enododerm, and then appears in the primitive streak (Mohamed et al., 2004). The embryos lacking β-catenin do not develop a distal visceral endoderm

(DVE) suggesting that β-catenin plays a role in specification of DVE (Huelsken et al., 2000). The mesoderm also fails to develop in β-catenin -/- embryos (Huelsken et al., 2000), indicating the formation of mesoderm is also dependent on β-catenin signaling. In the mouse, *Dkk1* has been shown to play a role in regulating Wnt canonical signaling in the AVE migration process (Kimura-Yoshida et al., 2005). Besides *mDkk1, Sfrp1, Sfrp5, Fzd5* and *Fzd8* are also expressed in the DVE, suggesting tight control of Wnt signaling through multiple redundancy of Wnt antagonists (Kemp, 2007).

As mentioned above, Wnt signaling plays a cetral role in mouse anterior-posterior axis formation and mesoderm induction. As the DVE moves to the anterior side, Wnt3, is first expressed in the posterior visceral endoderm and then expands to the posterior epiblast (Rivera-Perez and Magnuson, 2005). Coincident with the formation of the primitive streak, other Wnt family members, *Wnt2b, Wnt5a, Wnt8a, Wnt3a, Wnt11* and *Fzd10,* are expressed in the primitive streak, promoting the correct anterior-posterior patterning (Kemp et al., 2005). In embryos lacking *Wnt3*, the primitive streak is lost while the AVE is intact and moves to the anterior side (Liu et al., 1999). This suggests a direct role of Wnt3 in regulating the formation of primitive streak but not in the movement of the AVE.

A transgenic reporter mouse line (BAT-gal), in which the *lacZ* gene is under the control of TCF binding elements, demonstrated the activation of canonical Wnt signaling in the primitive streak (Maretto et al., 2003). *LRP5; LRP6* double knockout embryos lack a primitive streak resembling embryos lacking

Wnt3 (Kelly et al., 2004). Embryos lacking *Axin*, a negative regulator of canonical wnt signaling, develop duplicated axial structures (Zeng et al., 1997). Together, these data firmly place the canonical Wnt signaling at the center of the complex signaling networks during mouse gastrulation.

Nodal signaling

Nodal, a member of transforming growth factor β (TGFβ) super family of signaling molecules was identified as a mutation that affected gastrulation in a genetic screen of retrovirus mutated transgenic mouse strains (Conlon et al., 1991). In frogs, the TGFβ signals, such as activin and its relative Vg1, serves as mesoderm inducers *in vivo* (Schier and Shen, 2000).

Nodal ligands activate TGFβ signaling pathways through serine/threonine kinase receptors to regulate downstream target gene expression (Schier, 2003). A simple outline of the canonical Nodal signaling transduction pathway is presented in Figure.1.8. When Nodal is present on the cell surface, the signal is transduced by type I and II Activin receptors and EGF-CFC co-receptors, resulting in phosphorylation of Smad2, which forms a complex with Smad4. This complex then enters the nucleus to associate with members of the FAST family of transcription factors to regulate the expression of downstream target genes.

During early mouse development, Nodal has been suggested to play central roles in four main aspects: axis formation, mesoderm formation, neural patterning and left-right asymmetry patterning (Schier, 2003). Nodal is present in

Figure 1.8

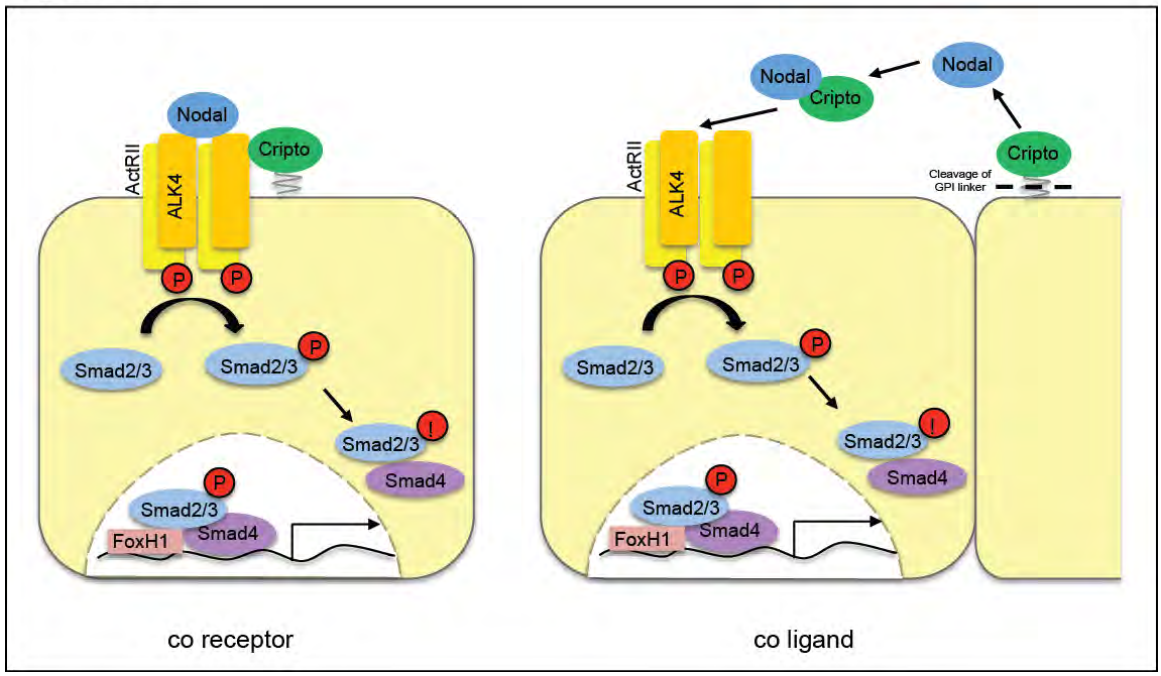
Nodal
Cripto
ActRII
ALK4
P
Smad2/3
Smad4
FoxH1
Cleavage of GPI linker
co receptor
co ligand

Figure 1.8. Schematic representation for the dual roles of Cripto in Nodal signaling pathway. Cripto acts as a coreceptor for Nodal (left panel). In addition Cripto can act together with Nodal as a paracrine signal following by the cleavage of the GPI linkage (right panel). The binding of Nodal, Cripto and ActRIIA/ActRIIB receptors leads to the activation of Smad2. The phosphorylated Smad2 and Smad 4 form a complex to enter into nucleus, further interact with the transcriptional factor FAST1 to control downstream target gene expression. This figure is adapated from the figure in the webpage (http://cisreg.cmmt.ubc.ca/cgi-bin/tfe/articles.pl?tfid=171) .

the inner cell mass of the blastcyst (Tam and Loebel, 2007). At egg cylinder stages, the Nodal mRNA is present in the whole epiblast and overlaying visceral endoderm (Varlet et al., 1997). As development advances, the expression of Nodal forms a proximal-distal gradient. Coincident with the emergence of the primitive streak, the expression of nodal is present in the nascent primitive streak (Brennan et al., 2001). In *Nodal* mutant embryos, the distal visceral endoderm also fails to develop and move to the anterior side of the embryo, indicating nodal plays a role in DVE specification and migration. In addition, the embryos deficient for *Nodal* show the loss of the primitive streak and mesoderm, lacking posterior gene expression,such as *Wnt3, Brachyury* and *Cripto* (Zhou et al., 1993). The embryos lacking *Smad2,* the downstream effector of Nodal signaling, also show early patterning defects, causing ectopic expression of *Wnt3*, *Cripto* and *Eomes* all over the epiblast at a high levels, indicating that Nodal signaling plays a role in maintaining posterior pattern features in early development (Brennan et al., 2001). Nodal signaling is also required for left-right patterning and asymmetric organogenesis in later development (Schier, 2009).

Fgf signaling

The first fibroblast growth factor (FGF) ligands, FGF1 and FGF2, were purified from human and murine fibroblasts as mitogenic factors (Gospodarowicz and Moran, 1975). Twenty-two FGF family members have been indentified and four FGFR (FGF receptor) genes, which generate various FGF receptors

isoforms through alternative splice (Dorey and Amaya, 2010).

The FGF ligands binds to FGF receptors and lead to dimerization of the receptors, which in turn result in phosphorylation of the intracellular tyrosine residues (Dorey and Amaya, 2010). This transduces the signal to downstream cytoplasmic signaling pathways, such as Ras/ERK and the Akt or PKC pathways in, which further activate the downstream genes to affect cell proliferation, differentiation, survival and migration (Dorey and Amaya, 2010).

In early vertebrate embryos, FGF signaling plays roles in many aspects, such as cell fate decision, axes patterning and morphological movements. In *Xenopus* and *Zebrafish*, FGF signaling is required for axial mesoderm and paraxial mesoderm formation. In mice, Fgf8 and Fgf4 are coexpressed in the primitive streak of the gastrulating mouse embryo.

Fgf8 mutant mice initiate gastrulation but show failure of mesendoderm migration which results in accumulation of cells in the primitive streak and subsequent lethality (Sun et al., 1999).

In embryos lacking of both FGF8 and FGF4, no embryonic mesoderm- or endoderm-derived tissues develop due to the defects in coordinated epiblast cell movements, which suggest Fgf signaling is required for early gastrulation and cell migration in the primitive streak (Sun et al., 1999).

Bmp signaling

Bone morphogenetic proteins (BMPs) constitute a subgroup of the transforming growth factor β superfamily (Dutko and Mullins, 2011). Although initially discovered as osteogenic fators in demineralized bone, BMPs are also implicated in many aspects during early embryonic development, such as patterning embryonic axial structure, nerual crest cell differentiation and limb bud patterning (Bandyopadhyay et al., 2013)

The BMP signaling pathway shares some similarities with other TGF-β signaling pathway components. First, BMP ligand dimers bind type I and type II serine-threonine kinase receptors, resulting in phosphorylation of the Smad intracellular effector proteins (Smads1/5/8). These activated Smads then recruit Smad4 to enter into nucleus and regulate downstream gene expression (Dutko and Mullins, 2011).

In the mouse and chick embryo, bone morphogenetic protein 4 (Bmp4) is required in extra-embryonic ectoderm for normal formation of node and primitive streak (Fujiwara et al., 2002). In mouse embryos, there is no evidence that Bmp signaling is activated at the pre-implantation stage embryo. The expression of Bmp4 mRNA is present in the extraembryonic ectoderm adjacent to the epiblast around E6.0 (Winnier et al., 1995). Coincident with the emergence of the primitive streak, the expression of Bmp4 is present in the forming primitive streak (Winnier et al., 1995). In Bmp4 null embryos, the phenotype varies. Some fail to develop a primitive streak, while some form a primitve streak, indicating Bmp4 plays a role in gastrulation (Winnier et al., 1995). However, whether Bmp4 plays

a role in initiating the gastrulation or maintaining the gastrulation process remains unknown. Another BMP ligand, BMP2 expressed in anterior visceral endoderm (AVE) signals to epiblast derivatives to initiate ventral folding morphogenesis during gastrulation and initial stages of morphogenesis (Pfister et al., 2007). All these indicate Bmp signaling plays important roles during early development.

In mice, complex molecular crosstalks between extraembryonic and embryonic tissues are involved at the stage when the mouse embryo is establishing its axial polarity. Evolutionarily canonical Wnt signaling is present in posterior visceral endoderm and also the top candidate to induce the formation of primitive streak. In addition, Bmp signaling from extra-embryonic ectoderm could be the potential regulator to activate Wnt signaling. TGF-β/Nodal signaling plays a role in regulating DVE specification and Cripto-dependent Nodal signaling functions importantly in driving the AVE movements.

CHAPTER II:

THE AVE BLOCKS *WNT3* EXPRESSION IN THE ANTERIOR EGG CYLINDER TO POSITION THE PRIMITIVE STREAK

Preface

The work shown in this chapter is part of the manuscript “Extra-embryonic *Wnt3.*is essential for mouse gastrulation currently under review in *Developmental Biology*”. The *Wnt3*^{lacZ} knock-in mice were generated by Dr. Maki Wakamiya. The rest of the work described here was designed by Dr. Jaime Rivera and Tingting Huang and performed by Tingting Huang.

Abstract

During early mouse embryogenesis, temporal and spatial regulation of gene expression and cell signaling influences lineage specification and embryonic polarity. Two extra-embryonic tissues, the anterior visceral endoderm (AVE) and the posterior visceral endoderm (PVE), located on opposite sides of the embryo, are thought to play an important role in establishing the antero-posterior (AP) body axis. This chapter focuses on studying the interaction between AVE and PVE cells and the molecular cross-talk between epiblast and extra-embryonic tissues in establishing the pattern of Wnt expression responsible for positioning the primitive streak at early post-implantation stages.

Introduction

The formation of the organizer, an area that releases a cocktail of factors and plays a central role in the formation of the embryonic axis, is one of the most fundamental events in establishing the primary body axes during early vertebrate development. The mouse equivalent to the organizer is the primitive streak, which forms in a localized region of the epiblast adjacent to the extra-embryonic ectoderm where it marks the future posterior side of the embryo (Figure.1.6). During gastrulation, the primitive streak serves as a conduit for the generation of mesoderm and definitive endoderm (Tam and Gad, 2004).

The visceral endoderm plays a pivotal role in establishing the anterior-posterior axis of the mouse embryo, but the molecular nature of the signals required remains to be determined. Loss-of-function mutations of *Otx2, Cripto, Nodal, and Wnt3* have been shown to disrupt the signaling cascade, in which the embryo fails to establish the A-P axis (Acampora et al., 1995; Liu et al., 1999; Schier and Shen, 2000). Here, I examine the interaction between AVE and PVE cells and the molecular cross-talk between epiblast and extraembryonic tissues in the establishment of the pattern of expression of Wnt3 and other primitive streak markers and their effect on axial development.

This work began with the observation that the AVE and *Wnt3* expression occupy complementary regions in E6.5 mouse embryos. As mentioned above, the AVE, first occupies the distal tip and then moves to the anterior side of the

egg cylinder. The AVE expresses the Wnt antagonists *Dkk1*, *Sfrp1* and *Sfrp5*. On the other hand, *Wnt3*, has been shown to be essential for gastrulation in loss of function studies (Liu et al., 1999) and our lab has provided evidence that Wnt3 emanating from the posterior visceral endoderm is the main signal that controls the formation of the primitive streak (Tortelote et al., 2013). These observations led us to hypothesize that the AVE prevents Wnt3 activity from reaching the anterior side of the embryo.

Two models for primitive streak formation

Mammalian embryos arrive at gastrulation in a shape that differs from other vertebrate embryos in two main aspects: first mammalian embryos inherit a restricted amount of maternal components and thus the embryos need to activate the zygotic genome as early as the two-cell stage (Schultz, 2002). Second, the number of epiblast cells when mammalian embryos initiate gastrulation is much smaller than in *Xenopus* (a few hundred cells in mice vs thousands of cells in *Xenopus*) (Solnica-Krezel and Sepich, 2012) .

Two regions of the early post-implantation mouse embryo have been proposed to be responsible for the formation of the primitive streak (Conlon, 1995; Bachvarova et al., 1998). One is the extra-embryonic ectoderm, a tissue that abuts the proximal epiblast. In this model, Bmp4 from the extra-embryonic ectoderm signals to the adjacent epiblast, to activate primitive streak markers, among them *Brachyury* (*T*). The induced epiblast then undergoes an epithelial to

mesenchymal transition to become the primitive streak, allowing gastrulation and the subsequent generation of mesoderm and endoderm (Beddington and Robertson, 1998). Several genetic and embryological arguments have been provided to support this hypothesis (Beddington and Robertson, 1999; Donnison et al., 2005; Ben-Haim et al., 2006; Arnold and Robertson, 2009) (Figure.2.1A)

An alternative signaling center is the prosterior visceral endoderm, an extra-embryonic component of the mouse conceptus located adjacent to the regioin of the epiblast that becomes the primitive streak. It was proposed that the posterior visceral endoderm serves as a signaling center that directs the formation of the primitive streak and that Wnt3 is the effector molecule (Rivera-Perez and Magnuson, 2005). In this model, Wnt3 emanating from posterior visceral endoderm, signals to the adjacent epiblast, to activate primitive streak markers, among them Brachyury (T). Several lines of evidence support this PVE signaling model. The embryos lacking *Wnt3,* show the complete loss of primitive streak, while the DVE cells are specified and move to the prospective anterior side, which suggests the formation of primitive streak is dependent on the *Wnt3* expression, while independent on the relocation of DVE to the prospective anterior side (Liu et al., 1999). The loss of the canonical Wnt signaling effector, β-catenin, causes the embryos to die around early post-implantation stages, without developing a correct anterior-posterior axis (Huelsken et al., 2000). The embryos homozygous for *Axin1* or *APC* null alleles, both of which are essential components in β-catenin degradation machinery Axin/GSK/APC, develop A-P

axis duplication (Zeng et al., 1997; Ishikawa et al., 2003) (Figure.2.1B).

In addition unpublished data from our laboratory has shown that inactivation of *Wnt3* in the posterior visceral endoderm of mouse embryos leads to a phenotype that phenocopies the phenotype of *Wnt3* null embryos, suggesting that *Wnt3* function in the posterior visceral endoderm is essential for the initiation of the primitive streak. Morever posterior visceral endoderm-signaling model was further supported by experiments in which *Wnt3* was conditionally inactivated in the epiblast of developing embryos (Tortelote et al., 2013). Embryos lacking *Wnt3* in the epiblast fail to thrive but still establish the antero-posterior axis and initiate gastrulation (Tortelote et al., 2013). Interestingly, in these embryos, *Wnt3* expression is temporarily present in the posterior visceral endoderm (Tortelote et al., 2013) suggesting that *Wnt3* signaling from the posterior visceral endoderm is responsible for this initiation of gastrulation.

Figure 2.1

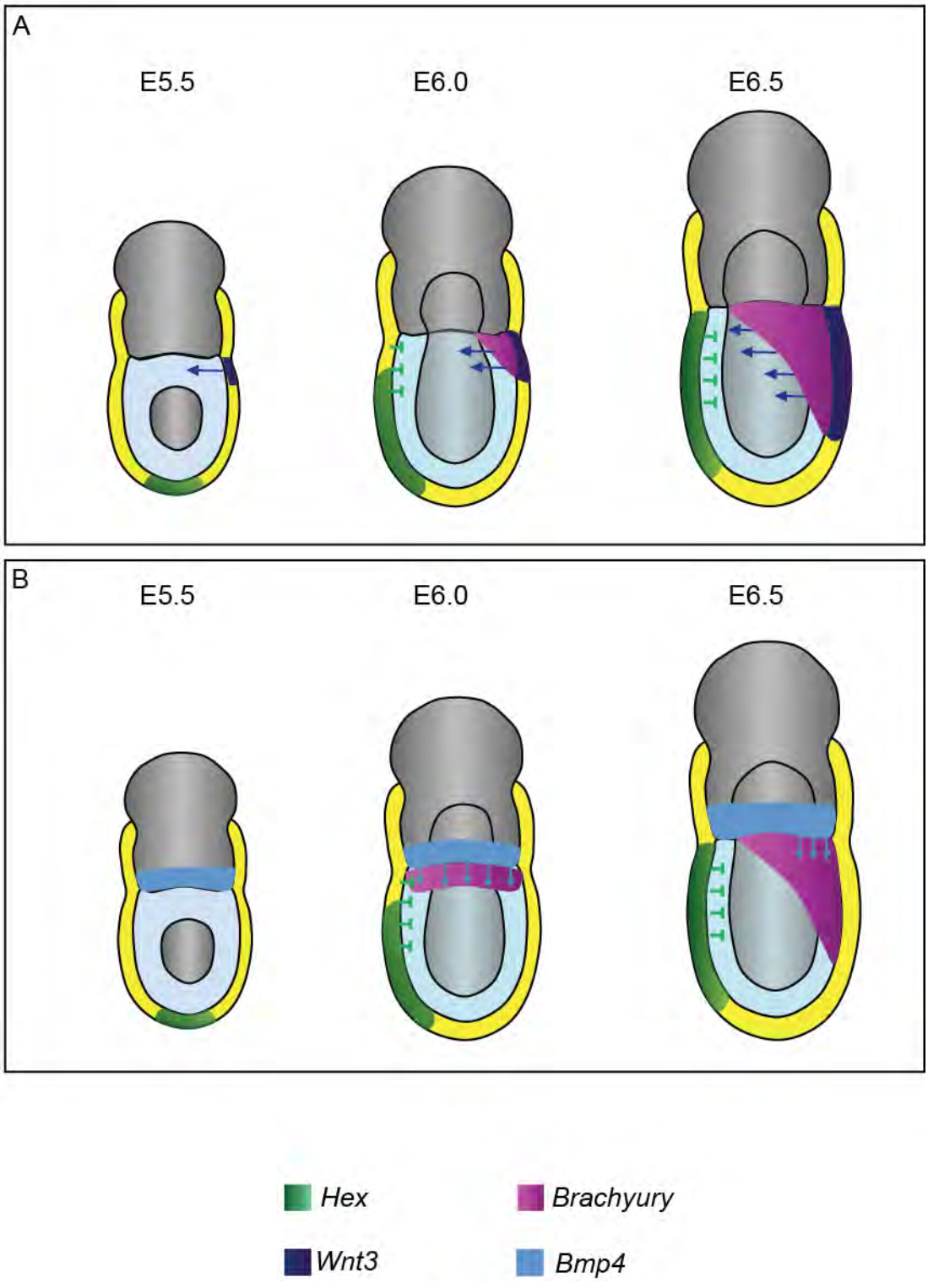

Figure 2.1. Schematic representation of the posterior visceral endoderm and extra-embryonic ectoderm signaling models.. (**A**) Posterior visceral endoderm model. *Wnt3* expression begins in the posterior visceral endoderm at E5.5, and then it activates primitive streak makers in the posterior epiblast (blue arrows). At E6.0, *Wnt3* signaling expands anteriorly, however, the anterior visceral endoderm (green) located in the anterior side at this time of development, releases Wnt antagonists that block *Wnt3* expansion to the anterior side of the egg cylinder. This process restricts the formation of the primitive streak in the posterior side of the embryo. (**B**). Extra-embryonic ectoderm signaling model**.** *Bmp4* (blue arrows) expressed in the extra-embryonic ectoderm induces the adjacent epiblast to express markers of the future primitive streak such as *Brachyury* and *Cripto*. Later, *Hex*-expressing (green) distal visceral endoderm cells move to one side of the epiblast. These cells then inhibit *Bmp4* signaling in the anterior side, which leads to the expression of the primitive streak makers only in the posterior epiblast and hence the formation of the primitive streak. Figure. A is adapted from the paper (Rivera-Perez and Magnuson, 2005) and Figure. B is adapted from the paper (Beddington and Robertson, 1998).

Cripto and EGF-CFC family

Cripto, is the founding member of EGF-CFC family of signaling molecules. The EGF-CFC family members contain a cystein rich domain called the Cripto, FRL-1 and Cryptic (CFC) motif and an epidermal growth factor (EGF) - like motif.

The EGF-CFC gene family is conserved in vertebrates, including Cripto, Cryptic, frog FRL-1, and zebrafish one-eye pinhead (oep) (Persico et al., 2001). Genetic evidence in fish and mice demonstrated the EGF – CFC family members play a key role in early embryonic development in patterning the early embryo (Griffin et al., 1998; Ding et al., 2005). *Cripto* has been shown to be essential for mouse anterior-posterior patterning (Ding et al., 1998) and *Cryptic* is required for left-right axis formation (Yan et al., 1999). Maternal – zygotic *oep* mutants show lack of endoderm and mesoderm, and defects in anterior-posterior patterning (Schier et al., 1997). In Nodal signaling pathway, Cripto can act as a co-receptor and co-ligand for Nodal (Figure. 1.8). A mammalian cell culture assay by using a luciferase reporter showed Cripto, in addition to its role as a coceptor for Nodal ligands, can also function as a secreted signaling factor in cell coculture assays, suggesting that it may also act as a coligand for Nodal (Yan et al., 2002). In Xenopus, Frl1 has been implicated in Wnt pathway and also shown to be a coreceptor for Wnt11 (Tao et al., 2005).

Cripto mRNA is present in the blastocyst stage embryo (Pfister et al., 2007). As development proceeds, Cripto is expressed uniformly in the epiblast of egg cylinder stage embryos and then in the primitive streak as gastrulation starts.

In mice, *Cripto* is required for the shift of the AVE to the anterior side of the embryo (Ding et al., 1998). Chimeric analysis shows that Cripto acts non-cell autonomousily way during axial mesendoderm formation in the mouse embryo, which suggests the possibility of transducing intercellular signaling (Chu et al., 2005). Current models suggest that in early mouse emrbyogenesis, Cripto acts as a coreceptor to facilitate Nodal binding to an type I and II Activin receptor complex (Shen and Schier, 2000). However, another study also showed Cripto regulates mouse anterior – posterior axis specification via a Nodal-independent signaling pathway (D'Andrea et al., 2008). *In vitro* studies showed Cripto can activate a ras – raf –MAP kinase signaling pathway (Bianco et al., 2003).

Here I hypothesized the relocation of DVE to the future anterior side, a fundamental step during early mouse embryogenesis, regulates the formation of primitive streak via blocking the expression of *Wnt3* into the anterior side.

Results

Cripto expression is present in the whole epiblast at E5.5 and then is restricted to the primitive streak

Cripto expression is known to mark the primitive streak during gastrulation (Ding et al., 1998). We analyzed *Cripto* RNA in embryos dissected at stages from E5.5 to E6.5 using a full length coding sequence and portions of the 5’ and 3’ untranslated region. *Cripto* expression is restricted to the epiblast. In embryos at E5.5, *Cripto* RNA was detected in the whole epiblast (Figure 2.2). Later, *Cripto* expression forms a gradient along the proximal–distal axis of the epiblast with higher expression in the proximal and lower expression in the distal regions. Coincident with the emergence of the primitive streak, the *Cripto* expression was exclusively restricted to the primitive streak (Figure 2.2). All the embryos show no *Cripto* expression in the extra-embryonic ectoderm and visceral endoderm.

Figure 2.2

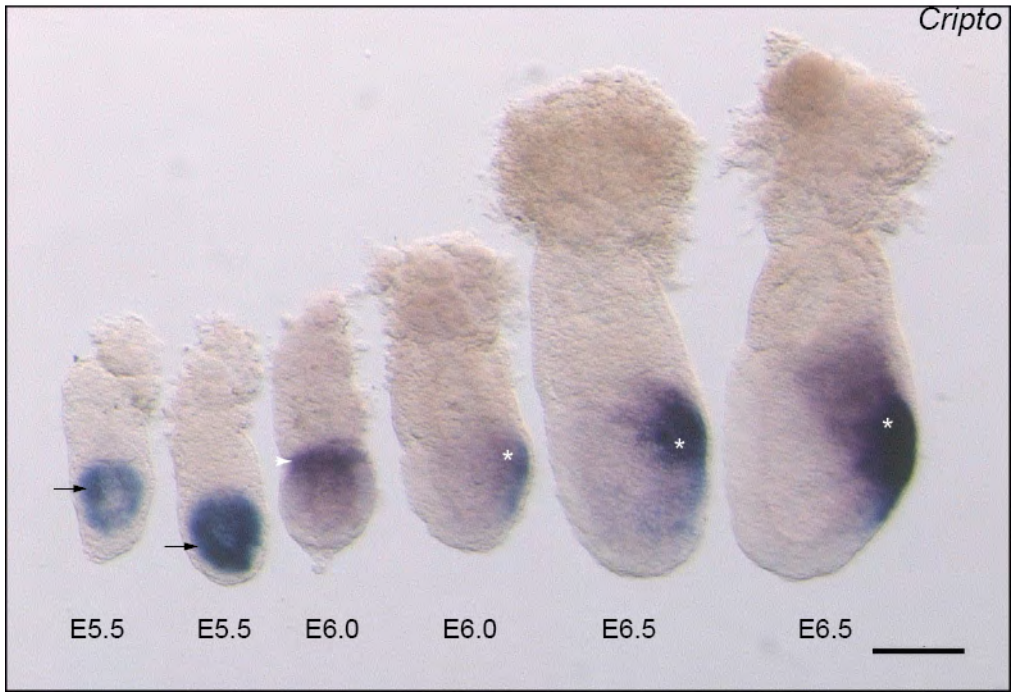

Figure 2.2. Whole-mount *in situ* hybridization of *Cripto* expression in embryos dissected between E5.5 and E6.5. *Cripto* RNA is first detected in the whole epiblast of the egg cylinder in E5.5 embryos (arrows) and then forms a proximal-distal gradient at around E5.75 (white arrowhead). Starting at E6.0, the expression of *Cripto* mRNA becomes restricted to the posterior epiblast and later to the primitive streak (asterisks). Scale bar: 100 μm.

Wnt3 is essential for primitive streak formation

As previously described, embryos homozygous for a *Wnt3* null allele lack primitive streak, mesoderm and node (Liu et al., 1999). The *Wnt3* allele I used is a null allele which carries a lacZ cassette and a floxed PGKneobpA cassette in exon 4 (Figure 2.3A) (Tortelotte et al., unpublished). The *Wnt3* promoter driven lacZ allele recapitulates the endogenous expression pattern of *Wnt3* and the mice homozygous for *Wnt3lacZ* gene generate a null mutation that phenocopies the straight knockout phenotype of *Wnt3* (Figure 2.3 C - E).

To inactivate *Wnt3* in the early developing mouse embryo, the homozygous mutant embryos were obtained from the intercross between *Wnt3* $^{lacZ/+}$ heterozygous mutant mice (Figure. 2.3B). Morphological analysis of *Wnt3* mutant embryos at E6.5 revealed the absence of primitive streak, as shown in the previous study (Liu et al., 1999) (Figure. 2.3 C, D). To determine if the primitive streak was specified in *Wnt3* null embryos, we analyzed the expression of *T (Brachyury)* (n=8) and *Cripto* (n=5). These genes mark the primitive streak and its precursors in the epiblast (Pfister et al., 2007). *T* also marks the distal third of the extra-embryonic ectoderm adjacent to the proximal epiblast (Perea-Gomez et al., 2004; Rivera-Perez and Magnuson, 2005). *Wnt3* null embryos did not show expression of any of these markers at E6.5 (Figure. 2.3C, D). Expression of *T* in the extra-embryonic ectoderm was present but reduced showing that although its initial expression in this tissue is independent of *Wnt3*

function in the visceral endoderm *Wnt3* is required to maintain *T* expression in the extra-embryonic ectoderm (Figure.2.3C). Expression of *Cripto* in the epiblast is absent in *Wnt3* mutant embryos (Figure.2.3D). From this set of experiments we conclude that *Wnt3* function is essential for the specification of the primitive streak in the mouse embryo.

It has been suggested that *Bmp4* emanating from the extraembryonic ectoderm induces the formation of the primitive streak (Winnier et al., 1995). Therefore, we wondered if the absence of the primitive streak in *Wnt3* mutants was an indirect effect of an absence of *Bmp4* expression in the extraembryonic ectoderm. To address this question, we analyzed the expression of *Bmp4* in *Wnt3* mutant embryos (*Wnt3* $^{lacZ/lacZ}$) dissected at E6.5. All the mutant embryos tested (n=5), expressed *Bmp4* in the distal third of the extraembryonic ectoderm comparable to control embryos (Figure. 2.3E). Since no primitive streak is observed in *Wnt3* mutant embryos, these results suggest that Bmp4 is not sufficient for the formation of the primitive streak.

Figure 2.3

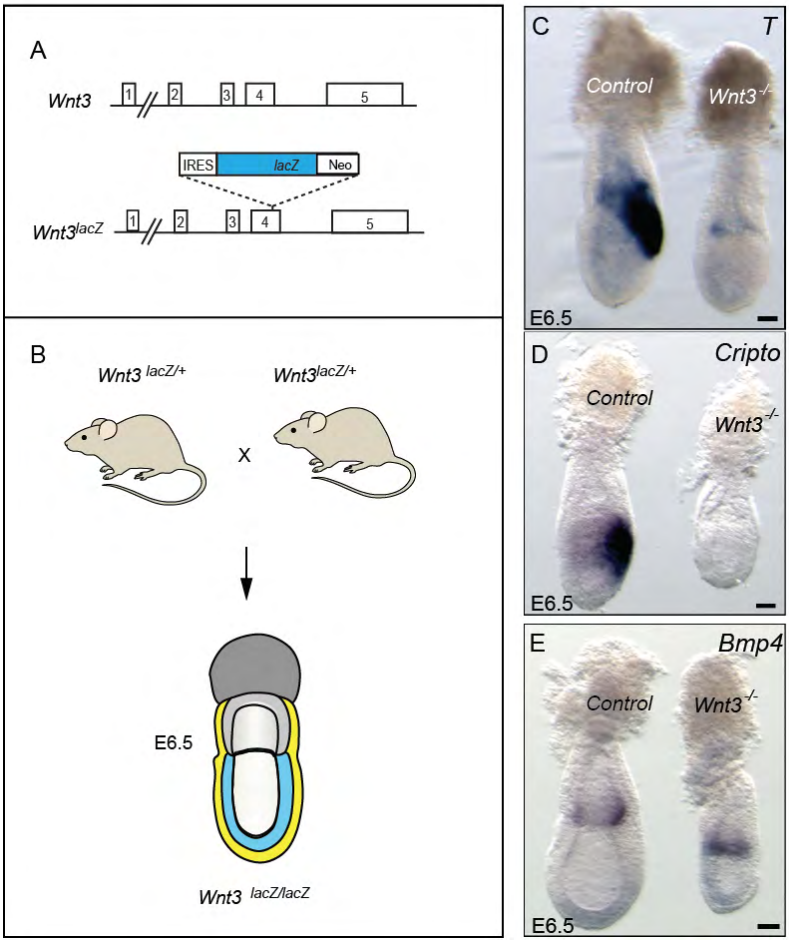
A
Wnt3
1
2
3
4
5
IRES
lacZ
Neo
Wnt3lacZ
B
Wnt3 lacZ/+
Wnt3lacZ/+
X
E6.5
Wnt3 lacZ/lacZ
C
T
Control
Wnt3-/-
E6.5
D
Cripto
Control
Wnt3-/-
E6.5
E
Bmp4
Control
Wnt3-/-
E6.5

Figure 2.3. *Wnt3* function in early mouse development. A. Schematic representation of the *Wnt3* locus and targeted $Wnt3^{lacZ}$ allele. **B.** Genetic strategy to generate. $Wnt3^{lacZ/lacZ}$ embryos. **C-E**. Control and *Wnt3* mutant embryos dissected at E6.5 and hybridized with *Brachyury (T), Cripto* and *Bmp4*. *Wnt3* mutant embryos express *T* in the extra-embryonic ectoderm but here is no expression of *Cripto. Bmp4* is normally expressed in the extra-embryonic ectoderm. Scale bars: 50 µm.

The location of DVE/AVE is complementary to *Wnt3*-expression in pre-gastrulating embryos

Anterior visceral endoderm cells shift to one side of epiblast from E5.5 to E5.75 marking the future anterior side of the embryo (Thomas et al., 1998; Rivera-Perez et al., 2003). On the posterior side of the embryo, *Wnt3* is present in the posterior visceral endoderm starting as early as E5.5 and expands anteriorly in a pattern complementary to the position of the AVE (Rivera-Perez and Magnuson, 2005). To confirm these observations, we compared the position of the AVE marked by fluorescence provided by the *Tg(Hex-eGFP)ARbe* transgene (Thomas et al., 1998) and the expression of *Wnt3,* marked by the $Wnt3^{lacZ}$ allele (Figure. 2.4A). *Hex* is a marker for the AVE during early mouse embryogenisis (Thomas et al., 1998).

At E6.5 embryos, the *Hex* expression domain was clearly restricted to anterior visceral endoderm and extended from the distal tip to the extra-embryonic boundary, while the expression of Wnt3 extended to half the length of the epiblast and overlying visceral endoderm and tapered anteriorly encompassing the whole circumference of the egg cylinder. The overlaying image shows that *Hex* transcripts remain localized to the visceral endoderm diametrically opposite the streak. These results provide direct evidence that the anterior visceral endoderm is located just opposite to the area where *Wnt3* is expressed at pre-gastrulation stages (Figure 2.4B-D).

Figure 2.4

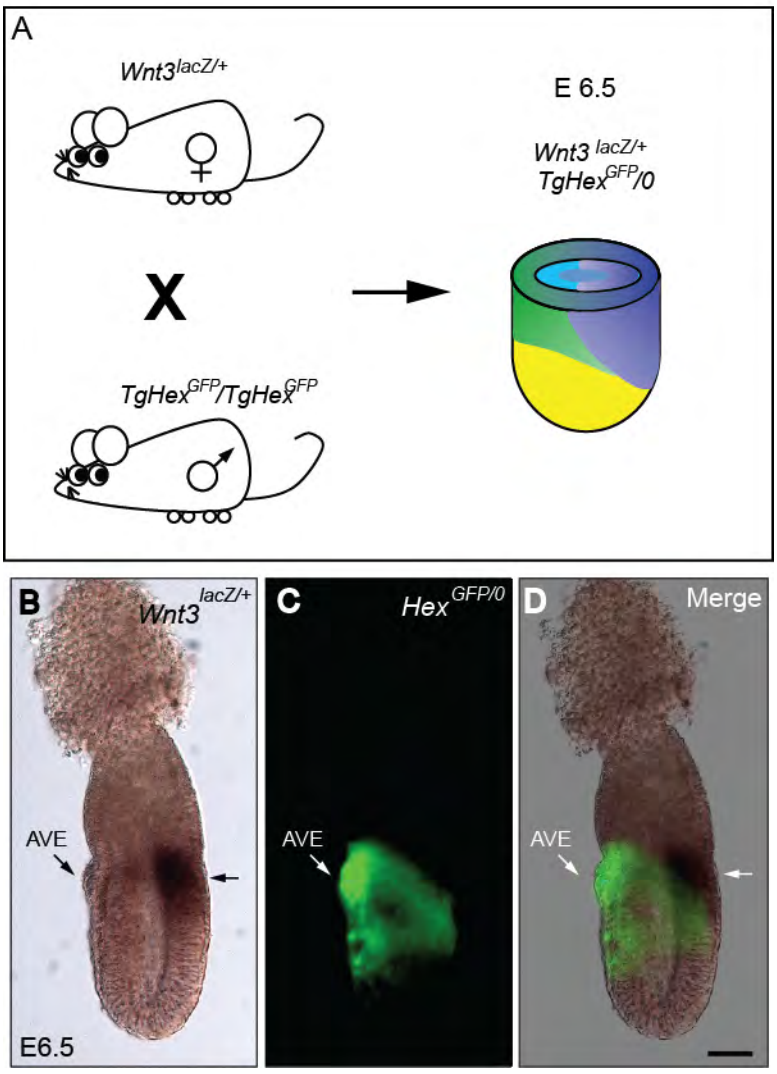
A
Wnt3lacZ/+
E 6.5
Wnt3 lacZ/+
TgHexGFP/0
X
TgHexGFP/TgHexGFP
B
Wnt3lacZ/+
AVE
E6.5
C
HexGFP/0
AVE
D
Merge
AVE

Figure 2.4. Comparison between the location of the AVE and *Wnt3* expression domains. A. Schematic representation of the genetic strategy to generate embryos heterozygous for *Wnt3*^{lacZ} and hemizygous for the *TgHex*^{GFP} transgene. **B-D.** E6.5 *Wnt3*$^{lacZ/+}$;*TgHex*$^{GFP/+}$ embryos assayed for β-galactosidase activity. The location of the AVE is revealed by green fluorescence generated by *TgHex*^{GFP}. *Wnt3* expression is complementary to the location of the AVE. Scale bar: 50 µm. Right arrow: posterior visceral endoderm.

Wnt3 forms a ring of expression in the proximal region of _Cripto_ mutant embryos

The above observations led us to postulate that the AVE prevents Wnt3 activity in the anterior side of the embryo. To address this question we took advantage of *Cripto* mutant embryos. In *Cripto* mutants (Figure. 2.5), the AVE fails to localize to the anterior side of the epiblast and remains at the distal tip of the conceptus (Ding et al., 1998), which is evident by the distal visceral endoderm thickening. We postulated that *Wnt3* was radialized in *Cripto* mutant embryos.

Analysis of *Wnt3* expression in *Cripto* null embryos (n=11) revealed that *Wnt3* expression was indeed radialized in mutant embryos forming a ring of expression around the proximal epiblast region (Figure. 2.6A). Histological analysis showed that *Wnt3* expression was mainly present in the visceral endoderm layer and was nearly absent from the epiblast (Figure. 2.6B). These results indicate that the AVE prevents the expansion of Wnt3 expression to the anterior side of the embryo and that *Wnt3* expression is downstream of *Cripto* in the epiblast.

Figure 2.5

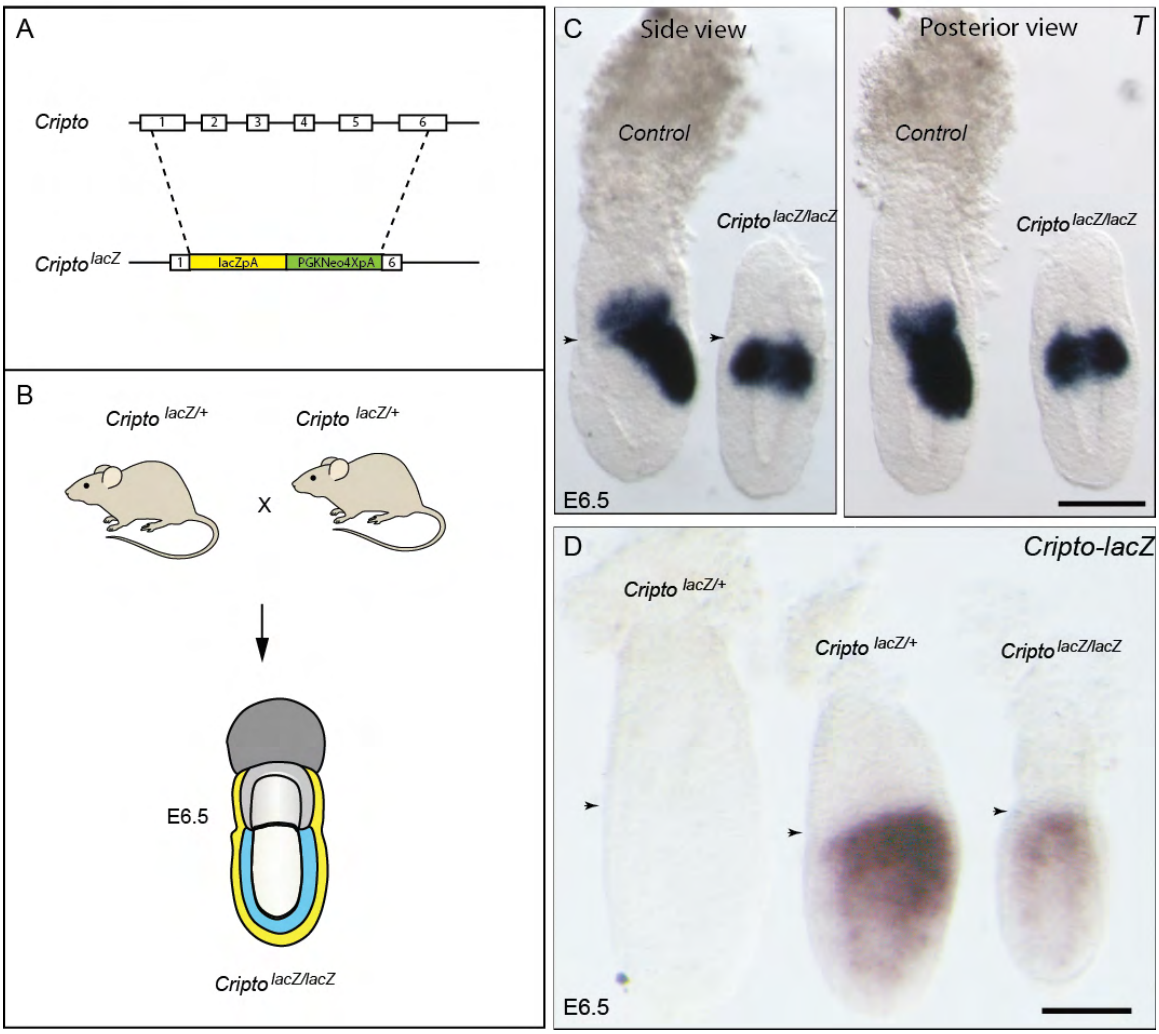
A
Cripto
1
2
3
4
5
6
Cripto lacZ
1
lacZpA
PGKNeo4XpA
6
B
Cripto lacZ/+
Cripto lacZ/+
X
E6.5
Cripto lacZ/lacZ
C
Side view
Control
Cripto lacZ/lacZ
Posterior view
T
Control
Cripto lacZ/lacZ
E6.5
D
Cripto-lacZ
Cripto lacZ/+
Cripto lacZ/+
Cripto lacZ/lacZ
E6.5

Figure 2.5. Analysis of *Cripto* function in early mouse development. A. Schematic representation of the *Cripto* locus and targeted *Cripto*^{lacZ} allele. **B.** Genetic strategy to generate *Cripto*$^{lacZ/lacZ}$ embryos. **C**. Control and *Cripto* mutant embryos dissected at E6.5 and hybridized with *Brachyury (T). Cripto* mutant embryos show radialized *T* expression in the proximal epiblast. **D.** Wild type, heterozygous and homozygous for *Cripto*^{lacZ} embryos dissected at E6.5 and assayed for β-galactosidase activity. *Cripto* mutants show *Cripto* promoter activation in the proximal epiblast region, while heterozygous *Cripto* mutants mainly show *Cripto* promoter activation in the primitive streak region. Arrowheads mark the extra-embryonic/embryonic boundary. Scale bars: 100 μm in C and D.

Figure 2.6

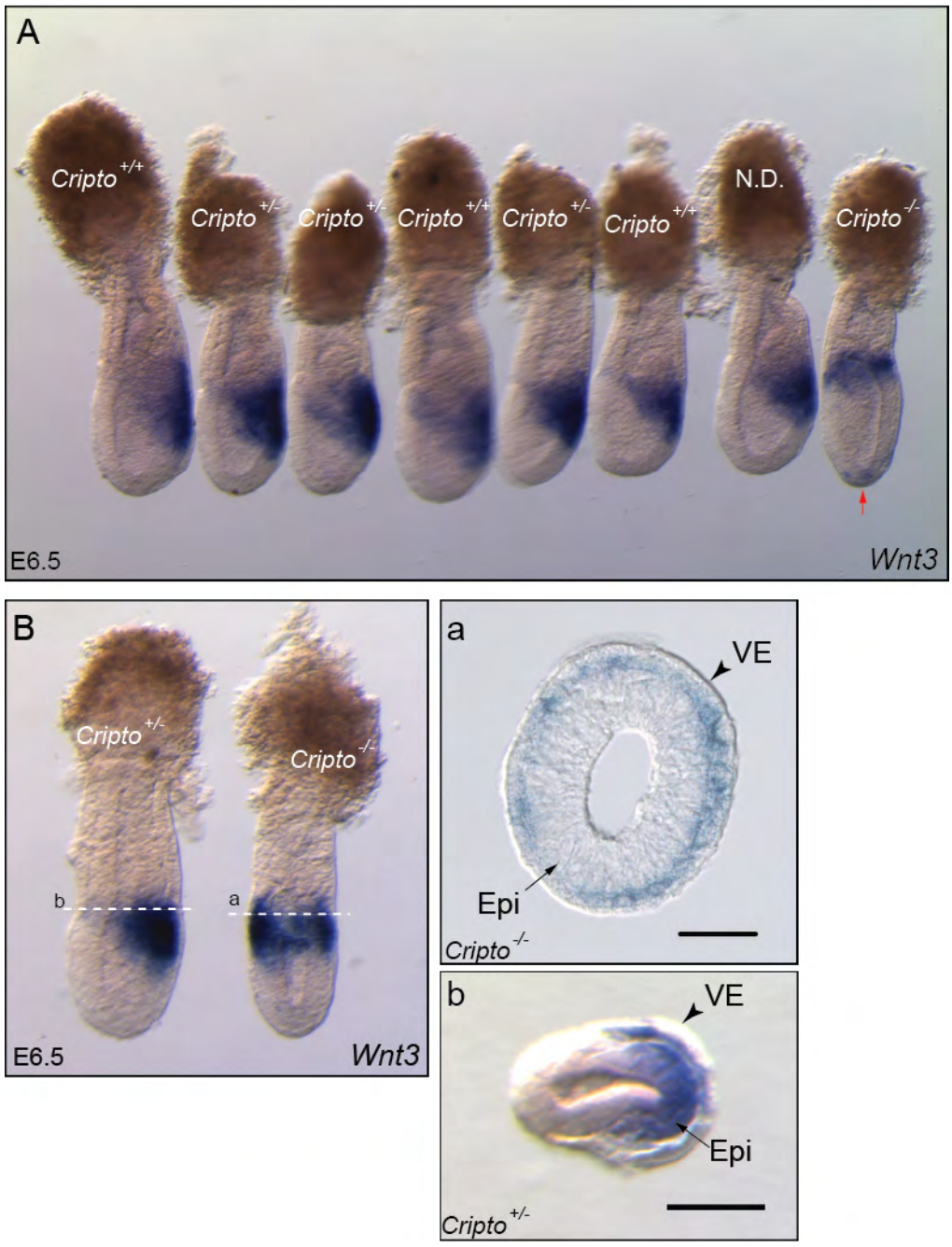
A
Cripto+/+
Cripto+/-
Cripto+/-
Cripto+/+
Cripto+/-
Cripto+/+
N.D.
Cripto-/-
E6.5
Wnt3
B
Cripto+/-
Cripto-/-
b
a
E6.5
Wnt3
a
VE
Epi
Cripto-/-
b
VE
Epi
Cripto+/-

Figure 2.6. Whole mount *in situ* hybridization analysis of *Wnt3* expression in *Cripto* mutant embryos. A. *Wnt3* expression in a litter dissected at E6.5 obtained from heterozygous for *Cripto*^{lacZ} crosses. The red arrow marks the location of the AVE in a mutant embryo. **B.** Heterozygous and *Cripto* mutant embryos dissected at E6.5 and hybridized with a *Wnt3* probe. In the *Cripto* mutant embryo, *Wnt3* expression is mainly radialized in the proximal visceral endoderm region (a) while in the heterozygous embryo, it is present in both the epiblast and the visceral endoderm (b). The dotted lines in B, represent the approximate location of the sections shown in a and b. Scale bars 30 µm. Epi, epiblast; VE, visceral endoderm.

Primitive streak markers are present in the proximal epiblast of *Cripto* mutant embryos.

Analysis of *T* expression in *Cripto* null embryos (n=11) revealed that *T* expression was radialized in mutant embryos in the proximal epiblast region (Figure. 2.5C). Analysis of Cripto-promoter activation in *Cripto* null embryos (n=6) also revealed that the Cripto-promoter driven lacZ expression is present in the proximal region of epiblast, which suggests that *Cripto* expression, as reflected by $Cripto^{lacZ}$ activity, is also radialized in *Cripto* mutants. Surprisingly, histological analysis showed that *Wnt3* expression was restricted to the visceral endoderm layer and was absent from the epiblast (Figure. 2.5D). These results indicate that the AVE prevents the expansion of Wnt3 signaling to the anterior side of the embryo and that *Wnt3* expression is downstream of *Cripto* in the epiblast. *T* expression in the epiblast depends on *Wnt3* (Liu et al., 1999; Barrow et al., 2007; Tortelote et al., 2013)**.**

***Brachyury* expression is completely abolished in the *Cripto/Wnt3* double mutant embryos.**

To determine if the ectopic expression of *Wnt3* in the visceral endoderm was responsible for the expression of *T* in the anterior epiblast, we removed *Wnt3* activity from *Cripto* mutants by generating *Cripto/Wnt3* double mutant embryos. We generated 87 embryos from double heterozygous (*Wnt3*$^{lacZ/+}$;*Cripto*$^{+/-}$) crosses and obtained five *Cripto/Wnt3* double mutant embryos. In all these double mutant *Wnt3/Cripto* embryos, the *Brachyury* expression is completely abolished (Figure. 2.7). Therefore, the radialized expression of *Wnt3* in the proximal visceral endoderm of *Cripto* mutants leads to ectopic activation of *T* in the anterior epiblast.

These results indicate that in *Cripto* mutant embryos, *Wnt3* expression in the posterior visceral endoderm is sufficient to induce primitive streak markers in a non-cell autonomous manner.

Figure 2.7

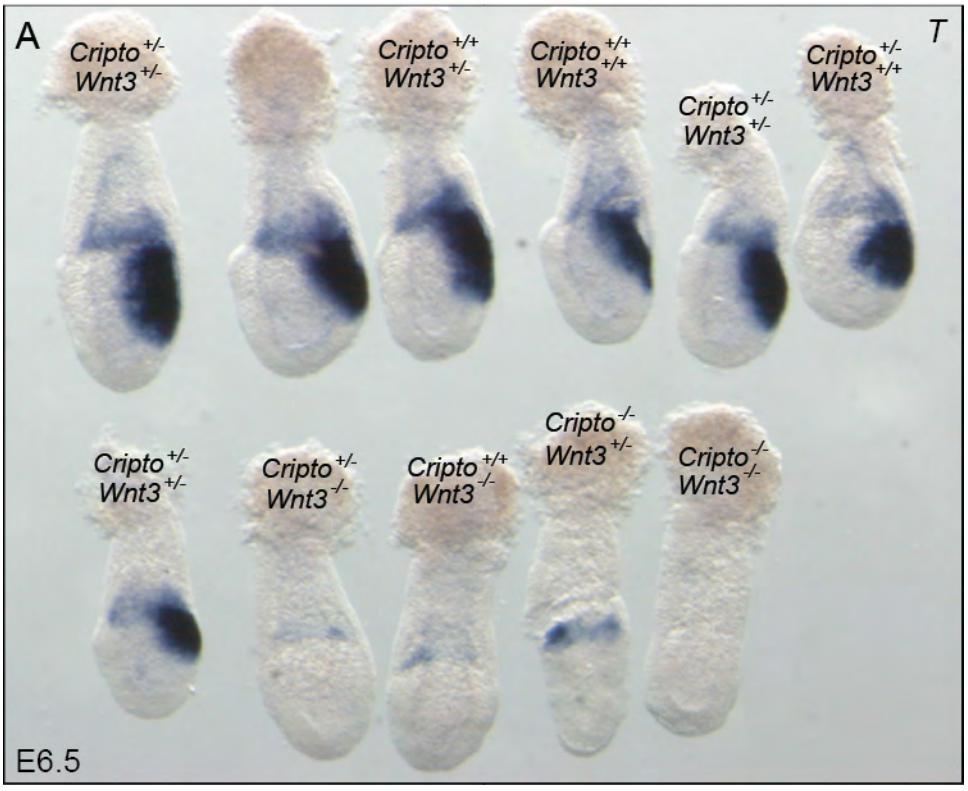
A
T
Cripto +/- Wnt3 +/-
Cripto +/+ Wnt3 +/-
Cripto +/+ Wnt3 +/+
Cripto +/- Wnt3 +/-
Cripto +/- Wnt3 +/+
Cripto +/- Wnt3 +/-
Cripto +/- Wnt3 -/-
Cripto +/+ Wnt3 -/-
Cripto -/- Wnt3 +/-
Cripto -/- Wnt3 -/-
E6.5

Figure 2.7 cont.

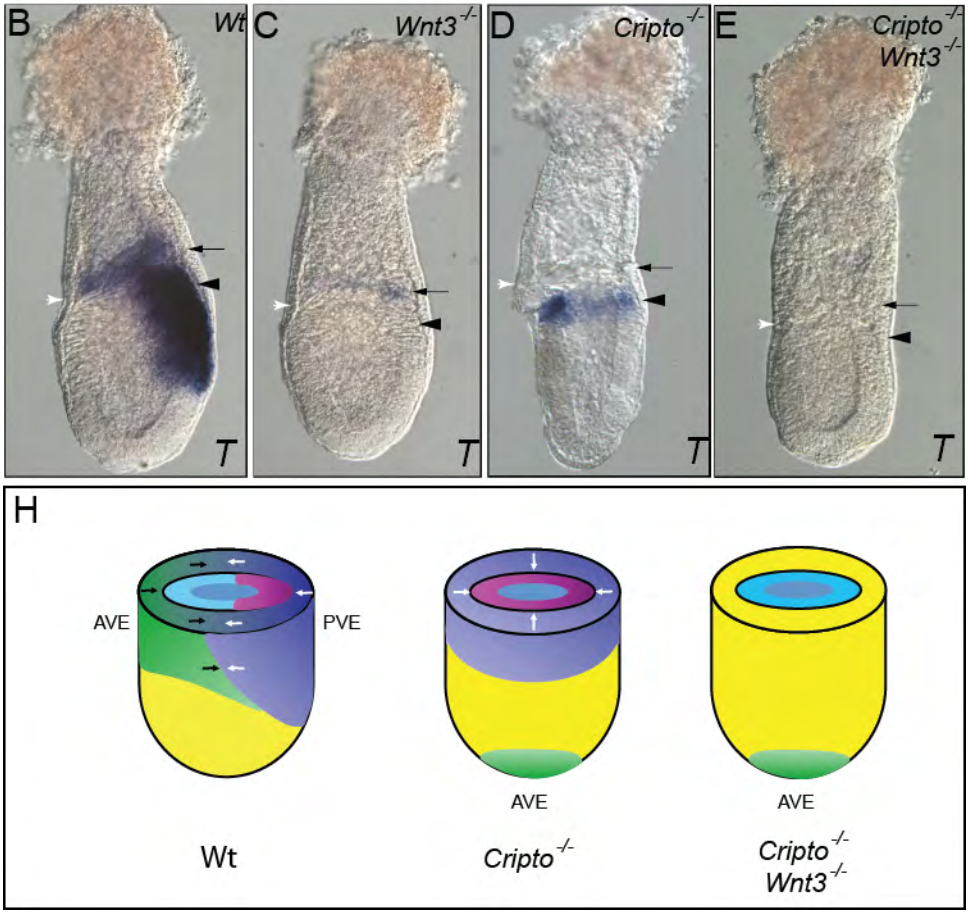

Figure 2.7. Whole mount *in situ* hybridization analysis of *Brachyury* in double mutant *Cripto/Wnt3* embryos. A. A litter dissected at E6.5 obtained from double heterozygous *Cripto*$^{lacZ/+;}$*Wnt3*$^{lacZ/+}$ crosses. **B-E.** *Cripto* Heterozygous (B), *Wnt3* mutant (C), *Cripto* mutant (D) and double *Wnt3/Cripto* mutant (E) embryos dissected at E6.5 and hybridized with *Brachyury*. *Brachyury* is expressed in the extra-embryonic ectoderm (arrow) and epiblast (black arrowhead) of wild-type embryos and weakly in the extra-embryonic ectoderm of *Wnt3* mutants. The double mutant embryo completely lacks *Brachyury* expression showing that in *Cripto* mutant embryos *Wnt3* is essential for radialized *Brachyury* expression. The white arrowhead represents the extra-embryonic-embryonic boundary. **H.** Schematic representation of the events occurring in wild type, *Cripto* heterozygous and Cripto/Wnt3 double mutant embryos. In *Cripto* mutants, the anterior visceral endoderm remain at the distal tip of the eg cylinder, allowing expansion of Wnt signaling to anterior region of the embryo. This causes the radialized expression of primitive streak markers in Cripto mutants. The removal of *Wnt3* in *Cripto* mutants causes a complete abolishment of the expression of primitive streak markers.

Materials and Methods

Embryo staging

Embryos were staged based on morphological landmarks as previously described (Downs and Davies, 1993; Rivera-Perez et al., 2010) or described in terms of dissection time. Noon of the day that a mating plug was observed was considered embryonic day 0.5 (E0.5) of gestation. All embryos were derived from mice maintained on a CD-1 genetic background.

Generation of *Wnt3*^{lacZ} knock-in mice

The targeting vector contained a 6 kb NotI-BamHI genomic DNA fragment (129S6/SvEvBrd) containing exons 3-4 of the *Wnt3* locus (Figure 2.3A). A *lacZ* cassette and a floxed PGK*neo*bpA cassette were inserted into the ClaI site in exon 4. The *lacZ* cassette contained an internal ribosomal entry site (IRES) and an SV40 polyA signal sequence. An HSV-*tk*pA cassette was added to the 5'-homologous arm. Gene targeting in ES cells was performed as previously described (Mishina et al., 1995). A total of 192 G418; FIAU double-resistant ES cell colonies were screened for homologous recombination by Southern blotting using a *Wnt3* 3' UTR probe (Liu et al., 1999). Twenty-seven lines were positive in the initial screening, and two lines gave rise to germ-line chimeras. Heterozygous mutants were normal and fertile. The phenotype of the *Wnt3*^{lacZ} homozygous mutants was indistinguishable from that of *Wnt3* null mutants previously reported

(Liu et al., 1999; Barrow et al., 2007) (Figure 2.3A), indicating that the *Wnt3*^{lacZ} allele is a null allele.

Mouse strains and genotyping

Cripto $^{lacZ/+}$ mice (Ding et al., 1998) were obtained from crosses between mixed stock heterozygous males and CD-1 females. Heterozygous *Wnt3* $^{lacZ/+}$ mice were also maintained by the same strategy. Male mice heterozygous for *Wnt3* $^{lacZ/+}$ were crossed with female mice heterozygous for *Cripto* $^{lacZ/+}$ to generate the mice double heterozygous for the *Wnt3* $^{lacZ/+}$ allele and the *Cripto* $^{lacZ/+}$ allele. All the CD-1 mice were obtained from Charles River Laboratories.

Embryos were genotyped retrospectively after wholemount *in situ* hybridization or after the β-galactosidase assay. Each litter was pictured before genotyping to allow unique identification of each embryo. Embryos were placed in 15-20 µl of PCR lysis buffer (50 mM KCl, 10 mM Tris-HCl pH8.3, 2.5 mM $MgCl_2$, 0.1 mg/ml gelatin, 0.45% IGEPAL and 0.45% Tween 20) containing 100 mg/ml Proteinase K and incubated overnight at 56^{o}C. After lysis, proteinase K was inactivated at 95^{o}C for 5 min and 1 µl of the sample was use for the PCR reaction. Mice were genotyped at postnatal day 10 using a 2 mm tail tip piece.

PCR for *Cre*, *LacZ* and *Wnt3*^{c} allele was carried out using Go Taq Flexi DNA polymerase (Promega cat no. M8295) using the following PCR cycle conditions: 30 sec. at 95^{o}C, 40 sec. at 60^{o}C and 40 sec. at 72^{o}C repeated 31 times with an initial denaturation cycle of 5 min. at 95^{o}C and a final elongation

step of 7 min. at 72^{o}C. The *Wnt3*$^{3-4}$ allele was amplified using the following cycle: 1 min at 95^{o}C, 1 min at 58^{o}C and 1 min at 72^{o}C were repeated 35 times. We used the following oligonucleotides: Progeny of the above cross were genotyped using the following primers:

Cripto Fwd: 5'- CCT CCG AAG TCC TCA ATC AC-3'

Cripto $^{lacZ/+}$Rev*:* 5'-GAT TAA GTT GGG TAA CGC CAG-3'

Cripto Rev*:* 5'-TCC GAA GTG GCT ATC TCC AG-3'

LacZ Fwd*:* 5'-GCG TTA CCC AAC TTA ATC G-3'

LacZ Rev: 5'- TGT GAG CGA GTA ACA ACC-3'

Ptmw1: 5'- GAC TTC CTC AAG GAC AAG TAC G-3'

Ptmw2: 5'- GAA GAC GCA ATG GCA TTT CTC-3'

neoF2: 5'- TGG CTA CCC GTG ATA TTG CTG-3'

We amplified a around 300bp DNA fragment for *Cripto* allele by using *Cripto* Fwd and *Cripto* Rev primers, a 500bp DNA fragment for *Cripto* $^{lacZ/+}$ allele by using *Cripto* Fwd and *Cripto* $^{lacZ/+}$ Rev primers, a 300 bp DNA fragment for lacZ allele by using *LacZ* Fwd and *LacZ* Rev primers, a 300 bp DNA fragment for *Wnt3* allele, and a 300bp DNA fragment for *Wnt3* $^{lacZ/+}$ allele. We performed PCR reactions for different alleles separately.

Dissection and embryo staging

Dissections were conducted in DMEM (Dulbecco's Modified Eagle Medium) (Invitrogen, Cat. No. 31600-034) containing 10% heat inactivated fetal

bovine serum (Atlanta Biologicals, Cat. No. S11150), penicillin (100 U/ml), (Cat. No. 15140-122) and 20 mM HEPES (Fisher, Cat. No. BP310). Dissected embryos were examined on a Nikon diaphot microscope equipped with DIC optics. Embryos with any obvious mechanical damage or an extremely bent ectoplacental cone were not considered for further study. Embryos were photographed by using a CCD camera (Leica Inc. DFC420).

Whole mount *in situ* hybridization

Whole-mount *in situ* with digoxigenin-labeled probes was performed as previously described (Rivera-Perez and Magnuson, 2005). The plasmid used to generate the *Brachyury* probe was a gift from a gift from B. Herrmann (Duke University, Durham, NC). Plasmids for *Wnt3* probe were a gift from R. Behringer at Sealy Center for Cancer Cell Biology (University of Texas Medical Branch, Galveston. TX). Plasmids for *Cripto* probe were a gift from M. Shen at Department of Genetics and Development from Columbia University Medical Center.

Histology and salmon-gal staining

The protocol for Salmon-gal staining was previously described (Sundararajan et al., 2012). Embryos dissected at E6.5 were fixed in 2% formalin, 5 mM EGTA and 2 mM MgCl2 in 0.1 M phosphate buffer (pH 7.3) for 5 minutes. They were then washed three times in rinse solution: 0.1% sodium

deoxycholate, 0.2% IGEPAL, 2 mM MgCl2 and 0.1 M phosphate buffer (pH 7.3) for 20 minutes each. Embryos were then incubated in the dark in staining solution at 37°C. The staining solution consisted of 1 mg/ml Salmon gal (6-chloro-3-indolyl-β-D galactopyranoside) (Lab Scientific, catalog number X668) and 0.4 mM of TNBT (5-bromo-4-chloro-3-indoxyl phosphate) (VWR, catalog number 101108-494) in rinse solution.

Discussion

My studies show the relocation of the DVE from the distal to the prospective anterior region of the embryo results in restriction of Wnt signalling activity to the posterior side of the embryo. This in turn leads to the positioning of the primitive streak to one side of the epiblast commencing the process of gastrulation. These results support the novel view that interplay between the anterior and posterior visceral endoderm is a developmental mechanism for the proper establishment of the anteroposterior axis in mammals. The fact that ectopic expression of *Wnt3* in the visceral endoderm of *Cripto* mutants leads to the expression of *Brachury* in the proximal epiblast suggests *Wnt3* is sufficient to induce the formation of the primitive streak. The unpublished data done by Giovane Tortolotte from our laboratory showed the *Wnt3* in the visceral endoderm was essential for the formation of primitive streak, together with my data, implying an interesting parallel between the posterior visceral endoderm in mice and Nieuwkoop center of amphibians. Another study done by Jeff Barrow (Barrow et al., 2007) showed the expression of *Wnt3* is dispensable for mouse gastrulation, which is not consistent with Tortolotte's data. This could be due to the different mouse strains two groups used.

As this study and previous reports described, normal *Bmp4* expression was observed in *Wnt3*-null mutant embryos that had no primitive streak. This suggests that *Bmp4* is not sufficient to induce a primitive streak in mouse

embryos as previously suggested (Ben-Haim et al., 2006). More recent studies show that the *Wnt3*-visceral endoderm knockout embryos also do not develop a primitive streak while *Bmp4* is still present in the extraembryonic ectoderm abutting the epiblast (Tortelotte et al. unpublished), which indicate that *Bmp4* is dispensable for the initiation of gastrulation. However, a certain amount of embryos lacking *Bmp4* do not develop a primitive streak (Winnier et al., 1995), suggesting *Bmp4* plays a role in gastrulation albeit as a permissive rather than as an instructive signal. The presence of *Bmp4* in the extra-embryonic ectoderm in *Wnt3* mutant embryos shows that *Bmp4* expression in this region of the embryo is not dependent on *Wnt3*. This draws an intriguing linear gastrulation model in which *Bmp4* in the extra-embryonic ectoderm regulates *Wnt3* in the posterior visceral endoderm and then initiate the whole gastrulation process. To address this possibility, it would be interesting to study the expression of *Wnt3* in *Bmp4* mutant embryos.

Nodal is an important regulator for early mouse development. *Nodal* mutants have a small epiblast, lack a primitive streak and the AVE remains at the distal tip of the embryo (Conlon et al., 1994). During normal development, Nodal antagonistic action emanating from the AVE is necessary to restrict the formation of the primitive streak to the posterior side of the embryo (Perea-Gomez et al., 2002; Robertson et al., 2003). Interestingly, *Nodal* expression is lost in *Wnt3* mutants (Liu et al., 1999) and the regulatory region of *Nodal* that controls its expression in the primitive streak has TCF/LEF binding sites (Norris and

Robertson, 1999; Ben-Haim et al., 2006; Granier et al., 2011). Thus, *Nodal* expression in the posterior epiblast/primitive streak seems to depend on *Wnt3* signaling acting through the canonical Wnt signaling pathway. An intriguing possibility is that the AVE restricts a Wnt3-dependent Nodal activity in the epiblast to the posterior side of the embryo.

Apart from *Cripto* mutants, the DVE cells of *Otx2* mutant embryos fail to locate to one side of the embryo. In *Otx2* null embryos*, Wnt3* and *Brachyury* expression are present in the proximal region of the embryo (Kimura et al., 2001), suggesting the possibility that the proximal expression of *Wnt3* induces the corresponding *Brachury* expression in the proximal region in the *Otx2* mutants. This hypothesis could be addressed by generating double *Wnt3/Otx2* mutants to investigate the sufficiency of *Wnt3* expression in proximal region for maintaining *Brachyury* expression. The expected result is that the expression of *Brachyury* is lost after removing Wnt3 activity in *Otx2* mutants. The data from this experiment will reinforce the conclusion from the *Cripto* mutant experiment, that the relocation of DVE to the anterior side plays a role in mouse embryo patterning via blocking *Wnt3* expression. Moreover, testing the same hypothesis in two different models (*Otx2 -/-* and *Cripto -/-*) also exclude the possibility that it is the gene (*Cripto* or *Otx2*) but not the failure of AVE movements leads to the expansion of *Wnt3* expression.

The loss of *Cripto* leads to the failure to position the AVE even though the DVE may have been generated. In embryos lacking *Wnt3*, *Cripto* expression is

initiated in the whole epiblast at E6.0 (Tortelotte et al. unpublished), however could not be maintained later at E6.5 (Figure 2.3). This suggest that the initial expression of *Cripto* is not dependent on Wnt3, while *Cripto* expression in the primitive streak is dependent on *Wnt3*. Morever, complete loss of *Wnt3* in both epiblast and VE (Liu et al., 1999) does not seem to affect the formation of the AVE. Taking these two together, indicates that the loss of *Cripto* in the primitive streak would have no effect on the formation of the AVE, or contribute to the "radialization" of T expression. Thus, the initial expression of *Cripto* in the epiblast is most likely responsible for the DVE to AVE transition and affects the positioning of primitive streak (Figure 2.8).

Wnt antagonist (Dkk1) has been suggested as an attractive guidance cue to drive AVE migration to the prospective anterior side (Kimura-Yoshida et al., 2005). The embryos lacking *Otx2* die during early gastrulation and exhibit anterior-posterior patterning defects due to the failure of AVE positioning. In *Otx2* mutants, *Dkk1* expression in the DVE/AVE is missing and moreover, the A-P patterning defects could be partially resuced via removing one copy of β-catenin gene, which leads to the reduced canonical Wnt signaling activity. This further indicates the anatagonist role of DVE-expressing *Dkk1* in Wnt signaling during the establishment of the anteroposterior axis in mouse embryos (Kimura-Yoshida et al., 2005).

Since *Wnt3* mutants lack *Cripto* expression in the primitive streak, *Wnt3* functions upstream of *Cripto*. However, *Cripto* is required for maintaining *Wnt3*

expression in the epiblast, therefore, *Wnt3* acts downstream of *Cripto* in the epiblast. This paradox can be explained by placing the same molecules into different developmental time windows. Since Cripto is known to be a co-receptor for Nodal signaling pathway in vertebrate development (Yan et al., 2002), the loss of *Wnt3* expression in the epiblast in the *Cripto* mutants is likely to due to the distrupted Cripto-dependent Nodal signaling pathway in *Cripto* mutant embryos embryos. In addition, at E6.5, *Wnt3* is upstream of *Cripto* during the stage when primitive streak forms. However, the Wnt3 activity in *Cripto* mutant embryos could still exist even though the whole mount *in situ* for *Wnt3* is not sensitive enough to detect it, which is also revealed by p21 whole mount *in situ* and RT-PCR (Figure3.6).

The emerging view put forward by our results, suggests that the signaling cascades that pattern the mouse anteroposterior axis act in a spatially and temporally controlled manner (Figure. 2.8). Around E5.5, nodal precursors are produced in the epiblast, processed into a mature form in extraembryonic ectoderm and then released to the proximal epiblast. Nodal ligands from the epiblast activate the expression of several genes in visceral endoderm at the distal tip of the egg cylinder via Cripto-dependent or Cripto-independent signaling pathway (Tam and Loebel, 2007). Concurrently, Wnt3 emanates from posterior visceral endoderm, which provides a repulsive cue to guide AVE, while Wnt antagonist (Dkk1) from the distal visceral endoderm provides an attractive cue to guide AVE migration migration (Kimura-Yoshida et al., 2005). The AVE cells

actively migrate to the prospective anterior side of the egg cylinder around E5.75. At primitive streak stage (E6.5), Wnt3 signals from the posterior visceral endoderm to the adjacent epiblast to induce the expression of primitive streak markers among them *Cripto, Brachyury,* etc. *Cripto* expression in the epiblast is necessary for the expression of *Wnt3* in the epiblast, which is the reason that in *Cripto* mutant embryos, *Wnt3* expression in the epiblast is absent. The *Wnt3* expression in the epiblast is magnified via canonical Wnt signaling and the epiblast-expressing *Wnt3* is likely to signal back to the visceral endoderm to augment the *Wnt3* expression in the visceral endoderm via an autoregulatory loop. As *Wnt3* expression expands anteriorly, the AVE release Wnt antagonists (Dkk1, Sfrp1&5, etc) to block *Wnt3* expression in the epiblast and visceral endoderm. All these complex molecular crosstalks between visceral endoderm and epiblast ensure the right positioning of primitive streak during early gastrulating mouse embryos.

In conclusion, my data provide novel evidence that indicate that an interplay between the anterior and posterior visceral endoderm regulates gastrulation. These results open the way to dissect the complex network of visceral endoderm signaling *in vivo*. In the future, genetic manipulations, which selectively eliminate a subset of inhibiting activities will be crucial to dissect the complex functions of the AVE and its inhibitory role for Wnt signaling emanating from the posterior visceral endoderm. It will be important to determine, whether visceral endoderm specific double or triple mutant embryos for *mDKK1*, S*frp1*&5

and *Cer-l* can lead to the expansion of canonical Wnt signaling and a ectopic primitive streak.

Figure 2.8

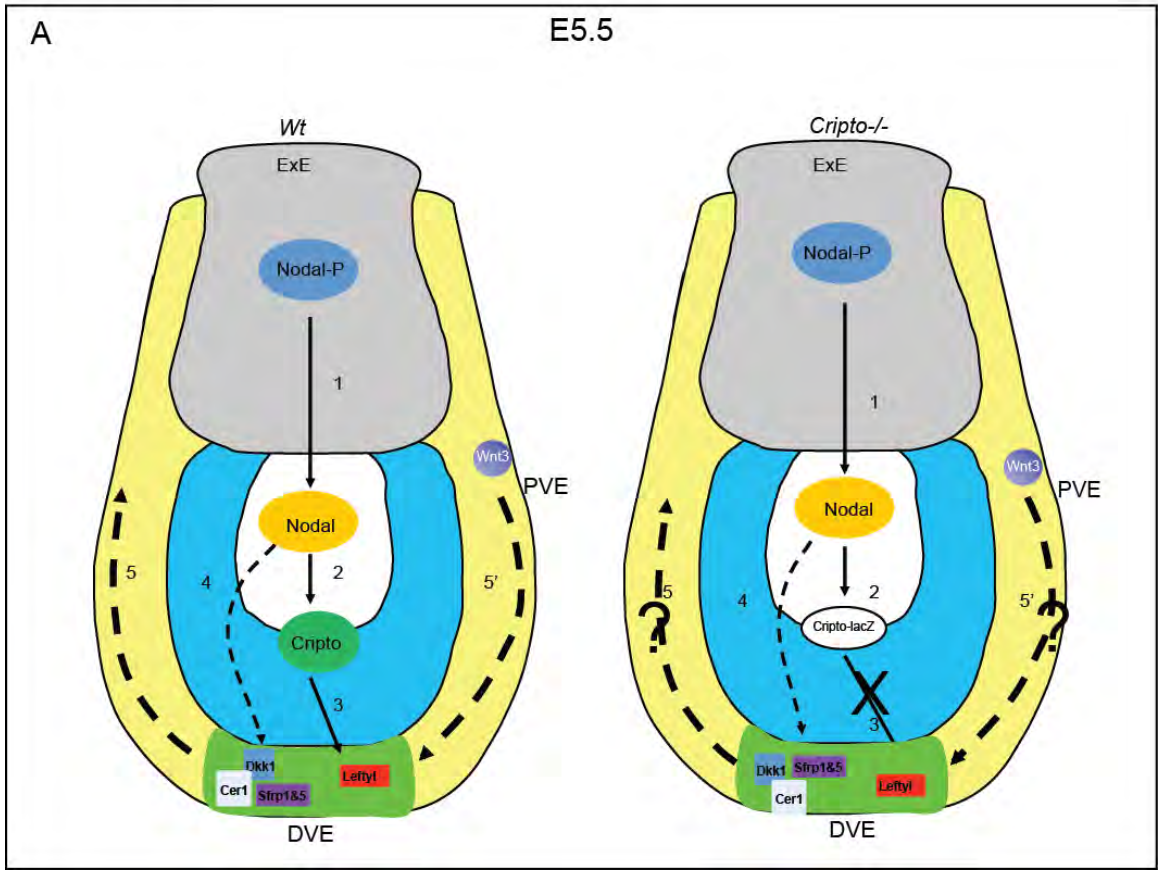
A
E5.5
Wt
ExE
Nodal-P
1
Nodal
2
Cripto
3
4
5
5'
Wnt3
PVE
Dkk1
Cer1
Sfrp1&5
Lefty1
DVE
Cripto-/-
ExE
Nodal-P
1
Nodal
2
Cripto-lacZ
3
4
5
5'
Wnt3
PVE
Dkk1
Sfrp1&5
Cer1
Lefty1
DVE

Figure 2.8

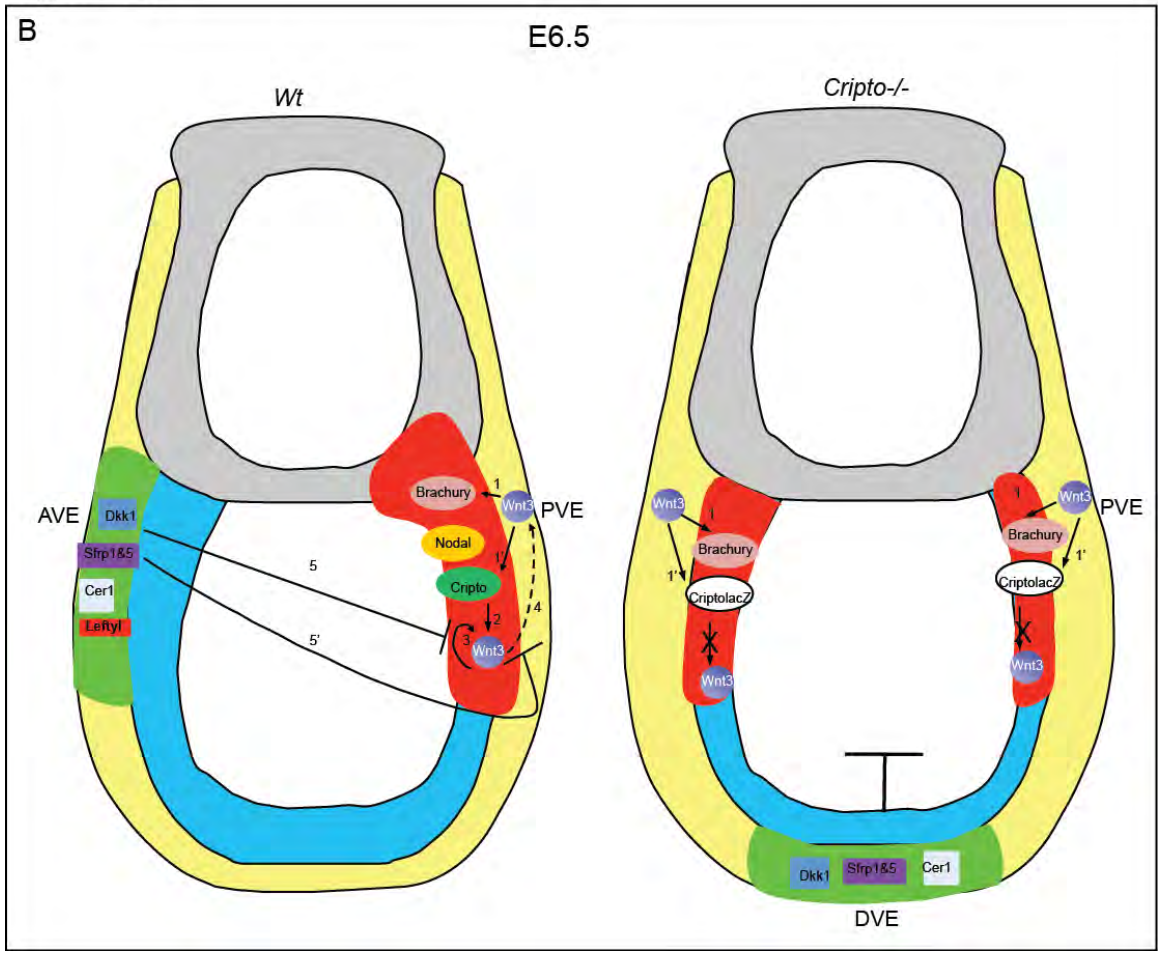
B
E6.5
Wt
Cripto-/-
AVE
Dkk1
Sfrp1&5
Cer1
Lefty1
Brachury
Wnt3
Nodal
Cripto
PVE
1
1'
2
3
4
5
5'
Criptolacz
DVE

Figure 2.8. Proposed model to explain the signaling events that pattern the early mouse embryo. (**A**). Signaling events at E5.5 mouse embryos. In wild type embryos, nodal precursor protein (Nodal-P) is processed in the extraembryonic ectoderm (ExE) (step 1). Nodal signals from the epiblast to maintain the expression of Cripto (step 2), which in turn works with Nodal to activate the expression of *Lefty1* in the distal visceral endoderm cells (step 3). Cripto-independent-Nodal signaling also maintains the expression of some other genes (*Dkk1, Sfrp1&5, CerI)*, which are required to specify DVE cells (step 4). Canonical Wnts and Wnt antagonists (Dkk1) are repulsive and attractive guidance cues respectively for relocating the DVE cells to the prospective anterior side by active cell migration (step 5). In *Cripto-/-* mutant, Cripto-dependent Nodal signaling is disrupted, which leads to the absence of *Lefty-1* in the DVE cells. The DVE cells fail to shift to the future anterior side by unknown mechanisms. (**B**). Signaling events at E6.5 mouse embryos. In wild type embryos, Wnt3 emanating from the posterior visceral endoderm activates primitive streak markers (*Brachyury, Nodal* and *Cripto)* in the adjacent posterior epiblast (step1 and 1'). The expression of *Wnt3* in the epiblast is dependent on *Cripto* expression (step 2). The expression of *Wnt3* in the epiblast is magnified potentially through canonical Wnt signaling (step 3) and canonical Wnt signaling also signals to the posterior visceral endoderm to magnify Wnt signals (step 4). The expression of *Wnt3* is prevented from reaching the anterior epiblast by the AVE cells which express multiple antagonists of Wnt signaling to block *Wnt3*

expression in the epiblast (step 5) and visceral endoderm (step 5'). In *Cripto* mutants, the AVE remains at the tip of the epiblast allowing expansion of *Wnt3* expression to the anterior visceral endoderm where it induces primitive streak markers leading to radialization of the primitive streak (step 1 and 1'). Abbreviations: Epi, Epiblast; AVE, anterior visceral endoderm; PVE, posterior visceral endoderm; ExE, extra-embryonic ectoderm.

CHAPTER III:

ANALYSIS OF SENESCENCE-ASSOCIATED β-GALACTOSIDASE STAINING IN EARLY MOUSE EMBRYOS INDICATES ACIDIC β-GALACTOSIDASE ACTIVITY PRESENT IN APICAL VACUOLES OF VISCERAL ENDODERM CELLS

Preface

The work shown in this chapter forms part of the article "**Senescence-associated β-galactosidase staining in early mouse embryos indicates acidic β-galactosidase activity present in apical vacuoles of visceral endoderm cells**". This paper is currently in press in the journal *Genesis*. Most of the work described here was designed by Jaime Rivera and Tingting Huang and all the work was conducted by Tingting Huang.

Abstract

Senescence-associated β-galactosidase (SA-β-gal) staining is widely used as a marker of cellular senescence and has been suggested to be an indicator of organismal aging. Here we conduct an analysis of SA-β-gal activity in early post-implantation mouse embryos and show that SA-β-gal staining marks the visceral endoderm, an extra-embryonic tissue, in predictable patterns that change as the embryo develops. However, both of the analysis of the cell proliferation in visceral endoderm and the whole mount *in situ* hybridization studies for analyzing the expression of *Cdkn1a* (p21), a marker of senescent cells, do not support the conclusion that the cellular senescence is occurring in the visceral endoderm at early post-implantation embryos. Detection of SA-β-gal activity and endocytotic labeling was conducted using a fluorescent β-galactosidase substrate in cultured embryos in the presence of rhodamine dextran. My results revealed the presence of SA-β-gal activity in apical vacuoles indicating the presence of acidic β-galactosidase. Taken together, our results show that in early mouse embryos SA-β-gal staining indicates acidic β-galactosidase activity in apical vacuoles of visceral endoderm cells. Previous studies have shown that SA-β-gal staining reflects the activity of lysosomal β-galactosidase in senescent cells, which might be the case in visceral endoderm cells since apical vacuoles are organelles with lysosomal activity.

Introduction

Normal somatic cells do not proliferate indefinitely in culture. At the end of their limited replicative lifespan, they enter a permanent growth arrest of cell division by a process termed cell senescence (Hayflick and Moorhead, 1961; Campisi and d'Adda di Fagagna, 2007). Some characteristics of senescent cells include an increase in cell size (Simons, 1967; Bowman et al., 1975; Meek et al., 1977; Schneider et al., 1977), growth arrest typical at G1-phase (Di Leonardo et al., 1994; Ogryzko et al., 1996; Serrano et al., 1997; Herbig et al., 2004) and apoptosis resistance (Campisi and d'Adda di Fagagna, 2007). Senescent cells also show altered gene expression, including increased expression of the Cdk inhibitor proteins p21 (*Cdkn1a*) and p16 (*Cdkn2a*) (Campisi, 2001), which function in parallel signaling pathways to maintain senescence growth arrest (Campisi, 2001; Espinosa et al., 2003; Ben-Porath and Weinberg, 2005; Jackson and Pereira-Smith, 2006).

The first and also the most extensively used biomarker of senescent cells is SA-β-gal staining (Dimri et al., 1995; Lee et al., 2006; Campisi and d'Adda di Fagagna, 2007). SA-β-gal activity is typically measured by *in situ* staining under acidic conditions using a chromogenic substrate. During an experiment designed to ectopically induce senescence in transgenic mouse embryos, we noticed that wild-type control embryos assayed for SA-β-gal activity developed staining in the visceral endoderm, an extra embryonic component of the developing conceptus.

This observation prompted us to expand these studies and explore the pattern of acidic β-gal activity in early post-implantation embryos.

A systematic analysis of embryos dissected at stages spanning embryonic days 5.5 and 9.5 (E5.5 –E9.5) revealed that SA-β-gal activity marks the visceral endoderm in predictable patterns that vary as the embryo progresses in development. This activity was first observed in the whole visceral endoderm layer of embryos at E5.5, approximately one day before the appearance of the primitive streak. After that, it was gradually restricted to extra-embryonic regions of the conceptus and by primitive streak stages it marked the extra embryonic and posterior visceral endoderm. Later, at gastrulation stages and during early organogenesis, SA-β-gal activity was detectable solely in the visceral yolk sac. Determination of the mitotic index of visceral endoderm cells using phospho-Histone H3 immunostaining and analysis of the expression of *Cdkn1a* (p21), a marker of senescent cells, did not reveal evidence of senescence in visceral endoderm cells. Instead they showed that visceral endoderm cells are actively proliferating. Moreover, we detected expression of *Cdkn1a* in the primitive streak, a region of high cellular proliferation, which is intriguing since p21 is a cell cycle negative regulator and normally associated with cellular senescence and apoptosis. Analysis of embryos cocultured with rhodamine dextran to mark endocytotic vesicles in combination with fluorescent SA-β-gal staining, revealed the presence of SA-β-gal activity in apical vacuoles an organelle that has lysosomal activity. From these studies, we conclude that the SA-β-gal activity

observed in visceral endoderm cells is not related to senescence but likely represents acidic β-galactosidase activity present in apical vacuoles and associated with the nutritional function of visceral endoderm at early post-implantation stages.

Replicative senescence

As Hayflick described in 1965, cellular senescence is encountered when cultured cells enter into a permanent cell cycle arrest at the end of their replicative life span (Hayflick, 1965). The classic experiment was done in human fibroblast cells. The human fibroblasts divide quickly at first multiple generations, then gradually lose the ability to proliferate. However, the non-dividing cells do not die for long time, and fail to proliferate even with sufficient living resources.

The study of the mechanism of cellular senescence contributes to the study of cancer research. The first indication of senescence being an anti-tumor mechanism came from the observation that the merge of an immortal cell and a normal cell give rise to a cell undergoing senescence, indicating senescence could be a potential therapeutic medical treatment for cancer (Smith and Pereira-Smith, 1996). Cellular senescence is also relevant to the regenerative medicine research since senescence is proposed as a process of recapitulating the process of aging *in vivo*. The loss of regenerative abitity of the tissues and the accumulation of senescent cells are always associated with aging process (Campisi and d'Adda di Fagagna, 2007).

Human adult fibroblast cells show enlarged cell size after the primary cells undergo senescence, sometimes increasing in size more than two-fold relative to the non-senescent counterparts (Hayflick, 1965; Simons, 1967). In addition, senescent cells show different characteristics from quiescent cells, which can reverse the growth cycyle arrest by resuming cell proliferation after spending long time intervals. However, senescent cells cannot reverse the permanent cell cycle arrest and start cycling (Campisi and d'Adda di Fagagna, 2007). Senescent cells also show high-level autofluorescence due to the accumulation of lipofuscin in lysosomal compartment, which could be detected by fluorescence/confocal microscopy (von Zglinicki et al., 1995; Hohn et al., 2010). Senescent cells also show altered gene expression, including increased expression of the Cdk inhibitor proteins p21 (*Cdkn1a*) and p16 (*Cdkn2a*) (Campisi, 2001), which function in parallel signaling pathways to maintain senescence growth arrest (Campisi, 2001; Espinosa et al., 2003; Ben-Porath and Weinberg, 2005; Jackson and Pereira-Smith, 2006)

Senescence can be induced by multiple stimuli. Aging cells are normally associated with the end-replication problem due to the dysfunctional telomeres, which trigger a DNA damage response (DDR) to induce senescence (Hemann et al., 2000; Martens et al., 2000; Gire et al., 2004). DNA damage, which creates DSBs, also trigger many cell types to undergo senescence (Di Leonardo et al., 1994; Parrinello et al., 2003). Both dysfunctional telomeres and DDR trigger senescence through p53-dependent pathway via p21 (Campisi and d'Adda di

Fagagna, 2007). The senescence phenotype can also be induced by other triggers, such as oxidative stress, oncogene activity, improper cell contacts and lack of nutrients/growth factors (Campisi and d'Adda di Fagagna, 2007).

Multiple stimuli converge on two major signaling pathways to induce senescence. Tumor suppressor proteins, p53 and Rb, play critical roles in the induction of senescence. Senescence-inducing signals activate p53, which in turn inactivate Rb to lead to the senescence growth arrest via p21 protein, an inhibitor of cyclin E/Cdk2 complexes. Senescence-inducing signals also activate the p16–pRB pathway by inducing the expression of p16, another CDK inhibitor that prevents pRB phosphorylation and inactivation. pRB promote cell senescence state by reducing the activity of E2F, a transcription factor that stimulates cell senescence (Ben-Porath and Weinberg, 2005; Campisi and d'Adda di Fagagna, 2007).

Markers of Replicative senescence

There are no exclusive markers for senescence. The senescence-associated molecules, such as p53, p21 and p16 are not specific to the senescent state. As a master regulator, p53 regulates the cell cycle and is invoved in many other cellular biological responses beside for senescence, such as cell proliferation and apoptosis (Farnebo et al., 2010). p16, an important regulator of senescence, is upregulated in many senescent cells, however, it is also upregulated in some tumor and apoptic cells (Al-Mohanna et al., 2004; Gil

and Peters, 2006). p21, which is upregulated in many senescence cells, is also involved in apoptosis beside cellular senescence (Gartel and Tyner, 2002; Al-Mohanna et al., 2004).

Senescence cells always show lack of DNA replication (Campisi and d'Adda di Fagagna, 2007). This characteristic can be usually detected by the incorporation of bromodeoxyuridine (BrdU) (Konishi et al., 2011). Another good marker to show lack of DNA replication is to immunostain for proteins such as PCNA, Ki-67 or phospho-histone H3 (Leonardi et al., 1992; Wei et al., 1999). However, this feature can not distinguish between senescent cells and quiescent cells. Some other senescent makers include senescence-associated secretory phenotype (SASP), senescence-associated heterochromatin foci (SAHF), DNA scars, γ-H2AX and etc (reviewed by (Campisi and d'Adda di Fagagna, 2007).

The most extensively used biomarker of senescent cells is SA-β-gal staining, which is detected at ph 6.0 cytochemically using a chromgenic substrate or by the use of 5-dodecanoylaminofluorescein di-β-D-galactopyranoside (C12FDG), a fluorogenic substrate for βgal activity, based on the alkalinization of lysosomes (Dimri et al., 1995; Debacq-Chainiaux et al., 2009). The quiescent cells do not develop positive staining SA-β-gal staining, making it a more specific way for senescent cells (Dimri et al., 1995). SA-β-gal staining comes from the accumulation of lysosomal residue during the process of cells undergoing senescence (Kurz et al., 2000).

The significance of senescence *in vivo*

Most of the senescence studies have been conducted in in vitro cell culture. Recently, animal models of ageing and human genetic diseases showed cellular senescence occurs and play an important role in age-related pathologies in vivo This is also supported by the study showing removal of $p16^{Ink4a}$-expressing senescent cells can postpone tissue dysfunction and extend health life, suggesting (Erusalimsky and Kurz, 2005; Campisi and d'Adda di Fagagna, 2007; Baker et al., 2011).

Senescence is a mechanism, which almost exists in all animals, except for the *hydra*, a kind of fresh-water animal that show radial symmetry and can consistently renew the body tissues (Martinez, 1998). In mice and humans, senescent cells accumulate more abundantly in old animals (Dimri et al., 1995; Erusalimsky and Kurz, 2005). An good explanation for this phenomenan is that senescence is programmed in order to limit population size or accelerate the turnover of generations (Kirkwood and Austad, 2000).

Senescence also contributes to normal somatic tissue repair (Campisi and d'Adda di Fagagna, 2007). Adult stem cells are central to tissue and organ regeneration process, as they maintain in the stem cell niche and retain the self–renew capability all the time and produce new cells to replace the old and damaged ones. The number of the cells in the stem cell niche marked by one or several senescence markers is increased with age, and the regenerative capacity of stem cells and their daughter cells appears to decrease during aging,

which suggests the senescence in old animals potentially cause the age-related functional decline of many tissues (Dimri et al., 1995).

Senescence is a important anti-tumor mechanism since it permanently arrests the cell cycle and stops cell proliferation (Campisi and d'Adda di Fagagna, 2007). Most stressers which induce senescence, such as oncogenes, are also be able to initiate the tumor formation (Campisi and d'Adda di Fagagna, 2007; Zhang, 2007). Also, the two major regulators for senescence, the p53 and pRB, are also tumor suppressors (Rodier and Campisi, 2011). In addition, cellular senescence is related to tumor regression in some tumor cell types, making it a very good therapeutic way for cancer treatments (Shay and Roninson, 2004). However, the role of cellular senescence in carcinogenesis could be beneficial or harmful depending on the age of the animal (Shay and Roninson, 2004).

Senescent cells are mostly associated with pathological situations, such as in tumor and ageing tissues (Campisi and d'Adda di Fagagna, 2007). The senescent cells are also found to accumulate in stellate cells during liver fibrosis and wound healing response in skin injury (Krizhanovsky et al., 2008; Jun and Lau, 2010). However, since most studies for senescence have been conducted in stress response situations, whether senescence cells are present during physiological circumstances remain unclear. Moreover, SA-β-gal activity is found in old quail mesonephros (Nacher et al., 2006). Two very recent studies surprisingly showed the senescent cells accumulate in inner ear, degenerating mesonepheric tubules and also apical ectodermal ridge during limb development

in murine embryogenesis, suggesting senescence, like apoptosis, is a fundamental mechanism to fine-tune the tissue and organ structures in early development (Munoz-Espin et al., 2013; Storer et al., 2013). Although senescence has been reported in renal and limb formation, its existence, if any during early post-implantation stages remains unknown.

Visceral yolk sac and microautophagy

Absence of the visceral yolk sac (VYS) leads to the miscarriage of human pregnancy, suggesting the VYS is essential for survival of human embryo during early development (Exalto, 1995). Human visceral yolk sac, a microvilli-covered structure, develops before the emergence of the blood flow via the placenta, and mainly plays a role for embryo nutrition through endocytosis (Zohn and Sarkar, 2010). In mice, like the endodermal-derived epithelial layer of the human VYS, the apical surface of visceral endoderm is also covered with microvilli and endocytotic machinery apparatus (Bielinska et al., 1999). As development proceeds, the visceral endoderm contributes to the endoderm epithelial layer of the VYS (Bielinska et al., 1999). Several mouse mutants, such as *hepatic nuclear factor 4-alpha* (*Hnf4*α*)* and *rab7 (rab7)*, show the initiation of A-P axis formation, however, are unable to absorb maternal nutrients and die around gastrulation (Chen et al., 1994; Kawamura et al., 2012).

The visceral endoderm can actively internalize the maternal nutrients into the cytoplasm through an endocytotic mechanism, which has been shown by

electron microscopy and immunohistochemistry studies (Wada et al., 2013). In mouse embryo, the lysosome-like organelle in visceral endoderm accumulates in the apical side and exhibits a multiple-arm structure, named the apical vacuole. The apical vacuole is a special form of lysosome in the VE, which is similar to lysosomes by exhibiting lysosome-associated member proteins, proteinase and enriched endocytotic markers (Wada et al., 2013). The delivery of early endosome to the apical vacuoles is via a microautophagy mechanism, a process by which the endosomes are engulfed into the apical vacuoles with double membranes, unlike the canonical lysosomal fusion, in which endosomes delivery to the lysosomes and form a continuous layer of memberane (Mijaljica et al., 2011; Kawamura et al., 2012) (Figure. 3.1).

Here I hypothezed the SA-β-gal activity in the visceral endoderm is derived from the lysosmal activity in the apical vacuole rather than linked to senescence.

Figure 3.1

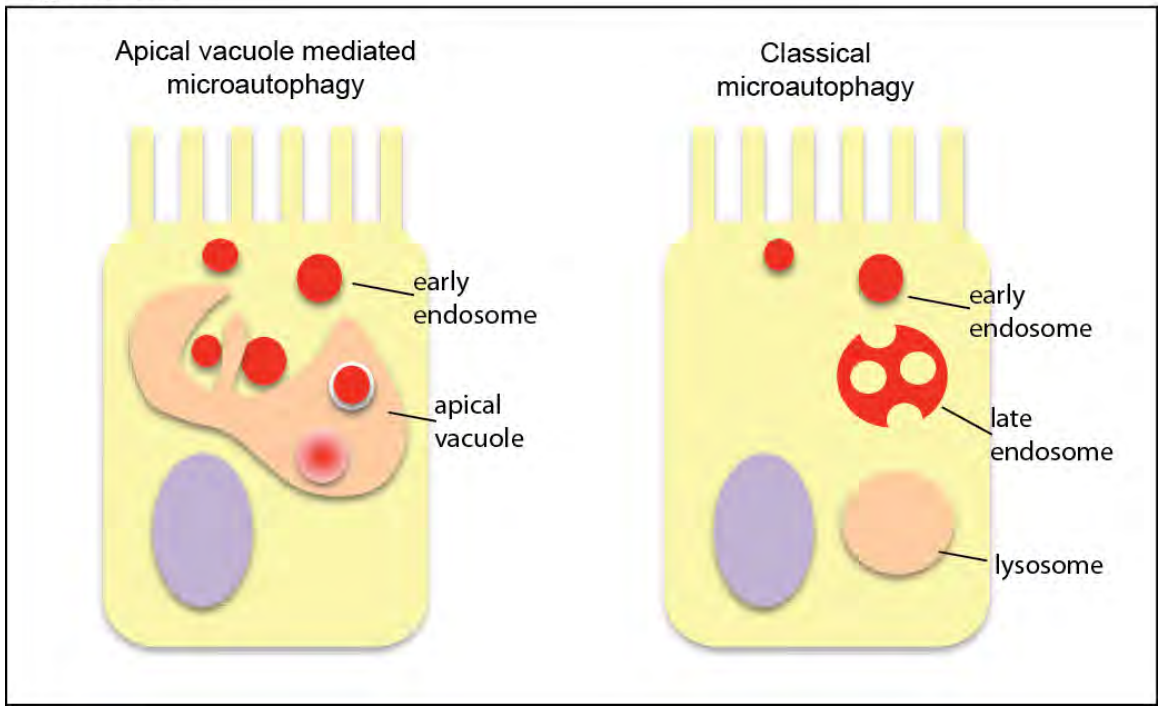
Apical vacuole mediated microautophagy
early endosome
apical vacuole
Classical microautophagy
early endosome
late endosome
lysosome

Figure.3.1 (A). A schematic model of apical vacuole mediated microautophagy in the visceral endoderm at early post-implantation mouse embryos. The VE cells contain large apical vacuoles, which is a multivesicular lysosomes, sharing several characteristics with lysosomes. **(B). A schematic model of classical microautophagy.** This figure is adapted from the figure 1 in the paper (Wada et al., 2013).

Results

SA-β-gal staining marks the visceral endoderm

To study the prevalence of SA-β-gal activity during early mouse embryogenesis, we characterize the spatial and temporal patterns of SA-β-gal activity in early mouse embryos, we dissected embryos at stages between E5.5 and E9.5 and subjected them to β-galactosidase assays at pH 6.0, the standard senescence assay. A systematic analysis of embryos revealed that SA-β-gal activity marks the visceral endoderm in predictable patterns that vary as the embryo progresses in development. DVE stage embryos dissected at E5.5 (n=10) showed widespread visceral endoderm staining that included both the embryonic and the extra-embryonic visceral endoderm. The epibast and extra-embryonic ectoderm were completely devoid of staining (Figure.3.2A).

At E6.5, coincident with the appearance of the primitive streak, acidic β-galactosidase staining marked only the extra-embryonic and posterior visceral endoderm with no labeled cells detected overlaying the rest of the epiblast region (n= 25) (Figure.3.2B). The staining in the posterior visceral endoderm region covered about one third to one half of the length of the epiblast and tapered anteriorly around the circumference of the embryo along the epiblast/extra-embryonic ectoderm boundary. The epiblast and extra-embryonic ectoderm remained clear of staining (Figure.3.2B).

At E7.5, acidic β-galactosidase-positive visceral endoderm cells were confined to the extra-embryonic region (n= 32) (Figure.3.3A - C). The area of staining extended over the sides of the embryo but was excluded from the posterior region of the embryo (Figure.3.3B, C). At later stages, acidic β-galactosidase staining was restricted to the visceral yolk sac in embryos dissected at E8.5 (n= 5, not shown) and E9.5 (n= 8) (Figure.3.4). At 21 to 27 somite stages (E9.5), acidic β-gal staining was also detected within the liver primordium while the rest of the embryo was completely devoid of staining (Figure. 3.4).

In summary, SA-β-gal activity initially marks the whole visceral endoderm of early post implantation embryos but as development progresses it becomes restricted to the extra embryonic and posterior visceral endoderm and later is limited to the visceral endoderm layer of the visceral yolk sac.

Figure 3.2

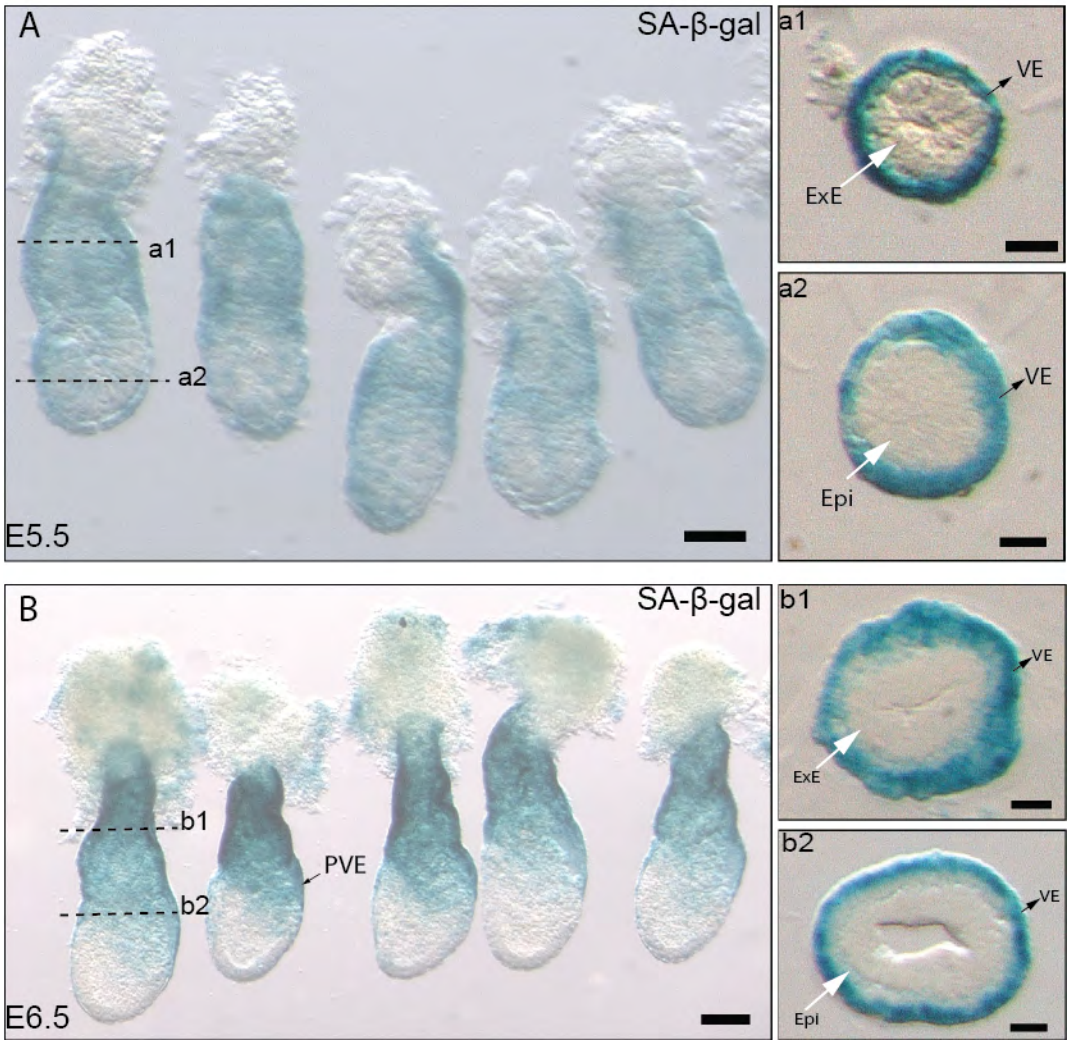
A
SA-β-gal
a1
a2
E5.5
a1
VE
ExE
a2
VE
Epi
B
SA-β-gal
b1
b2
PVE
E6.5
b1
VE
ExE
b2
VE
Epi

Figure 3.2. SA-β-gal activity marks the visceral endoderm of early post-implantation mouse embryos. A. Pattern of SA-β-gal staining in embryos dissected at E5.5. SA-β-gal staining marks the whole visceral endoderm. **B.** Pattern of SA-β-gal staining in embryos dissected at E6.5. At E6.5, the staining is restricted to the extra-embryonic and posterior visceral endoderm. The dotted lines represent the approximate level of the sections shown in (**a1, a2, b1, b2**). VE, visceral endoderm; ExE, Extra-embryonic ectoderm; PVE, posterior visceral endoderm; Epi, Epiblast. Scale bars: A, 50 µm; B, 100 µm; a1, a2, b1, b2: 20 µm.

Figure 3.3

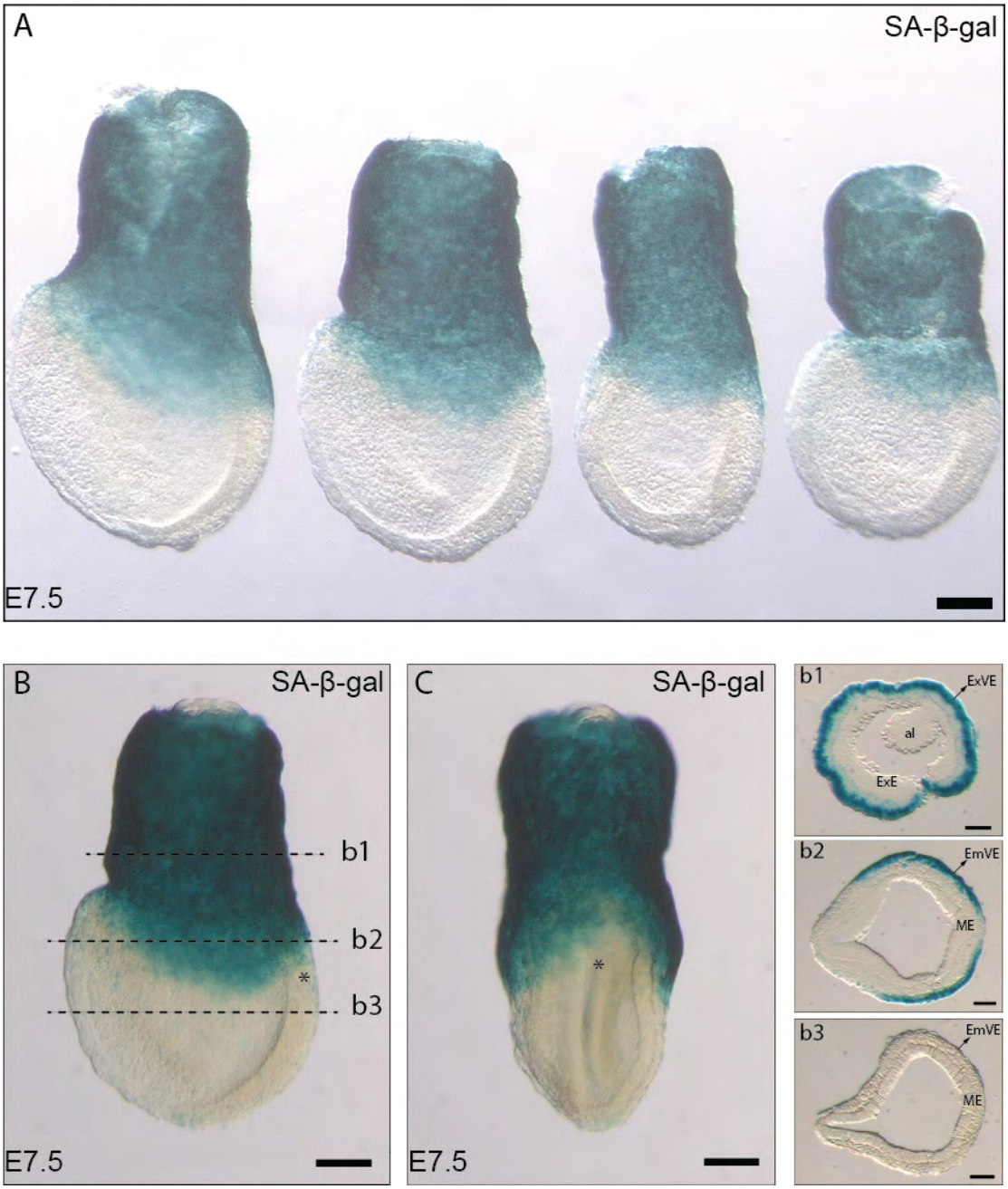
A
SA-β-gal
E7.5
B
SA-β-gal
b1
b2
b3
*
E7.5
C
SA-β-gal
*
E7.5
b1
ExVE
al
ExE
b2
EmVE
ME
b3
EmVE
ME

Figure 3.3. Pattern of SA-β-gal staining in embryos dissected at E7.5. A. In E7.5 embryos SA-b-gal activity is confined to the extra-embryonic visceral endoderm. **B, C**. Side (D) and posterior (E) views of the same E7.5 illustrate the lack of staining in the posterior visceral endoderm (marked by asterisks). The dotted lines represent the approximate level of the sections shown in (b1-b3). ExVE, extra-embryonic visceral endoderm; ExE, extra-embryonic ectoderm; al, allantois; EmVE, embryonic visceral endoderm; ExM, extra-embryonic mesoderm; ME, Mesendoderm. Scale bars: C, D, E, 100 µm; d1, d2, d3: 20 µm.

Figure 3.4

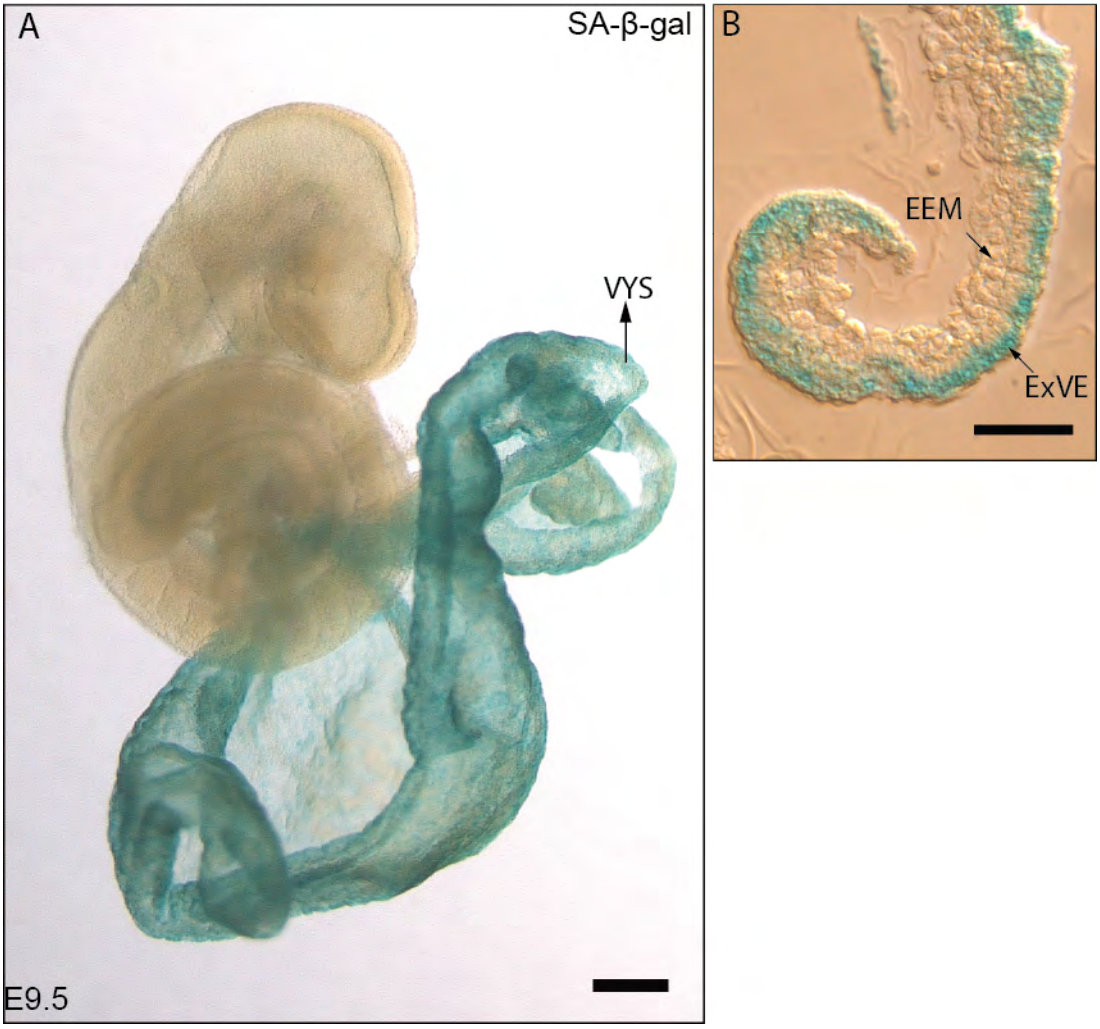

Figure 3.4. Pattern of SA-β-gal staining in embryos dissected in E9.5. A. SA-β-gal positive cells are restricted to the visceral yolk sac**. B.** Cross section of the visceral yolk sac showing that SA-β-gal staining is restricted to the visceral endoderm layer. VYS, visceral yolk sac. Scale bars: 250 µm in A and 50 µm in B.

SA-β-gal activity visceral endoderm cells are not senescent cells.

Senescent cells usually lack of DNA replication (Di Leonardo et al., 1994; Ogryzko et al., 1996; Serrano et al., 1997; Herbig et al., 2004), therefore, we assessed the proliferative status of visceral endoderm cells in E6.5 embryos using antibodies against Ki67, a general marker of proliferating cells but not quiescent cells (Wei et al., 1999; Chenn and Walsh, 2002). At E6.5, immunoreactive Ki67 (n=5) proteins were observed extensively in epiblast cells coincidental with the appearance of the primitive streak. There were also indeed Ki67 positive cells in the visceral endoderm layer of the conceptus, both in extraembryonic and embryonic region (Figure.3.5A - D).

Next, we immunostained embryos dissected at E6.5 by using phospho-histone H3 antibody (Figure.3.6). Phospho-Histone H3 is a specific marker for cells in mitotic metaphase that detects Ser-10 phosphorylation of histone. The mitotic index was calculated individually in extraembryonic and embryonic visceral endoderm compartments. The ratio between the number of cells in mitosis and the total number of cells in the extra-embryonic visceral endoderm is 2.06% while the ratio is 3.02% in the embryonic visceral endoderm (Figure.3.6C). The mitotic index for the epiblast is 10% at E6.5 embryos. The cells marked by phospho histone H3 were distributed randomly in the visceral endoderm (Figure.3.6B). These results indicate that visceral endoderm cells are actively cycling and contrast with the expected G1 arrest characteristic of senescent cells.

P21 is a cell cycle negative regulator that acts by inhibiting cyclineE/cdk2

Figure 3.5

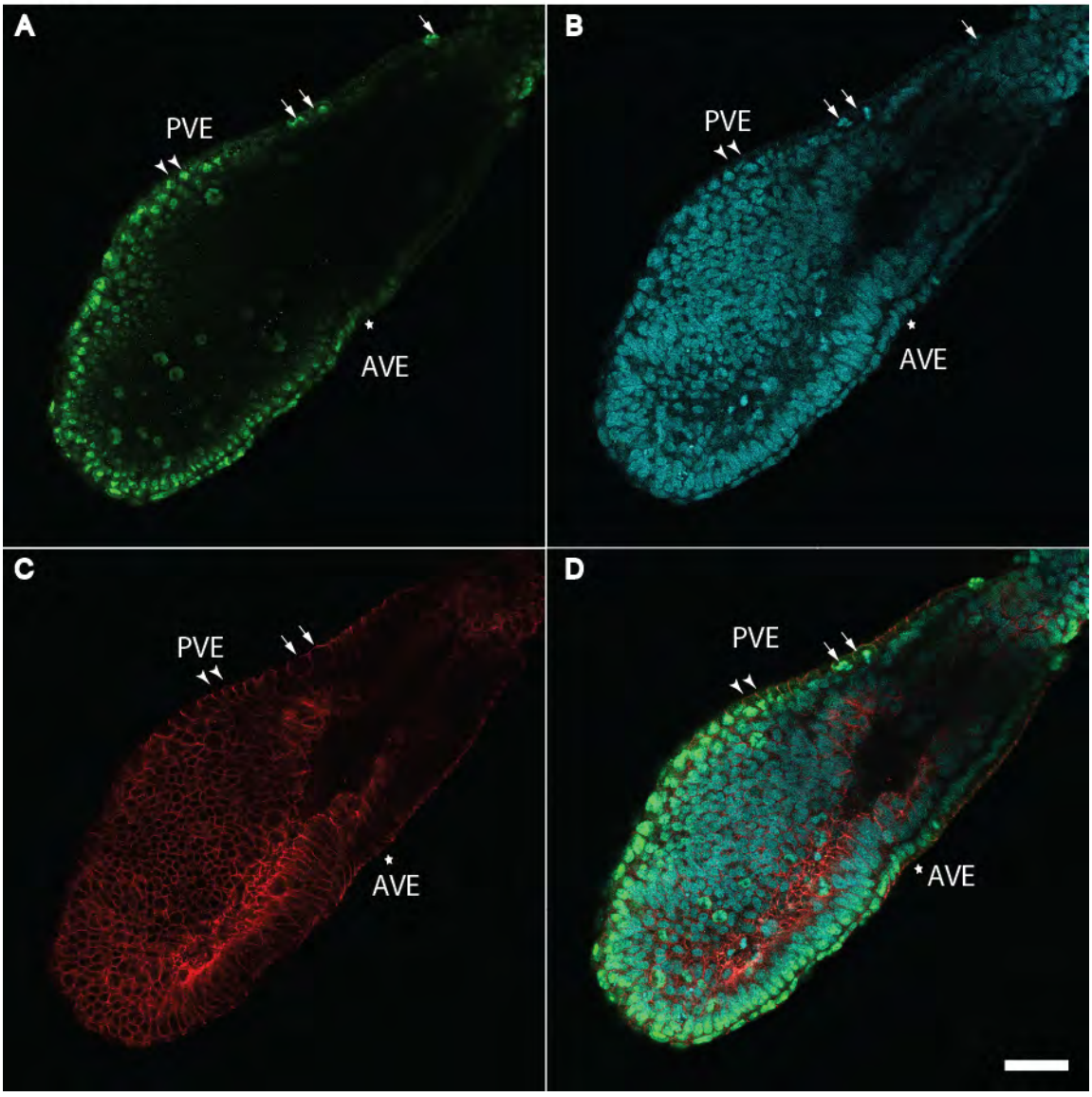

Figure 3. 5. Confocal analysis of cell proliferation in the visceral endoderm of E6.5 embryos using Ki-67 immunostaining . A. Staining for Ki67 to reveal cycling cells (green). The Ki67-stained nuclei are visible in the posterior visceral endoderm (arrowheads) and extra-embryonic visceral endoderm regions (arrows). **B.** Draq5 staining to reveal nuclei (blue). **C.** Immunostaining for E-Cadherin to reveal cell-cell boundaries (red). **D.** Merge of the three channels.. The asterisk represents anterior visceral endoderm. Scale bar: 50 μm.

Figure 3.6

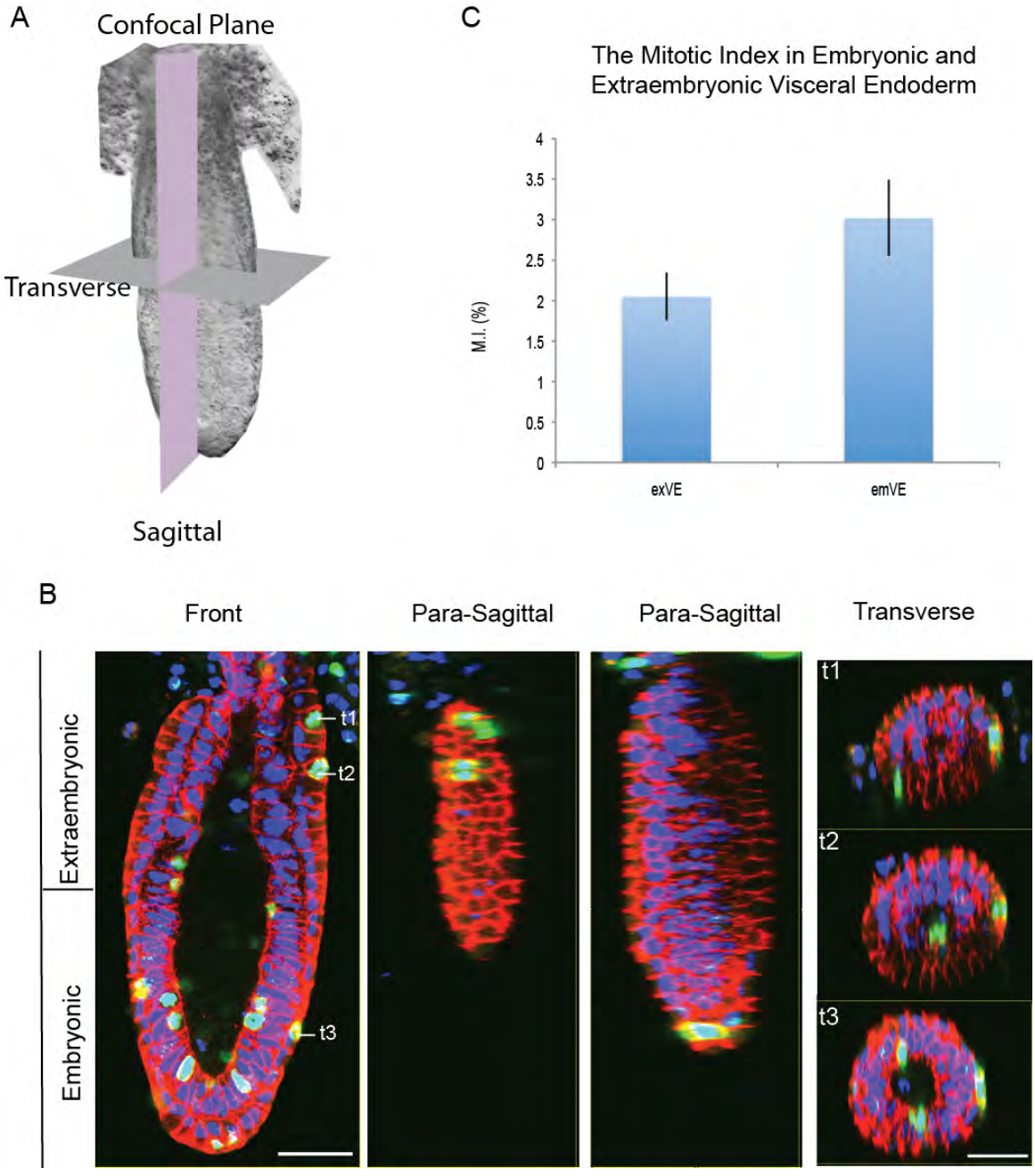
A
Confocal Plane
Transverse
Sagittal
C
The Mitotic Index in Embryonic and Extraembryonic Visceral Endoderm
M.I. (%)
4
3.5
3
2.5
2
1.5
1
0.5
0
exVE
emVE
B
Front
Para-Sagittal
Para-Sagittal
Transverse
Extraembryonic
Embryonic
t1
t2
t3
t1
t2
t3

Figure 3.6. Determination of the visceral endoderm mitotic index. A. Confocal optical planes in sagittal (pink) or transverse (grey) orientations. **B.** Wild-type E6.5 embryos were stained for phosphor-histone H3 (green), E cadherin (red) and DAPI (blue). Serial optical sections of whole mounted embryos were viewed under a laser confocal microscope. Sagittal,parasagittal and transverse focal planes are shown. Transverse sections (t1 – t3) were reconstituted from the serial optical sections. The approximate positions of extra-embryonic (t1 and t2) and embryonic (t3) sections are indicated. **C.** Quantification of the mitotic index in the extra-embryonic visceral endoderm and embryonic visceral endoderm. Scale bars indicate 50 μm. Abbreviations: ExVE, extra-embryonic visceral endoderm; EmVE, embryonic visceral endoderm.

complex. During senescence, expression of p21 has been shown to be upregulated by the tumor suppressor p53 in response to DNA-damage agents (Macleod et al., 1995). We stained E6.5 embryos using a p21 antibody and observed that the extra-embryonic and posterior visceral endoderm were positive for p21 antibody immunostaining, which are the same regions marked by SA-β gal staining (Figure.3.8). These results suggested that senescence is present in VE cells, however, they are inconsistent with the nature of the yolk sac that has to expand to encapsulate the growing embryo and also the proliferation analysis data.

To gain further evidence to support these results, we decided to look at the p21 mRNA expression pattern. Embryos were dissected at E6.5 and E7.5 and then lysed without cones to extract RNAs, which were reversely transcribed into cDNAs. The cDNAs were then used as templates to amplify a p21 fragment spanning over exon2 and exon3. The data showed the presence of p21 mRNA (Figure.3.7B). To confirm the immunostaining results obtained using p21 antibody, we conducted wholemount *in situ* hybridization using a p21 probe. p21 is encoded by the *Cdkn1a* gene. To determine the expression of *p21*, we used a 1,030 bp fragment of exon3 containing a 980 bp piece of 3'UTR (Figure.3.7A). We analyzed embryos dissected at E6.5 and E7.5. We did not detect expression at E6.5. At E6.5, we were not able to detect expression of Cdkn1a in any tissue of the conceptus (n= 5, not shown). At E7.5 (n=7), staining became apparent in the primitive streak region of embryos at early bud stages (Figure.3.7C). The

Figure 3.7

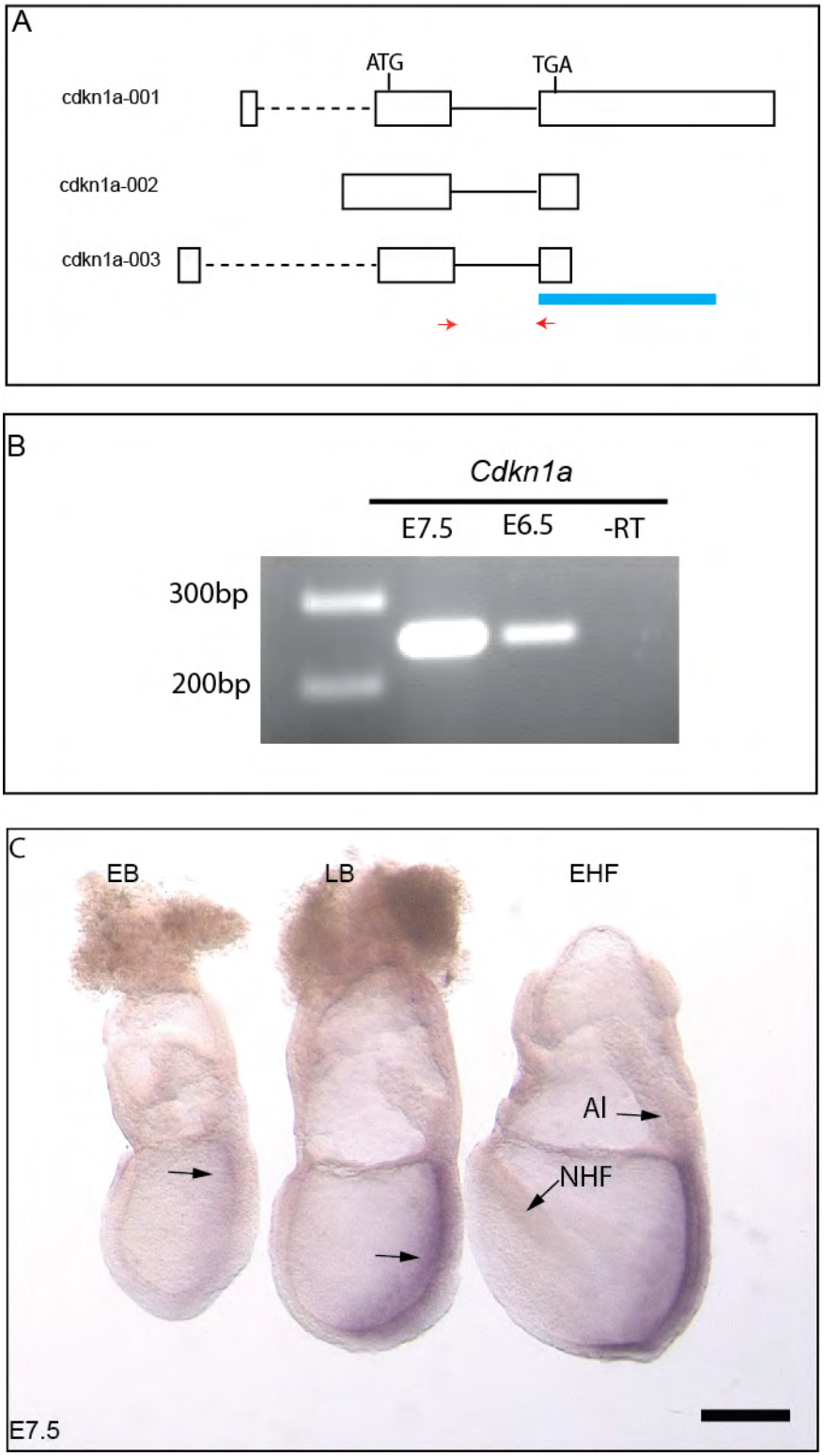
A
ATG
TGA
cdkn1a-001
cdkn1a-002
cdkn1a-003
B
Cdkn1a
E7.5
E6.5
-RT
300bp
200bp
C
EB
LB
EHF
AI
NHF
E7.5

Figure 3.7. Analysis of *Cdkn1a* (p21) expression in E7.5 embryos. A. Schematic representation of the *Cdkn1a* gene indicating the real time PCR primers and whole mount *in situ* probes used in this study. *Cdkn1a* have 3 transcripts which generate the same protein. *Cdkn1a* produces three transcripts. The blue bar indicates the location of the whole mount *in situ* probe used. Red arrows indicate the pair of RT-PCR primers used for RT-PCR. **B.** RT-PCR analysis for E6.5 and E 7.5 mouse embryos. **C.** Whole-mount *in situ* hybridization analysis in E7.5 embryos. *Cdkn1a* transcripts were present in the primitive streak (arrows). Scale bar: 200 µm. Abbreviations: EB, Early allantois bud stage; LB, Late allantois bud stage; EHF, Early headfolds stage; Al, allantois; NHF, neural head folds. Red arrows: the forward and reverse primers for RT-PCR.

Figure 3.8

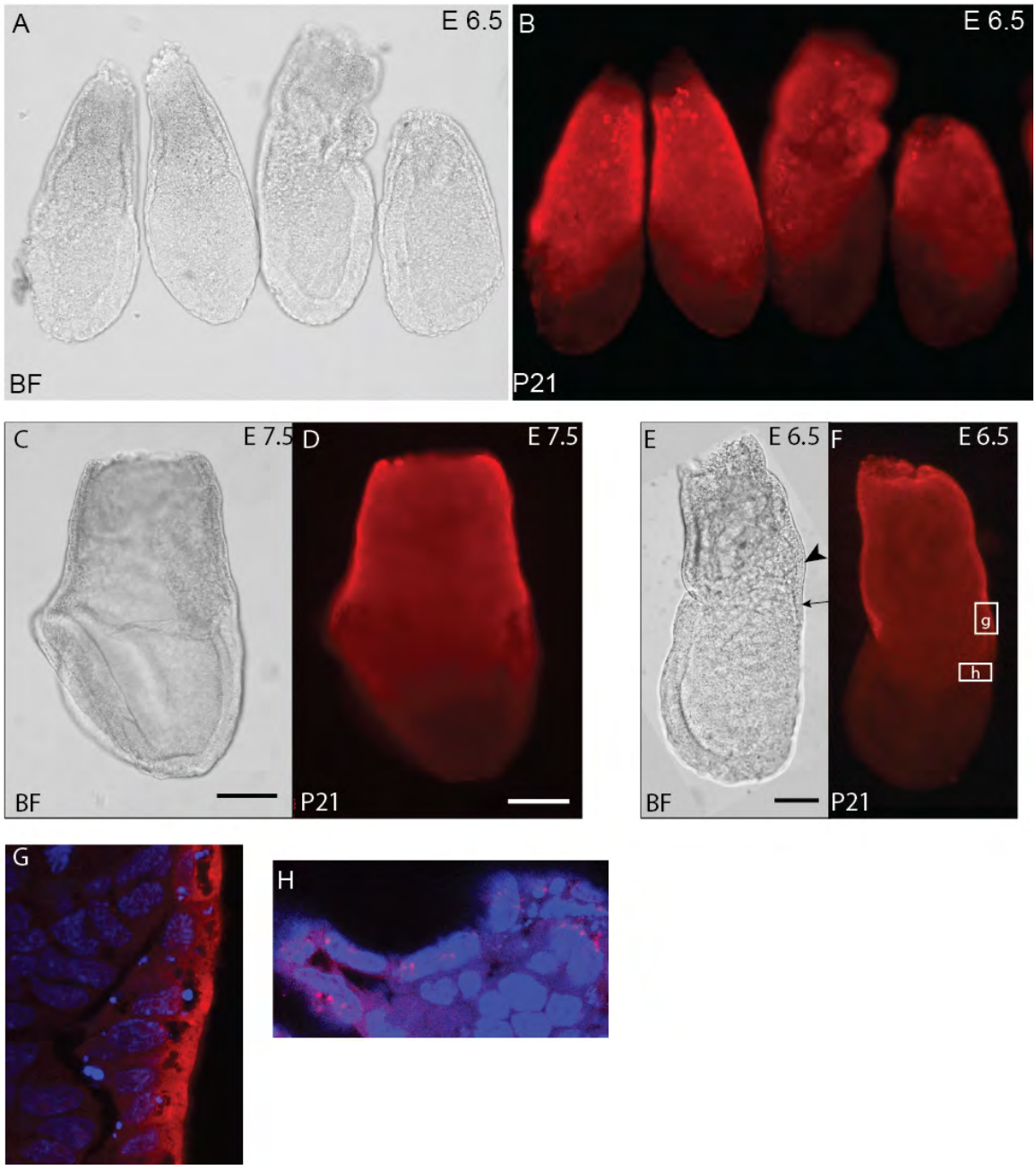

Figure 3.8. Immunostaining of early post-implantation embryos using an anti-p21 antibody. A, B. Immunohistochemistry using a mouse monoclonal antibody that detects all forms of p21 was performed in a litter of E6.5 embryos. Bright field (A) and fluorescence (B) views. **C, D.** P21 immunostaining (red) in E 7.5 embryos. **E, F.** E6.5 embryo showing approximate location of enlarged panels shown in **g** and **h**. **G, H:** Confocal study for different regions shown in (F). P21 is detected in the cytoplasm of visceral endoderm cells rather than in the nucleus (G). This staining likely represents an artifact that indicates maternal IgGs present in the visceral endoderm. In panel H, nuclear staining is observed at the base of the primitive streak. This pattern of staining is coincident with the pattern of expression of *Cdkn1a* which codes for p21. Scale bar: 200 µm in C and 100 µm in D. Arrow, posterior visceral endoderm; arrowhead, extra-embryonic visceral endoderm.

staining was mostly concentrated in the proximal region of the primitive streak. At a slightly later stage (late bud stage), the staining was clearly discernible along the entire length of the primitive streak region. This was also the case of embryos at early and late head fold stages. At these later stages, Cdkn1a expression was also evident in the epiblast layer of the node (Figure.3.7C). In neither case, however, we observed Cdkn1a expression in the visceral endoderm layer of the conceptus.

These results are not consistent with the p21 immunostaining data. Confocal microscopy analysis showed that the signal from the p21 immunostaining are not nuclearly located, suggesting it is not an active form of p21 (Figure.3.8E, F,G, H). All these led us to think that the immunostaining data might be an experimental artifact.

Taken all these results together, we conclude that visceral endoderm cells are not senescent cells. The question then shifted to understand what SA-β gal staining indicated in the visceral endoderm cells.

Detection of maternal Immunoglobins in the visceral endoderm

Previous studies have shown that the visceral endoderm cells internalize maternal components like transferrin, immunoglobulins (Ig), lipoproteins and albumins (Huxham and Beck, 1985; Ichimura et al., 1994; Assemat et al., 2005). Since the p21 antibodies were generated in mice, we suspected that the pattern of immunostaining observed in our immunostaining experiments reflected maternal immunoglobins present in the visceral endoderm. To determine if the visceral endoderm cell population that exhibited SA-β-gal activity corresponded to cells containing maternal IgGs, we conducted an immunostaining experiment using a goat anti mouse antibody conjugated with alexa 488.

Analysis of embryos dissected at E6.5 revealed maternal IgGs in the extra-embryonic and posterior visceral endoderm mimicking the pattern of staining observed in SA-β-gal assayed embryos (Figure.3.9A – C). As in the case of SA-β-gal embryos, the presence of IgGs was restricted to the apical surface of visceral endoderm cells (Figure.3.9D).

To address this question, we assayed mouse embryos using a secondary mouse anti IgG antibody. This resulted in the staining of extra-embryonic and posterior visceral endoderm, which exactly matched the p21 immunostaining results (Figure.3.9).

Therefore, the p21 immunostaining results are most likely the result of dectecting maternal immunoglobulins present in the visceral endoderm.

Figure 3.9

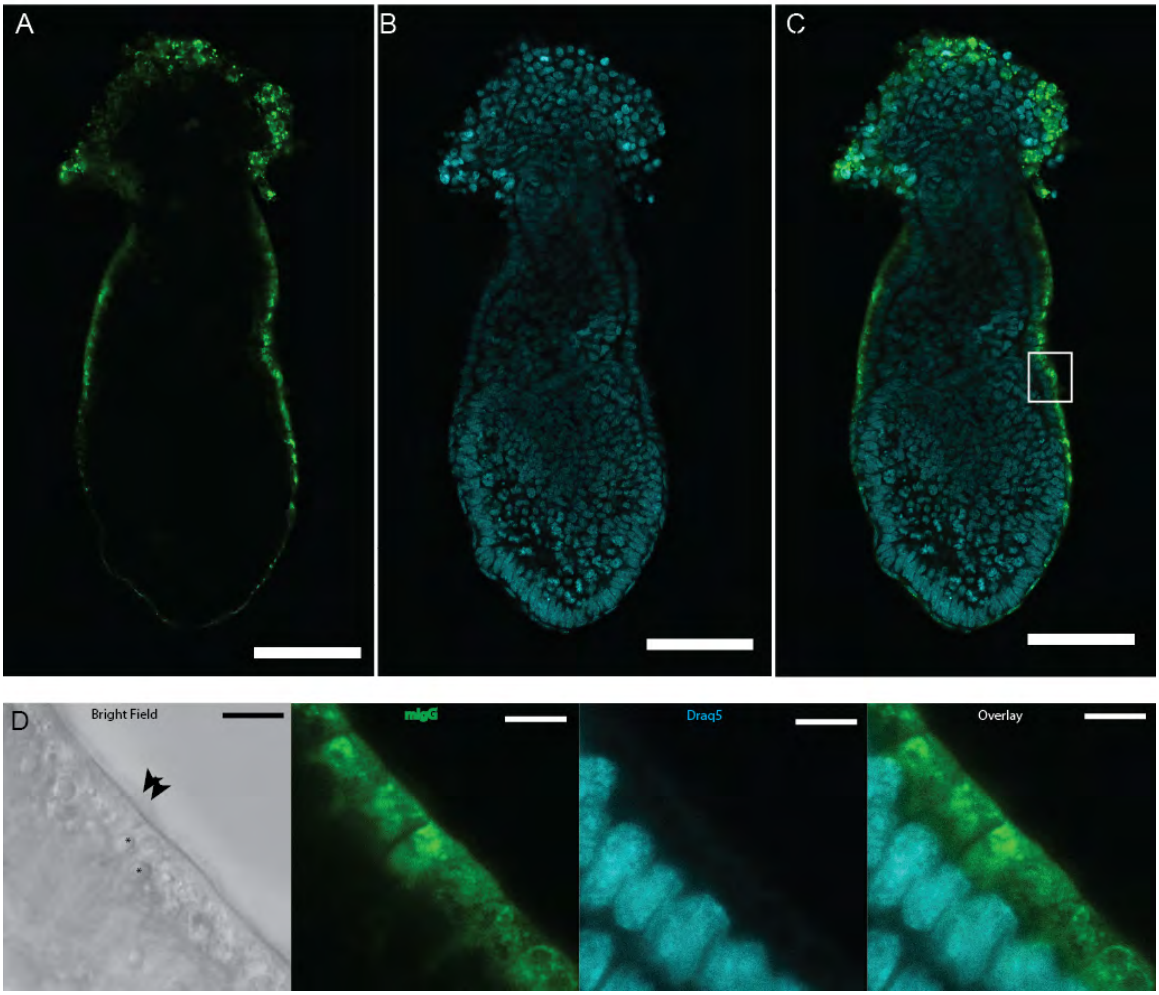

Figure 3. 9. Mouse embryos accumulate maternal IgGs in the apical side of the visceral endoderm. A-C. Detection of maternal IgGs in E6.5 embryos using a goat anti-mouse IgG antibody. The visceral endoderm, mainly the extra-embryonic and posterior visceral endoderm internalizes IgG from the maternal circulation through endocytosis. Panel A mouse IgG immunostaining (green). Panel B shows Draq5 staining to detect nuclei (cyan). Panel C is an overlay image of A and B. **D.** Magnification of the region marked with a square in panel (C). The internalized mouse IgGs are present in the apical side in the visceral endoderm. Arrows in D indicate microvilli present in visceral endoderm cells and the asterisks indicate apical vacuoles. Scale bars: 50 µm in A, B, C and 10 µm in D.

Visceral endoderm cells corresponded to acidic β-galactosidase activity present in apical vacuoles

The visceral endoderm is known to perform a nutritional role in early post-implantation embryos (Zohn and Sarkar, 2010). In addition, previous studies have shown that visceral endoderm cells capture maternal immunoglobins (Bernard et al., 1977). SA-β-gal activity marks apical vacuoles of visceral endoderm cells. The presence of SA-β-gal activity in visceral endoderm cells but absence of other senescence markers prompted us to investigate the origin of SA-β-gal staining in our embryos. Previous reports have suggested that the SA-β-gal assay reflects high lysosomal activity in senescent cells (Kurz et al., 2000). In addition, using human fibroblasts deficient for GLB1, the gene coding for lysosomal β-galactosidase, Lee and co-workers demonstrated that SA-β-gal staining reflects the activity of lysosomal β-galactosidase (Lee et al., 2006). Since the mouse visceral endoderm contains large apical vacuoles that exhibit lysosomal characteristics (Kawamura et al., 2012), we wondered if SA-β gal activity in the visceral endoderm cells was derived from lysosome activity linked to the nutritive role of the visceral endoderm cells. To investigate this possibility, we developed a technique to identify SA-β gal staining *in vivo* using a fluorogenic substrate for β-gal activity, (5-dodecanoylaminofluorescein di- β -D-galactopyranoside, C12FDG) (Figure.3.10). Our results revealed that the extra-embryonic visceral endoderm and posterior visceral endoderm were positive for

Figure 3.10

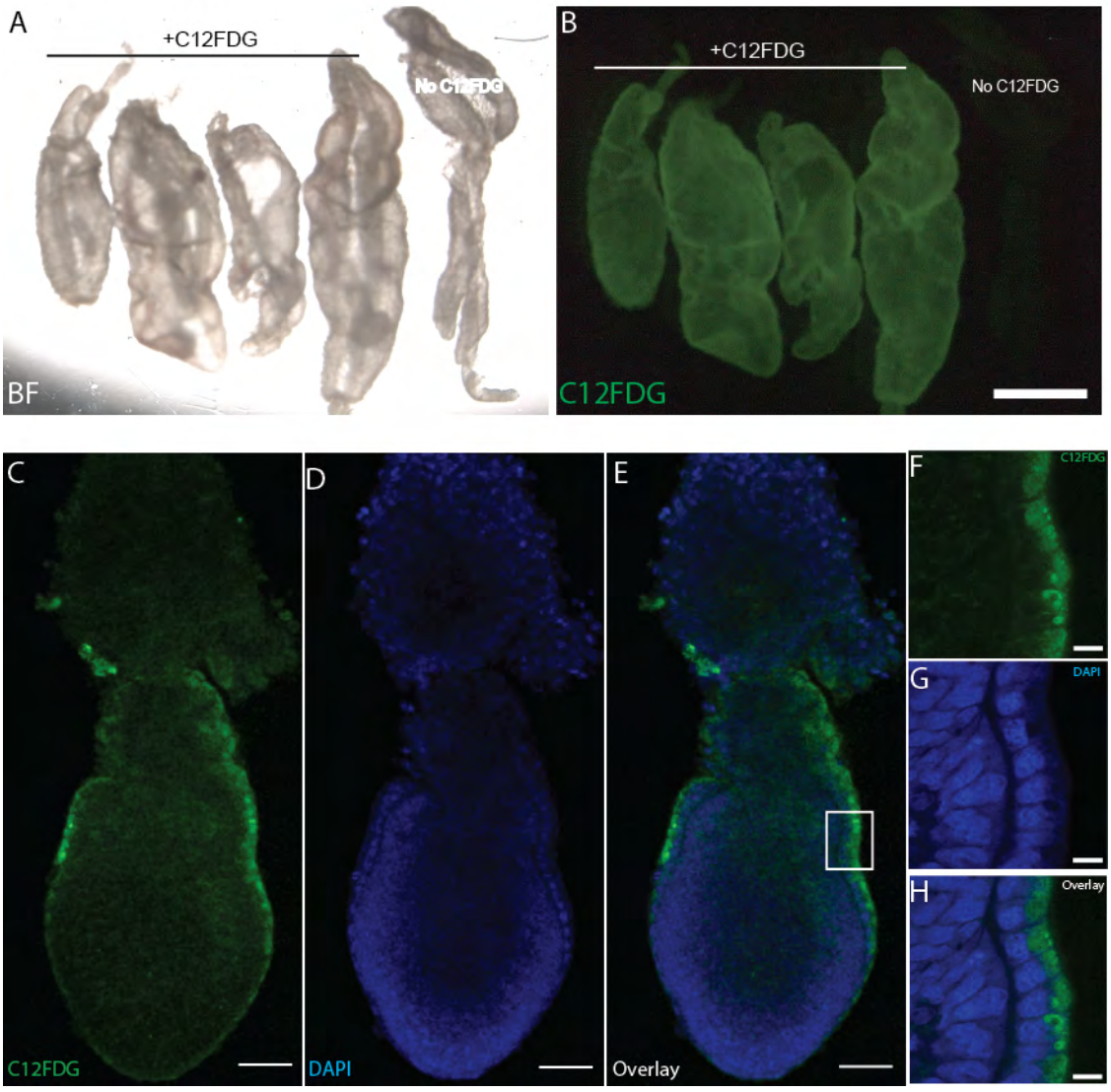
A
+C12FDG
No C12FDG
BF
B
+C12FDG
No C12FDG
C12FDG
C
C12FDG
D
DAPI
E
Overlay
F
C12FDG
G
DAPI
H
Overlay

Figure 3.10. Detection of SA-β-gal activity using C12FDG, a fluorescence substrate for β-galactosidase. A, B. Brightfield (A) and fluorescence illumination (B) of the visceral yolk sac of E9.5 embryos. SA-β-gal staining (green) marks the whole visceral yolk sac. The yolk sac shown at extreme right in B, is a control processed without incubation with C12FDG. **C - H.** SA-β-gal staining (green) labels the apical surface of extra-embryonic and posterior visceral endoderm cells. This is clearly visible in the higher magnification shown in insert (F). Scale bars: 1 mm in B; 100 µm in C, D, E and 10 µm in F-H.

C12FDG. At E9.5, the whole visceral yolk sac are marked by fluoregenic SA-β gal staining (Figure.3.10A, B). At E 6.5, only posterior visceral endoderm and extraembryonic visceral endoderm are marked by fluoregenic SA-β gal staining (Figure.3.10C - F).

We then combined this assay with an assay to label apical vacuoles using Lysinated Rhodamine dextran (LRDX). This compound has been used to mark apical vacuoles before (Kawamura et al., 2012). E6.5 embryos were labelled with LRDX *in vitro* for 15 min, and then incubated for 15 min in media lacking LRDX. During this chase period, most internalised LRDX was transported to the apical vacuoles. We then assayed the embryos for SA-β gal activity using C12FDG and imaged the embryos with confocal microscopy. We observed that SA-β gal fluorescence co-localized with the LRDX present in the apical vacuoles. Our results showed complete co-localization of green fluorescence produced by the fluorescent SA-β-gal assay and red fluorescence provided by LRDX in the apical vacuoles (Figure. 3.11)

From these studies, we conclude that the SA-β-gal activity observed in visceral endoderm cells is not related to senescence but likely represents SA-β-gal activity present in apical vacuoles and associated with the nutritional function of visceral endoderm at early post-implantation stages.

Figure 3.11

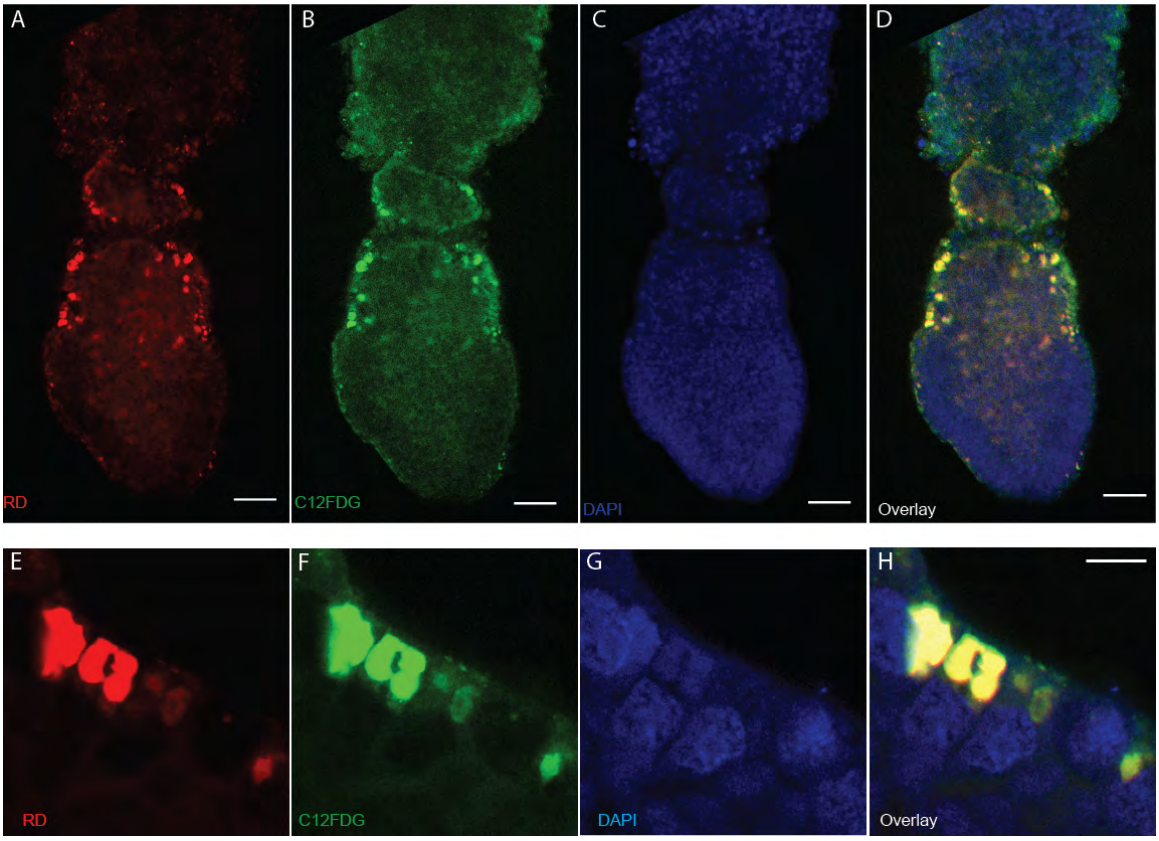

Figure 3.11. Detection of SA-β-gal activity in apical vacuoles of visceral endoderm cells. E6.5 embryo assayed for fluorogenic SA-β-gal activity and rhodamine dextran (RD) to label apical vacuolae. Panels **A** and **E**, show RD fluorescence (red). Panels **B** and **F** show SA-β-gal activity detected using C12FDG. Panels **C** and **G** show DAPI staining and panels **D** and **H** are overlays of the three channels. A-D are a rendering of all confocal sections in their particular channel. Confocal sections of the region in the dotted square are shown in E-H. SA-β-gal activity corresponds to the same areas marked by fluorescence dextran indicating its presence in apical vacuoles. Scale bars: 50 μm in A-D and 10 μm in E-H.

Materials and Methods

Mouse strains and embryo collection

Embryos were obtained from crosses between CD-1 mice (Charles River Laboratories). Postimplantation embryos were dissected in N-2 hydroxyethylpiperazine-N′-2 ethanesulfonic acid (HEPES) buffered Dulbecco's Modified Eagle's Medium (DMEM) containing 10% fetal bovine serum (FBS). Embryos dissected at 5.5 dpc were staged according to the position of the visceral endoderm thickening (Rivera-Perez et al., 2003) . Embryos dissected at 6.5 dpc and 7.5 dpc were staged as described (Downs and Davies, 1993). The middle of the dark cycle (midnight) that preceded the morning in which the copulation plug was observed was considered the beginning of gestation.

Whole mount *in situ* hybridization

CD-1 embryos were used in wholemount *in situ* hybridization. Embryos were fixed overnight in 4% paraformaldehyde prepared in PBS. After fixation, they were dehydrated in methanol series and stored in 100% methanol at -20°C. Hybridization was done at 70°C following the protocol of J. Rossant's laboratory (http://www.sickkids.ca/research/rossant/custom/protocols.asp). The cdkn1a-1 probe was transcribed from plasmid pcdkn1a-1wish. It consisted of a 1,030 bp fragment of exon3 of Cdk1a-1-3'U transcript containing a 980 bp piece of 3'UTR. For the wholemount in situ staining, embryos were fixed in 4% paraformaldehyde,

subjected to whole-mount in situ hybridization. Embryos hybridized with the Cdkn1a-1-3'U or Cdkn1a probes were treated for 5-8min with proteinase K (10 µg/ml) and allowed to be stained for 1-2 days in the color reaction solution. Embryos used in these experiments were littermates.

Immunofluorescence

Embryos obtained from CD1 crosses were fixed for 1 h in 4% paraformaldehyde prepared in PBS. After fixation, embryos were washed 3 times in PBS for 10 min and incubated in blocking solution (5% goat serum, 0.5% Triton X-100 and 1% bovine serum albumin in PBS) for 1 h. Subsequently, the embryos were incubated with primary antibody diluted 1:500 for 2 hours. After primary antibody staining, the embryos were washed three times in PBT (0.5% Triton X-100, 1% BSA in PBS) and incubated for 1 h at room temperature in secondary antibody diluted 1:500 in PBT. Embryos were then rinsed 3 times in PBT for 10 min, once in PBS for 5 min, counterstained with 1 µM Draq5 (Biostatus Cat. No. 4084), washed twice in PBS for 5 min and mounted in 50% Glycerol/PBS. Primary antibodies: Anti phospho-Histone H3 (EMD Millipore catalog number: 06-570) and rat anti E-cadherin IgG (Zymed catalog number 13-1900) Rabbit anti Ki67 (Abcam Cat. No. 66155) and mouse anti p21 (BD biosciences Cat. No. 556430). Secondary antibodies: Alexa-fluor 488 Goat anti Rabbit IgG (Molecular probes Cat. No. A11008), Alexa-fluor 594 Goat anti Rat IgG (MolecularbProbes, Cat. No. A-11007) and Alexa-fluor 568 Goat anti mouse

IgG (Life technologies, Cat. No. A-11004) . Mouse IgG immunostaining was done following the above procedure, excluding the primary antibody incubation, using Alexa-fluor 488 goat anti mouse IgG (Molecular probes Cat. No. A11001). Stained embryos were imaged using a laser scanning confocal microscope (Leica TCS SP5). Optical sections were obtained every 4µm.

Mitotic index (MI)

Confocal images of the embryo were captured on a Leica TCS SP5 Confocal Laser Scanning Microscope a 20x/0.70 immersion HC PL APO Lbd. Bl objective. z-stacks were taken at either 2um or 4 um intervals through the embryo, with each channel acquired sequentially. Stacks were then merged and reconstructed using ImageJ 1.46n. The number of the cells in M phase marked by green fluorescence (phoshop-histone H3) was scored manually by using imageJ Othogonal views function. The tranverse setions move along the whole y axis and the individual green spot in the visceral endoderm (periphery) was counted and double checked sagital view. The two adjacent green dots in the neighbouring cells are counted once. The green dots in the extraembryonic and embryonic boundary are separately scored in both extraembryonic and embryonic data set. The total number of the cells in the visceral endoderm was manually counted by using imageJ. The mitotic index (M.I.) is defined as the ratio between the number of cells in mitosis and the total number of cells. Each embryo was analyzed for M.I. separately in the extraembryonic visceral

endoderm and embryonic visceral endoderm.

Fluorescent SA-β-gal and endocytic labeling

Embryos obtained from CD-1 crosses were cultured in a 1:1 mixture of DMEM and rat serum (Rivera-Perez et al., 2003; Kawamura et al., 2012) containing 2 mg/ml fluorescent dextran (Molecular Probes, catalog number D-1818) and 20 mM C12FDG (5-Dodecanoylaminofluorescein Di-β-D-Galactopyranoside.Molecular Probes, catalog number D-2893) for 15 min(Debacq-Chainiaux et al., 2009). After the initial culture, the embryos were rinsed twice in culture medium (1:1 DMEM/rat serum) and incubated again in the same media for 15 min. After the secondary culture period, the embryos were rinsed twice in PBS and fixed for 10 minutes in 4% paraformaldehyde at room temperature. After fixation, the embryos were rinsed twice in PBS for 10 minutes each, stained with Draq5 diluted 1:5000 (1μM), washed twice in PBS for 5 min and mounted in a solution containing 50% Glycerol in PBS.

Discussion

SA-β-galactosidase activity is derived from lysosomal β-galactosidase that reflects increased lysosomal biogenesis in senescent cells(Kurz et al., 2000; Lee et al., 2006; Campisi and d'Adda di Fagagna, 2007). We showed that the SA-β-gal activity was present in the apical vacuoles of visceral endoderm cells, an organelle with lysosomal activity (Kawamura et al., 2012). Therefore we believe that the observed SA-β-gal activity corresponds to increased lysosomal activity present in these organelles. The visceral endoderm has a nutritional role at post-implantation stages before the establishment of the maternal-embryo circulation through the placenta (Zohn and Sarkar, 2010). A recent study has shown that the visceral endoderm endocytoses nutrients by a process of microautophagy in which endosomes are engulfed by large apical vacuoles (Kawamura et al., 2012). Hence, the high acidic β-galactosidase activity of visceral endoderm likely reflects the trophic activity of the visceral endoderm mediated by the apical vacules and lysosomes. Interestingly, acidic β-gal activity may be a characteristic of tissues involved in nutrient absortion since it has been found in intestinal cells (Going et al., 2002; Viotti et al., 2011).

Our results show that SA-β-gal activity marks the visceral endoderm of early post-implantation embryos, in predictable patterns, initially in the whole visceral endoderm at E5.5, then in the extra-embryonic and posterior visceral endoderm as the embryo progresses towards gastrulation and later in the

visceral yolk sac as the embryo proceeds through the initial stages of organogenesis (see Figure.3.12). This stereotyped pattern of staining resembles the pattern of expression of several markers of the visceral endoderm such as Alphafetoprotein (Afp) and Transthyretin (Ttr) (Going et al., 2002; Viotti et al., 2011). Alphafetoprotein is the embryonic equivalent of albumin a liver marker. Transthyretin is also a marker of the liver. These characteristics coupled with previous notions that the visceral endoderm mimics the function of the fetal large intestine and liver (Meehan et al., 1984) reinforce the view that SA-β-gal staining reflects the nutritional role of the visceral endoderm and suggest a shift of the source of embryo nutrition to the extra-embryonic visceral endoderm at early post-implantation stages. Kwon and co-workers reported that descendants of the embryonic visceral endoderm are incorporated into the definitive endoderm layer of the embryo (Nielsen et al., 1999; Kwon et al., 2008). This process involves a functional transition of visceral endoderm cells into definitive endoderm(Nielsen et al., 1999; Kwon et al., 2008).

Our results suggest that lost of acidic β-galactosidase activity in embryonic visceral endoderm precedes this transition since acidic β-galactosidase staining is not evident in the embryonic visceral endoderm at the time that definitive endoderm cells emanating from the primitive streak intercalate between the visceral endoderm layer of the embryo. A number of molecular changes found in senescent cells in vitro resemble those occurring in somatic cells during the process of aging in vivo (Mishima et al., 1999; Nielsen et al., 1999; Campisi and

d'Adda di Fagagna, 2007; Kawamura et al., 2012) and SA-β-gal activity has been associated with organismal aging (Mishima et al., 1999; Pendergrass et al., 1999; Sigal et al., 1999; Melk et al., 2003). It seems paradoxical then that SA-β-gal activity is present during embryogenesis. This is also the case of p21 another marker of senescence, whose transcripts are present in the primitive streak, a region with high levels of cell proliferation during embryogenesis (Snow, 1977; Stuckey et al., 2011). Our study shows that these two markers are not only markers of senescence or aging and highlight the contrasts encountered when conducting studies in cell culture and at the organismal level.

Since first described in 1995 (Dimri et al., 1995), the SA-β-gal assay has been widely used as a biomarker of senescent cells. However, our studies reveal that SA-β-gal staining marks the visceral endoderm of early post-implantation embryos. Morever, the SA-β-gal activities at early post-implantation stage are enriched in the apical vacuole, most likely linked to the nutritive role of the visceral endoderm cells rather than a senescent cell population. Firstly, the analysis of Ki67 immunostaining revealed that a good portion of visceral endoderm cells are actively are proliferating, however, almost all the extraembryonic visceral endoderm and posterior visceral endoderm cells are stained by SA-β-gal staining, suggesting the SA-β-gal staining and Ki-67 immunostaining patterns are not exclusive to each other, which in further implies the SA-β-gal patterning does not infer senescence in this case. In addition, determination of the mitotic index showed that visceral endoderm cells are

actively cycling, confirming previous studies (Stuckey et al., 2011). Moreover, analysis of the expression of the senescence marker *p21* did not reveal expression in the visceral endoderm but rather on the highly proliferative primitive streak. All of these suggest the SA-β-gal activity in the visceral endoderm is not linked to senescence. In additioin, we demonstrated the SA-β-gal activity in the visceral endoderm mostly likely comes from apical vacuole, a specialized form of lysosome.

Previous studies have shown that SA-β-gal staining can be encountered in non-senescent situations *in vitro* and *in vivo*. For example, a small number of β-galactosidase positive cells at pH 6.0 were found in growing 3T3 fibroblast cultures (Yegorov et al., 1998) and acidic β-galactosidase staining was found in the glomerular basement membrane of kidney cells (Melk et al., 2003). More studies showed that senescent cell populations are present in some pathological situations, such as wound healing and liver fibrosis (Krizhanovsky et al., 2008; Jun and Lau, 2010). In addition, two recent studies came out at the end of last year showed the senescence, the same as apoptosis, is a fundamental mechanism to fine tune embryo development (Munoz-Espin et al., 2013; Storer et al., 2013). However, in the stage we studied, early post-implantation (E 5.5 – E 9.5), instead of representing senescent cells, the SA-β-gal stained visceral endoderm cells are localized in the apical vacuoles, presumbably linked to the

Two papers just came out demonstrated the senescence, similar to apoptosis, is a basic mechanism for shaping the embryo development (Munoz-

Espin et al., 2013; Storer et al., 2013). The cause of the discrepancy is the developmental time windows. The embryo stage I worked on is mainly between 5.5 to E9.5, while the stage is much later in the other two published papers. Thers is also another possibility that a sub-population of visceral endoderm cells are senescent even though the visceral endoderm is not. To address this question, the analyses of dual markers, Ki67 and SA-β-gal, for instance, need to be examined on the cellular level to investigate if there is a strong association between SA-β-gal activity and absence of proliferation.

The SA-β-gal activity linked to senescence is derived from the increased lysosomal residue contents (Kurz et al., 2000; Lee et al., 2006), and the SA-β-gal activity is dispersed in the whole cytoplasm. However, the SA-β-gal activity I observed in visceral endoderm cells is restricted in apical vacuole and this could be due to that the increased lysosomal lipase activity inside the apical vacuole, which somehow mimicks the accumulation of lysosomal residue contents in the whole cytoplasm when cells undergo senescence. It also indicates SA-β gal activity is specific indicator for a consequence of accumulation lysosomal contents but not senescence. One potential candidate for this lysosomal origin of SA-βgal activity is GLB1, the gene encoding the classic lysosomal enzyme (Lee et al., 2006).

Figure 3.12

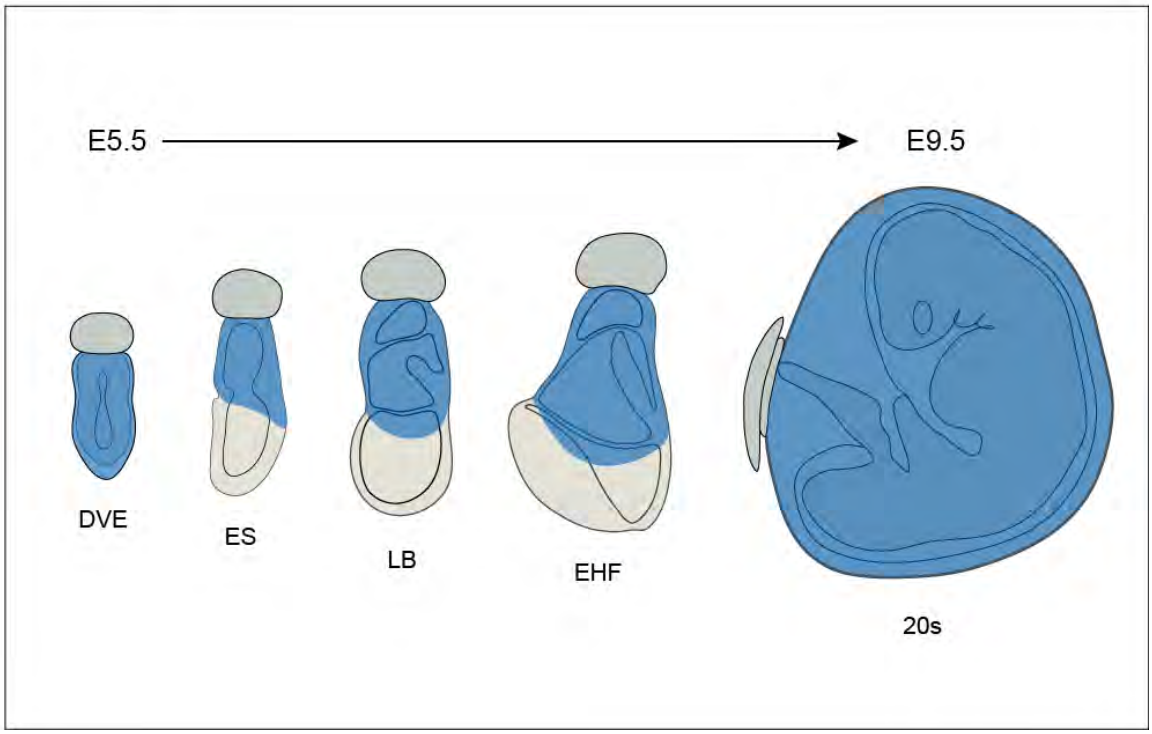

Figure 3.12. Schematic representation of SA-β-gal staining between E5.5 and E9.5. SA-β-gal staining (shown in blue) marks the entire visceral endoderm at DVE stage (~E5.5) but it marks the extra-embryonic and posterior visceral endoderm by primitive streak stages (~E6.5). At gastrulation stages (~E7.5) SA-β-gal staining is observed to the extra-embryonic portion of the conceptus, and eventually, it is present to the yolk sac (E9.5). Abbreviations: DVE, Distal Visceral endoderm stage; ES, early streak stage; LB, Late allantoic bud stage; EHF, Early head folds stage; 20s, 20 somite stage.

CHAPTER IV:

GENERAL DISCUSSION

Vertebrates have diverse shapes and a unique appearance. Such sophisticated body architecture develops from a conserved body plan laid out during early embryonic development. One of the earliest decisions for any embryo is to decide where to form the head opposite to the tail along the anteroposterior axis.

In anamniotes such as *Xenopus* and zebrafish, the anteroposterior axis is determined by the organizer, a specialized region that releases signaling factors to promote the formation of the three germ layers. The organizer is induced by the evolutionarily conserved Wnt signaling-based Nieuwkoop center (Harland and Gerhart, 1997; Tao et al., 2005; Lu et al., 2011). However, whether the Nieuwkoop center exists in amniotes such as mice and chick is unknown. In humans, a study of fetuses with tetramelia found linkage to a non-sense mutation in *WNT3* that leads to a truncated form of the protein (Niemann et al., 2004). Since these fetuses were able to undergo gastrulation, *WNT3* does not seem to direct gastrulation in humans.

The mouse is the most amenable model organism to represent mammalian embryo development, however, the mouse embryo has stark differences to anamniotes and also to chick embryos. First, mouse embryos do not carry much maternal components and the zygotic genome is activated at a much earlier stage than other vertebrates, implying that cues to lay down the primary body axes are not present in the fertilized eggs. Second, mouse embryos have a simple epiblast consisting of a relatively small number of embryonic cells

while sophisticated patterned extra-embryonic tissues compose the rest of the conceptus at the beginning of gastrulation. Third, morphological evidence of the anteroposterior axis is evident almost a week after fertilization at E6.5. These features pointed to a fundamental role of extra-embryonic tissues in patterning the early mouse embryos.

4.1. Evolutionarily conserved “Nieuwkoop center” during vertebrate development

The existence of abundant extraembryonic tissues implies a potential role of murine extraembryonic tissues in regulating early developmental events, which is further evidenced by tissue specific gene knockout studies. Embryos lacking a few genes (*Nodal, Smad2* and *Otx2)* in the visceral endoderm show embryonic leathality and fail to establish the primary body axes (Beddington and Robertson, 1998; Waldrip et al., 1998; Perea-Gomez et al., 2001)

In *Xenopus*, the most well studied model organism for axial specification, the Nieuwkoop center produces signals to induce the Spemann organizer which in turn releases a cocktail of factors to establish axial polarity. Figure.1.6 is a modified figure from the Beddington and Robertson’s 1998 review to explain how the topological relationship between the organizer derivatives and Nieuwkoop center observed in frog might be conserved in chick and mice. According to the model, it is suggested that the Nieuwkoop center equivalent in mice is the posterior visceral endoderm (Figure.1.6) (Beddington and Robertson, 1998).

In a classical transplantion experiment, juxtaposing the posterior visceral endoderm to anterior ectoderm leads to respecification of anterior epiblast to a posterior mesodermal fate by forming the blood cell progenitors and expressing endothelial markers (Belaoussoff et al., 1998). *Wnt3*, a gene essential for gastrulation (Liu et al., 1999), was identified as a candidate molecule in expression studies (Rivera-Perez and Magnuson, 2005). In early post-implantation embryos, *Wnt3* mRNA is first observed in the posterior visceral endoderm of embryos dissected at embryonic day 5.5 (E5.5) and expands to the adjacent epiblast tissue a few hours later by E5.75 (Rivera-Perez and Magnuson, 2005). Based on these studies, it was proposed that the posterior visceral endoderm directs the formation of the primitive streak and that Wnt3 is the effector molecule (Rivera-Perez and Magnuson, 2005). Recently, evidence to support a posterior visceral endoderm-signaling model was provided by experiments in which *Wnt3* was conditionally inactivated in the epiblast of developing embryos (Tortelote et al., 2013). Embryos lacking *Wnt3* in the epiblast establish the anteroposterior axis and initiate gastrulation but fail to thrive. Intriguingly, in these embryos, *Wnt3* expression is temporary present in the posterior visceral endoderm suggesting that Wnt3 signaling from the posterior visceral endoderm is responsible for the initiation of gastrulation (Tortelote et al., 2013).

In order to determine if *Wnt3* function in the posterior visceral endoderm is required for the generation of the primitive streak, our lab inactivated *Wnt3* in the

posterior visceral endoderm of mouse embryos and analyzed their phenotype at early post-implantation stages. Our results show that embryos lacking *Wnt3* in the visceral endoderm phenocopy *Wnt3* null embryos failing to produce a primitive streak. Hence, *Wnt3* function in the posterior visceral endoderm is essential for specification of the primitive streak.

The first part of my work focused on studying the interaction between two visceral endoderm lineages; the posterior and anterior visceral endoderm. From initial observations that suggested interplay between these tissues in patterning early mouse embryo, we provided evidence that the PVE can induce the formation of the primitive streak in an ectopic region. These studies complement unpublished studies from our laboratory that showed that Wnt3 emanating from the PVE is necessary to form the primitive streak. Together these data provide evidence that Wnt3 derived from the PVE is necessary and sufficient to induce the primitive streak. Previous studies from our laboratory showed that Wnt3 acts through the canonical Wnt signaling pathway. Thus, the PVE appears to be an equivalent of the Nieuwkoop center of amphibians and fish. To our knowledge this is the first time that a signaling center responsible for the generation of the anteroposterior axis is identified in mammals.

4.2. Complex molecular mechanism patterns early mouse embryo

Studies in *Xenopus* have provided evidence that the Nieuwkoop center induces the formation of mesendoderm utilizing Wnt11, which activates the

canonical Wnt signaling pathway (Tao et al., 2005). In zebrafish, recent studies identified Wnt8a as the dorsal determinant also working through the canonical Wnt pathway (Lu et al., 2011). The involvement of the canonical Wnt signaling pathway in mesendoderm induction in *Xenopus*, *zebrafish* and mouse embryos suggest that this is an evolutionary conserved character of vertebrate gastrulation. However, different Wnt ligands, Wnt11, Wnt8a and Wnt3 respectively, appear to be the effector molecules. In humans, a study of fetuses with tetramelia found linkage to a non-sense mutation in *WNT3* that leads to a truncated form of the protein (Niemann et al., 2004). Since these fetuses were able to undergo gastrulation, *WNT3* does not seem to direct gastrulation in humans. Moreover, expression studies in *Xenopus* and *zebrafish* have shown that the ortholog of *Wnt3* in these organisms is not expressed at the time of gastrulation (Garriock et al., 2007; Clements et al., 2009). On the other hand, the knockout of *Wnt11* or *Wnt8a* orthologs in mice, do not produce a gastrulation phenotype (Majumdar et al., 2003; van Amerongen and Berns, 2006). Therefore different Wnt ligands appear to have been co-opted for anteroposterior axial specification during the evolution of vertebrates.

In mice, Wnt3 appears to be the central molecule in posterior visceral endoderm for mesoderm induction, while Bmp4 is also required for this process, even though not necessary for the initiation of gastrulation (Tortelote et al. unpublished). Whether Wnt3 and Bmp4 signaling can be integrated in the same signaling network to direct gastrulation remains unknown. Differentiation of stem

cells in vitro resembles the process of early stages of lineage specification since during differentiation, ESCs pass through a series of developmental events and express critical molecular markers that resemble those within the embryo (Keller, 1995; Hirst et al., 2006). It has been shown that Wnt3a or Bmp4 can direct the differentiation of embryonic stem cells to express mesoderm markers during certain temporal time windows, and in this case, the timing of addition of growth factors is critical for mesoderm induction (Jackson et al., 2010). Nodal is also able to induce the ESCs to express mesoderm markers, however, the time window for Nodal is 0.5-day-late compared to that for Wnt3a and Bmp4 (Jackson et al., 2010), indicating the order of these series of inductive events for mesoderm induction are mostly likely initiated by Wnt and Bmp signaling followed by Nodal signaling. In addition, Adding both Bmp4 and Wnt3a will robustly induce the mesoderm markers *T* and *Mixl1* and Bmp4 and Wnt3a by themselves will only weakly turn on mesoendoderm markers, suggesting that Wnt3a and Bmp4 can induce mesoderm induction in parallel signaling pathways.

The *in vitro* ESCs differention data mentioned above are indeed valuble, however, cannot directly fit into the *in vivo* signaling model. First, *Wnt3* instead of *Wnt3a* is the first Wnt signaling molecule expressed on the prospective posterior side of the embryo (Rivera-Perez and Magnuson, 2005). Second, some of the embryos lacking Bmp4 show a partial primitive streak, which suggest that mesoderm induction takes place in these *Bmp4* mutants (Winnier et al., 1995) while all the embryos lacking *Wnt3* show a complete loss of the primitive streak,

indicating that the initiation of mesoderm induction did not happen in these *Wnt3* mutants (Liu et al., 1999). These two lines of evidence, suggest the following model: *Wnt3* is the key molecule that initiates gastrulation, and *Wnt3* and *Bmp4* work in paralel to maintain the gastrulation process.

To better dissect the complex linear or parallel signaling pathways which shape the early mouse anteroposterior axes, several experiments could be made. First, to determine if Wnt3 is responsible for the partial primitive streak developed in *Bmp4* mutant embryos, we could generate double *Wnt3* and *Bmp4* knockout embryos to test if the primitive streak is completely gone in the double mutant embryos. Secondly, to test if Bmp4 could induce mesoderm through Wnt3, Wnt3 deficient ESCs could be generated to test if adding Bmp4 is sufficient to induce primitive streak markers. Or to test if Wnt3 requires Bmp4 to induce mesoderm, Bmp4 deficient ESCs could be generated to test if adding Wnt3 is sufficient to induce primitive streak markers.

4.3. An interplay between anterior and posterior visceral endoderm positions the primitive streak

One of the goals of my work was to define the role that the AVE played in the establishment of the anteroposterior axis. We addressed this issue genetically using *Cripto* mutant embryos in which the AVE fails to reach one side of the epiblast. We learned that the role of AVE is to restrict *Wnt3* activity to the posterior side of the embryo to regulate the position of the primitive streak.

Therefore, interactions between the anterior and posterior visceral endoderm establish axial patterning in mice.

There are several questions to address in the future, first, what is happening at the molecular level? Multiple Wnt antagonists are present in the AVE, including mDkk1, Sfrp1, Sfrp5, and Cer-I (Kemp et al., 2005; Pfister et al., 2007) and they regulate Wnt signaling through diverse mechanisms. The sFRP (secreted Frizzled-related protein) family, primarily binds to Wnt proteins and Dickkoff, binds directly with LRP5/6 and Kremen (Kawano and Kypta, 2003). This leads us to ask if Wnt antagonists in the AVE are blocking Wnt3 signaling? If so, how is this happening? An additional question is to determine if the AVE exerts its effects on the visceral endoderm, epiblast or both.

Another question that remains is whether this mechanism is conserved in other vertebrates. In *Xenopus*, the equivalent of the AVE resides in central yolk vegetal cells. In chick the AVE is equivalent to the anterior hypoblast. In zebrafish an AVE equivalent has not been described but a likely candidate is the dorsal syncitial layer (Beddington and Robertson, 1998). *Hex*, is a marker of the AVE in mouse. The Xenopus homologue of *Hex*, is present in the deep vegetal cells and the zebrafish homologue of *Hex* is expressed in the dorsal yolk syncitial cells before gastrulation (Beddington and Robertson, 1998). Wnt antagonists have been reported to restrict Wnt activity to form the organizer in other vertebrates. In *Xenopus,* FRZB-1, a Wnt antagonist, counteracts the ectopic activity of *Xwnt8* to induce a secondary organizer (Leyns et al., 1997).

All this data suggest that despite morphological differences, the morphogenetic and molecular mechanisms that control axial development in vertebrates have been conserved evolutionarily. It is tempting to speculate that in humans an equivalent would be present and that the canonical Wnt pathway will be involved in axial patterning. With the advent of high throughput sequencing technologies it may be possible to sequence naturally aborted fetuses at stages right after gastrulation at about two weeks of development to try to find out the responsible gene for human gastrulation.

4.4. The role of *Cripto* in Anterior Visceral endoderm movements

The expansion of Wnt signaling to the anterior side of the embryo is allowed by the failure of AVE movements in the *Cripto* mutants, suggesting that the shift of distal visceral endoderm cells to the future anterior side is a critical regulatory step for the proper embryonic development in mice. Using genetic and molecular studies, Ding et al. 1998 has shown that *Cripto* is required for correct anteroposterior axis formation in the mouse embryo (Ding et al., 1998).

Although the unilateral movement of AVE cells is crucial for embryo patterning, very little is known about how it takes place. The visceral endoderm There are two prevailing views. One is that it is a passive movement due to the different proliferative rate of anterior or posterior visceral endoderm cells (Lawson and Pedersen, 1987; Yamamoto et al., 2004). The other view suggests the AVE migrates as a single layer in direct contact with the epiblast, which indicates the

epiblat layer serves as a buttress for supporting AVE movement or even provide directional cues (Srinivas et al., 2004).

The process of AVE movements consists of a series of coordinated cellular changes and movements. At E5.5, the visceral endoderm cells located at distal tip are specified to express multiple genes, such as *Hex, mDKK1, Sfrp1&5, Lefty1* CerI (Tam and Loebel, 2007). These cells then shifts to the prospective anterior side in 7 hours (Thomas et al., 1998; Rivera-Perez et al., 2003) (Figure.2 8). Multiple signaling pathways have been indicated in involving the AVE movement process. TGF-β/ Nodal signaling promotes DVE specification (Brennan et al., 2001; Tam and Loebel, 2007) (Figure.2 8) and the Nodal antagonists Cerl and Lefty1 are also involved in AVE movements by controlling cell proliferation in the visceral endoderm layer (Yamamoto et al., 2004). Moreover, canonical Wnt ligands and Wnt anatagonist Dkk1 has been suggested to function as repulsive and attractive guidance cues to predict the direction of AVE movement (Kimura-Yoshida et al., 2005) (Figure.2 8).

Cripto is a major member of EGF-CFC proteins attached to the cell membrane through a glycosylphosphatidylinositol linkage. Genetic and biochemical studies show that EGF-CFC proteins act as membrane-associated coreceptors for type I and type II activin receptors (Shen and Schier, 2000). The AVE cells in embryos lacking *Cripto* gene stay distally instead of moving anteriorly (Ding et al., 1998). *Cripto* is exclusively expressed in the epiblast at egg cylinder stage and then the expression of *Cripto* shifts to the primitive streak

conincident with the emergece of the primitive streak, indicating the epiblast-expressing *Cripto* plays a role in the process of AVE movements. Furthermore, cell culture and chimeric analysis show Cripto can work in a non cell autonomous manner in cell culture and also during during axial midline formation (Yan et al., 2002; Chu et al., 2005). All this evidence indicates that absence of Cripto in the epiblast leads to the mislocalization of anterior visceral endoderm in the Cripto mutants. However, the detailed mechanism for dissecting the role of *Cripto* in anterior visceral endoderm has not been done yet. More detailed information regarding on the question on epiblast-expressing *Cripto* affects AVE movements could be gained by the following experiments.

To gain more information about AVE cell fate and cell movements in *Cripto* mutants at pre-streak stage we can conduct cell lineage assays. The abnormal location of AVE at the distal tip of mutant *Cripto* embryos suggest defects either in the genetic cascade that controls the expression of the transgenes, or in the displacement of distal visceral endoderm cells. To determine whether the distal visceral endoderm cells at 5.5 dpc stay remain distally located or give rise to anterior descendants that lack DVE/AVE markers, the individual cells of distal visceral endoderm (DVE) in both wild type and *Cripto* mutant embryos could be labeled with a mixture of horseradish peroxidase (HRP) and Lysinated Rhodamine Dextran (LRDX) (Lawson and Pedersen, 1987) to study their movements. Iontophoresis is a microinjection technique that utilizes electric current to deliver ions into cells. If absence of *Cripto* affects cell

movement, we expect to see that in *Cripto* mutants, the labeled cells remains distally, while in wild type embryos, the labeled cells move to anterior side of the epiblast after 7-hour culture.

Iontophoresis is previously tested single cell lablling technique, which leads to a negligible volume change and minimal damage in the labeled cell. There are potential complications such as limited detection of 6 divisions of labeled descendants, however, these does not affect the experiment design, since only 1-2 cell division for visceral endoderm cells is expected from E5.5 to E6.5.

Another question, which needs to be addressed, is how epiblast-expressing *Cripto* plays a role in regulating the cell movements in the viscereal endoderm layer. The expression of Cripto is exclusively and uniformly distributed in the epiblast at pre-streak stage (Ding et al., 1998), suggesting Cripto protein, might diffuse through the epliblast-visceral endoderm boundary to mediate intercellular response in distal visceral endoderm cells. Cell coculture studies demonstrated Cripto could also function as a secreted signaling factor with Noda (Yan et al., 2002) and moreover, chimera analysis provides evidence that shows a potential non-cell-autonomous role for Cripto during axial midline formation (Chu et al., 2005). I postulate that Cripto is secrected by the epiblast cells to function as a signal molecule to regulate the displacement of the AVE in a non-cell-autonomous way.

To address this question, Cripto-soaked beads could be attached to distal visceral endoderm cells in *Cripto* mutant embryos. The distal visceral endoderm cells could be visualized using *Hex-eGFP* fluorescence, which make it much easier to conduct these experiments. The method to attach protein-soaked beads to tissues has been described in chick to study limb development, or mouse to study the repulsive and attractive cues for AVE movement (Kimura-Yoshida et al., 2005). If our hypothesis that soluble Cripto protein can act non-cell-autonomously to rescue the displacement of AVE is correct, we would expect to see the movements of AVE cells in Cripto mutants when we apply the Cripto-soaked beads.

There are some potential difficulties for this experiment, for example, the Cripto-soaked beads can be attached to certain points, however, it is not clear at which site the Cripto protein is required to regulate AVE movements. The distal tip is the top potential candidate site for bead attachment since it is clear that Nodal/Cripto signaling takes place to direct DVE specification (Brennan et al., 2001). An alternative approach for this experiment is to add Cripto soluble protein directly into the embryo culture medium for falicitating a uniform and continuous supply of Cripto ligand.

The next question addresses the role of Lefty1-dependent Cripto signaling in regulating AVE movements. The anterior visceral endoderm cells are specified at the distal tip at E5.5, expressing AVE markers (*Hex*) or Wnt/Nodal signaling antagonists (*mDKK1, sFRP1&5, Cerl, Left1,* etc) (Beddington and Robertson,

1999). Lefty1 expression begins randomly in the inner cell mass (ICM) of the blastocyst. *In situ* hybridization experiments have previously shown that Lefty1 is asymmetrically expressed in the visceral endoderm of E5.5 mouse embryo, during AVE movements (Oulad-Abdelghani M et al. 1998). The embryos lacking both *CerI and Lefty1* develop an ectopic primitive streak (Perea-Gomez A et al. 2002). In *Cripto* mutant embryos, although many AVE genes are expressed in distal visceral endoderm, Lefty1, was absent (Kimura et al., 2001; D'Andrea et al., 2008). Cell-based assays show that *Lefty1* interacts with EGF-CFC proteins and prevent their ability to form part of a Nodal receptor complex, suggesting the loss of *Lefty1* might be the reason for the failure of AVE movements in *Cripto* mutants.

To determine whether the absence of Lefty1 causes the misplacement of the AVE, *Lefty1* fused to a GFP tag, will be ectopically expressed, in the visceral endoderm of E5.25 Cripto mutant embryos. The vector containing a full coding sequence of *Lefty1* followed by a GFP tag, could be introduced into visceral endoderm cells on the distal side of E5.25 mouse embryos using iontophoresis. If the hypothesis that the absence of Lefty1 protein causes the displacement of AVE is correct, we would expect to see the movements of *AVE* cells in Cripto mutants when we re-express Lefty1 in the cells of distal visceral endoderm in Cripto mutants.

The potential difficulties for this experiment design are the technical barrier of injecting DNA vector into the E5.25 embryos and if the induced promoter could be successfully activated in the visceral endoderm cells. A good alternative

strategy is to establish a floxed transgenic line for *Lefty1* and set up genetic crosses to specificly activate the expression of introduced *Lefty1* gene in distal visceral endoderm cells.

An additional question is to study an indirect role of Cripto in AVE movement. In tumorigenesis, Cripto activates the MAPK signaling pathway to control cell proliferation. The hypothesis is that decreased cell proliferation in Cripto mutants correlate with displacement of the AVE. To determine whether the Cripto null embryos have a decreased rate in cell proliferation, the immunostaining analysis for mKi-67 and Oct4 for E 5.5 *Cripto* mutants and wild type embryos could be conducted and the epiblasts for mutants and wild type embryos will be analysed to calculate the percentage of the proliferating cells in the epiblast. The mouse Ki-67 protein is cell proliferation marker strictly associated with cell proliferation. During all active phases of the cell cycle (G1, S, G2, and mitosis), but is absent from resting cells (G0) (Wei et al., 1999; Chenn and Walsh, 2002). The Oct 4 antibody recognize mouse Oct4 proteins. Oct4 is a transcription factor expressed by undifferentiated embryonic stem cells and embryonic germ cells and marks all the cells of the epiblast.

If Cripto affects cell proliferations, I expect to see a difference between the percentage of proliferating cells between E5.5 *Cripto* null and wild type embryos. This is a straightforward approach. The main technical issue is to differentiate dividing cells present in the epiblast and other tissues such as visceral endoderm. This can be done using confocal microscopy.

4.5. Senescence-associated β-galactosidase activity marks apical vacuoles

The second part of my work showed that senescence-associated β-galactosidase activity marks the visceral endoderm and visceral yolk sac. Through the analysis of several markers and cell proliferation assays, we concluded that this phenomenon most likely reflects increased lysosomal activity in visceral endoderm cells that in turn, is linked to the nutritional role of the visceral endoderm layer of the conceptus. This is a previously unknown phenomenon of early embryos that has several implications. First, we noted that SA-β-gal staining follows a stereotypic pattern as the embryo progresses in development. This serves as a new cue for staging early post-implantation mouse embryos. Second, SA-β-gal staining appears to mark nutritional tissues. As such, analysis of SA-β-gal activity could help monitor the health of the embryo. Both of these characteristics are very useful in the analysis of mutant mouse embryos. From the human health point of view, this is particularly important since the visceral endoderm and yolk sac provide the nutrition of the embryo before the embryo-maternal interphase is established through the placenta (Zohn and Sarkar, 2010).

An intriguing discovery from our studies is that in mouse embryos the SA-β-gal assay does not indicate senescence as it does in *in vitro* studies. This is a sobering lesson that illustrates the caveats of directly extrapolating *in vitro* results to *in vivo* studies. As mentioned before, SA-β-gal staining marks senescent

human fibroblasts indicating acidic β-galactosidase activity ((Dimri et al., 1995). In this respect it is similar to reports that showed that SA-β-gal reflected acidic β-gal activity present in lysosomes of senescence cells and reflects high lysosomal activity. Therefore, there is no discrepancy between our results and those obtained in senescence studies using this assay, rather the problem seems to be in drawing conclusions from the extrapolation of tissue culture results to an organismal situation.

It is important to note that several studies published in respected journals have used the SA-β-gal assay to study senescence and aging (Liu et al., 2007). A cautionary note should be given to studies of senescence or aging in tissues involved in absortion of nutrients, since as our results suggest, the SA-β-gal assay marks nutritional tissues *in vivo*. Therefore, several markers of senescence should be used before a senescence diagnostic is given. In addition, two papers just came out demonstrated the senescence, similar to apoptosis, is a basic mechanism for shaping the embryo development (Munoz-Espin et al., 2013; Storer et al., 2013).

Overall, my work does not only enhance our understanding of normal mouse development, but also provide new insights that could impact human disease.

The study of abnormal developmental occurrences helps us broaden our knowledge and understanding about that how and why normal and abnormal

development occurs. Thirty percent of all human pregnancies are lost at early post-implantation stages when the embryo is establishing its axial polarity. Also, assisted reproduction technologies, have led to an increase in the number of monozygotic twins, which brings multiple problems such as birth weight discordance and premature births. Our understanding of the role of the visceral endoderm in embryonic patterning will provide some basic knowledge to prevent these defects.

Oncogenesis may be considered a recapitulation of embryogenesis in an inappropriate temporal and spatial manner. The genes known to perform critical roles during early embryogenesis are also expressed during the development of cancer. Cripto is an evident example. During gastrulation, Cripto is also expressed in primitive streak, which is an excellent model for the study of epithelial to mesenchymal transition (EMT). EMT has a role in cancer progression, specially the metastasis of carcinomas. Hence, understanding how the mechanisms of primitive streak formation will broaden our knowledge in cancer research.

My work leaves several questions unanswered, in the case of axial development and gastrulation there is a need to study the cell behaviours and advance to the molecular level to determine how exactly is the AVE controlling the expansion of Wnt signaling derived from the PVE. My studies on SA-β-gal staining provide new tools to study mechanisms of cellular transport in nutritional tissues. There is also a need to explore the utility of the SA-β-gal assay in other

mammals and in vertebrates in general. Such studies could help define homologies that in turn can illuminate novel paths of research in vertebrate developmental biology. New and exciting technologies are currently being developed for addressing these questions *in vivo* focusing on populations of cells that will make future studies highly rewarding.

APPENDIX I:

GENERATION OF A CONDITIONAL *WNT3* TRANSGENIC LINE USING THE *PIGGYBAC* TRANSPOSON SYSTEM

In *Cripto* mutants, the radialized expression of *Wnt3* in the visceral endoderm leads to radialized *Brachyury* expression in the proximal epiblast indicating an inductive event. However, we wanted to demonstrate that ectopic expression of *Wnt3* could lead to a secondary primitive streak using an independent method. Thus we aimed to create an inducible *Wnt3* trangenic mouse line to express *Wnt3* in the whole visceral endoderm using Ttr-Cre mice. In Ttr-cre mice, the transthyretin promoter drives the expression of Cre solely in the visceral endoderm layer. Transthyretin (Ttr) is a thyroid hormone transport protein secreted exclusively by cells of the visceral endoderm at early postimplantation stages (Kwon and Hadjantonakis, 2009).

We aimed to be able to induce a primitive streak in the extra embryonic ectoderm, a region of the embryo that has been shown to be responsive to canonical Wnt signaling (Popperl et al., 1997). To achieve this goal, we used the *piggybac* (*PB*) transposon system to generate a transgenic mouse line stably expressing *Wnt3*. The *PiggyBac* (*PB*) transposon can efficiently transpose vectors and chromosomes via a "cut and paste" mechanism (Figure.A1.1A).

We generated an inducible cassette to ectopically express *Wnt3* in a variety of tissues by combining it with tissue specific Cre driver transgenic lines. The piggybac construct contains a UbC (human ubiquitin) promoter, followed by a floxed β-galactosidase-neomycin resistance cassette containing a polyadenylation signal reiterated three times. This cassette is followed by a bicistronic construct consisting of the Wnt3 full coding sequence a 2A peptide

Figure. A1.1

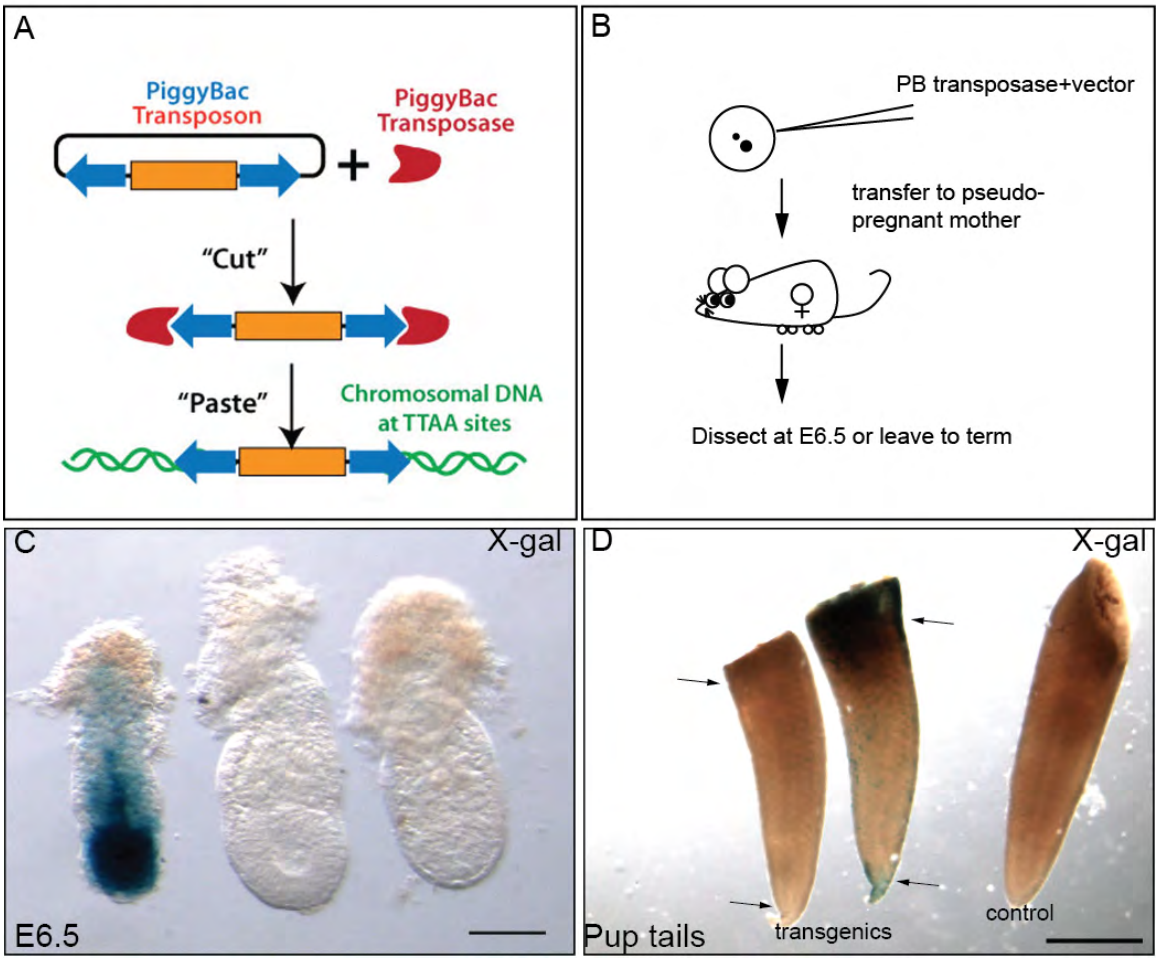
A
PiggyBac Transposon
PiggyBac Transposase
"Cut"
"Paste"
Chromosomal DNA at TTAA sites
B
PB transposase+vector
transfer to pseudo-pregnant mother
Dissect at E6.5 or leave to term
C
X-gal
E6.5
D
X-gal
Pup tails
transgenics
control

Figure A1.1. Generation of *Wnt3*-inducible transgenic mice using the *PiggyBac* transposon approach. A. Schematic representation of the *PiggyBac* transposon approach. The *PB* transposase cuts the gene fragment between the two ITRs and transfer it into target genomes. **B.** Strategy to generate transgenic animals. **C.** β-galatosidase assay to detect E6.5 transgenic embryos derived from founder parent. Transgenic embryos develops blue staining. **D.** X-gal staining for young transgenic founder animal tail. Two of the transgenic pups tails develops blue staining after β-galactosidase assay after one-hour staining developing time. Both of the transgenic tails are completely blue after one-day staining developing time, compared with the completely non-blue tails (Data not shown). Scale bars: 100 μm in C and 1 mm in D. Arrows in D mark skin cells positive for β-galactosidase staining.

linker and GFP. These sequences are flanked by specific inverted terminal repeat sequences (ITRs), which are recognized by the PB transposase. The powerful activity of the piggybac transposon system enables genes located between the two ITRs in the piggybac vector to be easily inserted into target genomes.

We microinjected *piggybac* transposase mRNA alongside with the piggybac vector into fertilized mouse eggs to generate transgenic animals (Figure.A1.1B). We obtained 13 mice from these injections and 10 were transgenic for a 77% success rate (Table.A1.1) (Figure.A1.1C, D). We also obtained 19 rats from these injections and 6 were transgenic for a 32% success rate (Table.A1.2). We analyzed 3 founders by crossing them with CD-1 females and analyzing the expression of the transgene using β-galactosidase assays (Figure.A1.2). Unfortunately, none of the transgenics expressed the transgene in visceral endoderm. The staining was present to the epiblast tissue and extraembryonic tissues but not in the visceral endoderm. These results prevented us from expressing the transgene in the visceral endoderm as originally planned.

The question of why the transgene is not expressed in the visceral endoderm cells remains unanswered. One possibility is that the transgenic embryos are mosaic, and the VE cells did not inherit the transgene. This is not likely since we have analyzed 3 lines and none of them show expression in the visceral endoderm. The mosaicism would also be reflected in epiblast cells.

Figure. A1.2

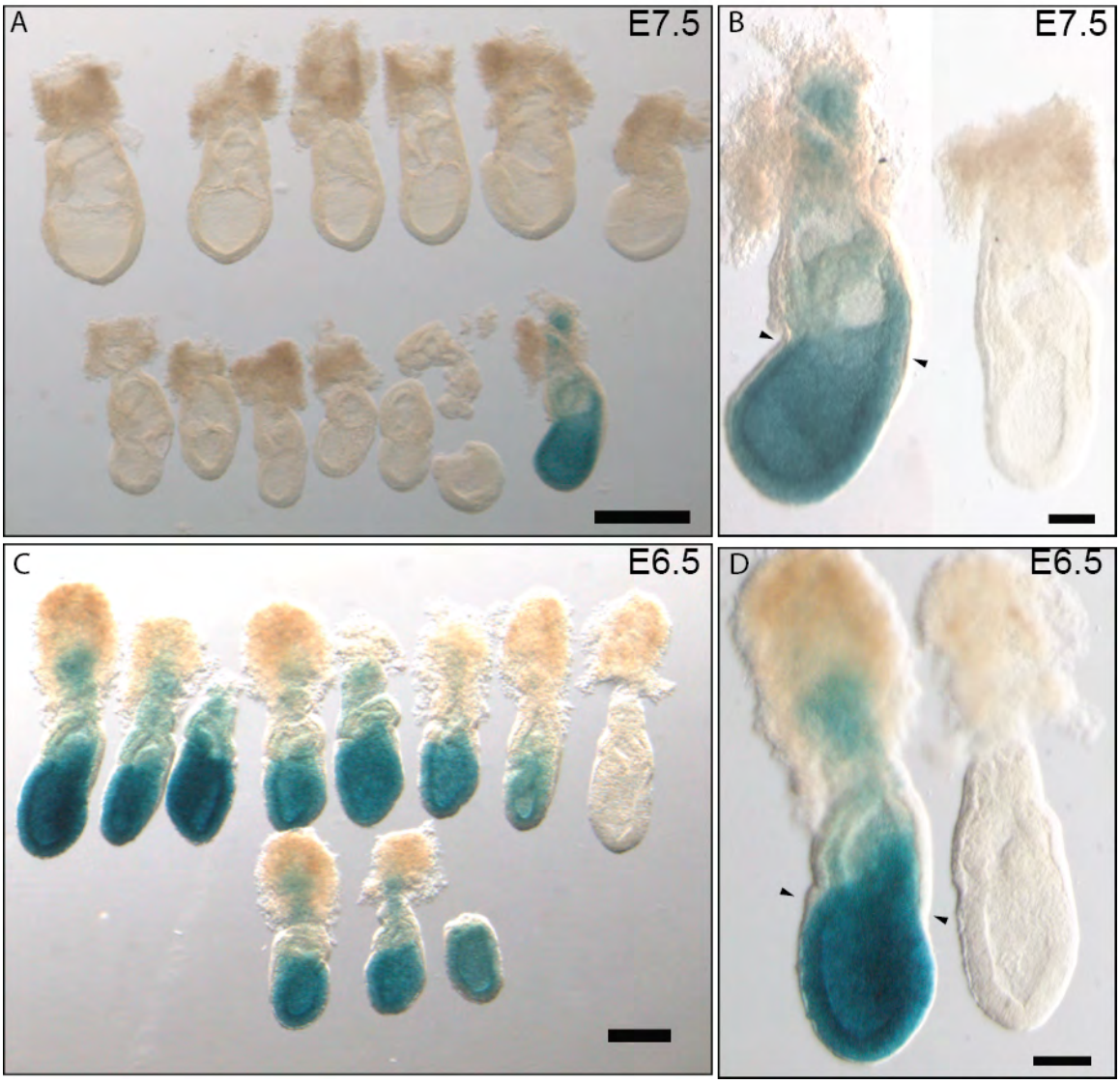

Figure A1.2. β-galactosidase analysis of F1 and F2 transgenic embryos. A. β-galactosidase staining for E7.5 F1 transgenic embryos. **B.** Higher magnification of stained and control embryos shown in A. The transgenic embryo show activation of the transgene in the epiblast, extra-embryonic ectoderm and parts of the ectoplacental cone but not in the visceral endoderm layer (arrowheads). **C.** β-galactosidase assay of E6.5 F2 transgenic embryos. **D.** Higher magnification a transgenic and a control embryo shown in C. The visceral endoderm does not express the transgene (arrowheads). Scale bars: 500 µm in A, 100 µum in B, 200 µm in C and 100 µm in D.

However, we did not observe mosaicism this tissue. The same argument can be put forward to disregard the possibility that the location of the transgene in the genome is to blame. Another possibility is that the human ubiquitin promoter is not active in visceral endoderm cells. This problem can be avoided by utilizing a promoter known to work in the visceral endoderm such as those of the *Transthyretin* and *Alfafetoprotein* genes (Kwon et al., 2006; Kwon and Hadjantonakis, 2009).

Regardless, these transgenic mice are useful in experiments designed to express *Wnt3* in embryonic tissues in combination with Cre reporter lines. More experiments are needed to generate a conditional mouse line that expresses *Wnt3* ectopically in the visceral endoderm.

The PB approach shows a much higher efficiency to produce transgenic animal comparted with the classic dsDNA pronuclear injection by microinjection double strand DNA into fertilized eggs (PB: 80% in mouse genome and 30% in rat genome vs. dsDNA 5% in mouse genome) (Costantini and Lacy, 1981; Stanford et al., 2001). The human genome has 35,000 human genes, which been sequenced and mapped. However, only 15% of them has related function assay. The *PB* transposon can be a promising way to serve as a gene-trap mutagenesis technique generates loss-of-function mutations and reports the expression of many mouse genes and thus promote the human genome study.

Table. A1.1. Summary of *PiggyBac* transgenic mouse experiments

Exp No.	Female No.	No. Embryos Transferred	No. Pups Born (% total)	No. Transgenics (% Pups Born)
1	1	19	2	1
2	3	57	11	9
Total	4	76	13 (17%)	10 (77%)

Table.A1.2. Summary of *PiggyBac* transgenic rat experiments

Exp No.	Female No.	No. Embryos Transferred	No. Pups Born (% total)	No. Transgenics (% Pups Born)
1	2	38	19 (50%)	6 (32%)

APPENDIX II:

EXPRESSION PROFILE OF THREE *TBX* GENES IN EARLY POST-IMPLANTATION MOUSE EMBRYOS

T-box genes are transcription factors characterized by a common DNA binding domain known as the T-box that binds a palindromic sequence as a dimer, with each monomer binding half of the sequence, or T-half site (5'-AGGTGTGAAATT-3') (Kispert and Hermann, 1993; Papapetrou et al., 1997; Naiche et al., 2005). The T-box gene family first came to the attention of mouse geneticists in 1927 with the discovery of a mutation, *Brachyury* (also known as *T*). Homozygous *T* embryos die at early post-implantation stages due to gastrulation defects but heterozygous embryos have truncated tails making them easy to recognize (Dobrovolskaia-Zavadskaia, 1927; Papaioannou, 1999).

The T- box genes are present in all metazoans, and are important regulators of a wide variety of developmental processes ranging from early embryonic cell fate decisions and axis formation to organogenesis (Naiche et al., 2005). The T-box genes also show dosage sensitivity in other species. In humans, mutations in T-box genes leads to dysmorphic syndromes and *Tbx2* and *Tbx3* have been implicated in tumorigenesis (Naiche et al., 2005).

Due to their fundamental role in development we decided to characterize the expression of Tbx genes in early mouse development. Initially, we conducted RT PCR analysis of early post-implantation embryos ranging from E5.5 to E6.5. From these experiments we decided to concentrate on four genes, *Tbx3*, *Tbx4* and *Tbx20* that were clearly expressed in early embryos.

In order to characterize their expression pattern, whole mount *in situ* hybridization studies were conducted for all three genes. Our results revealed

robust expression in specific regions of the embryo as opposed to ubiquitous expression.

Tbx3 is strongly expressed in the extra-embryonic visceral endoderm at E 6.5 and E 7.5 embryos (Figure.A2.1). *Tbx3* homozygous mutant mice are embryonic lethal and have yolk sac, limb and mammary gland defects (Naiche and Papaioannou, 2003). *Tbx3* expression in extra-embryonic visceral endoderm can explain the yolk sac defects. Limb and mammary gland defects are likely due to later expression of *Tbx3* in these tissues.

Tbx4 expression is restricted to the developing allantois at E 7.5 embryos (Figure.A2.2A). Tbx4 mutations cause hind limb and allantois defects in mice. The heterozygous mice for *Tbx4* mutation causes reduced allantois growth rate, while the homozygous mice died of allantois defects (Naiche and Papaioannou, 2003). The expression is correlated well with the mutant phenotype.

Tbx20 is present in a crescent shape pattern that demarcates the primary heart field and the developing allantois (Figure.A2.2B). *Tbx20* is involved in heart development, including cardiogenic mesoderm, cardiac crescent and looping heart tube. The heterozygous mice for *Tbx20* mutation causes abnormal heart chamber formation and congenital heart diseases in mice (Stennard et al., 2005). The expression on the heart crescent is correlated well with the mutant phenotype. However, there is no report of *Tbx 20* expression in the allantois before.

The expression of *Tbx4* and *Tbx20* overlaps on the heart crescent region

during early development suggesting these two proteins have the potential to heterodimerize to regulate the heart formation. The relevance for this interaction between these two T-box proteins during the development of heart will be an interesting topic to be addressed.

Figure. A2.1

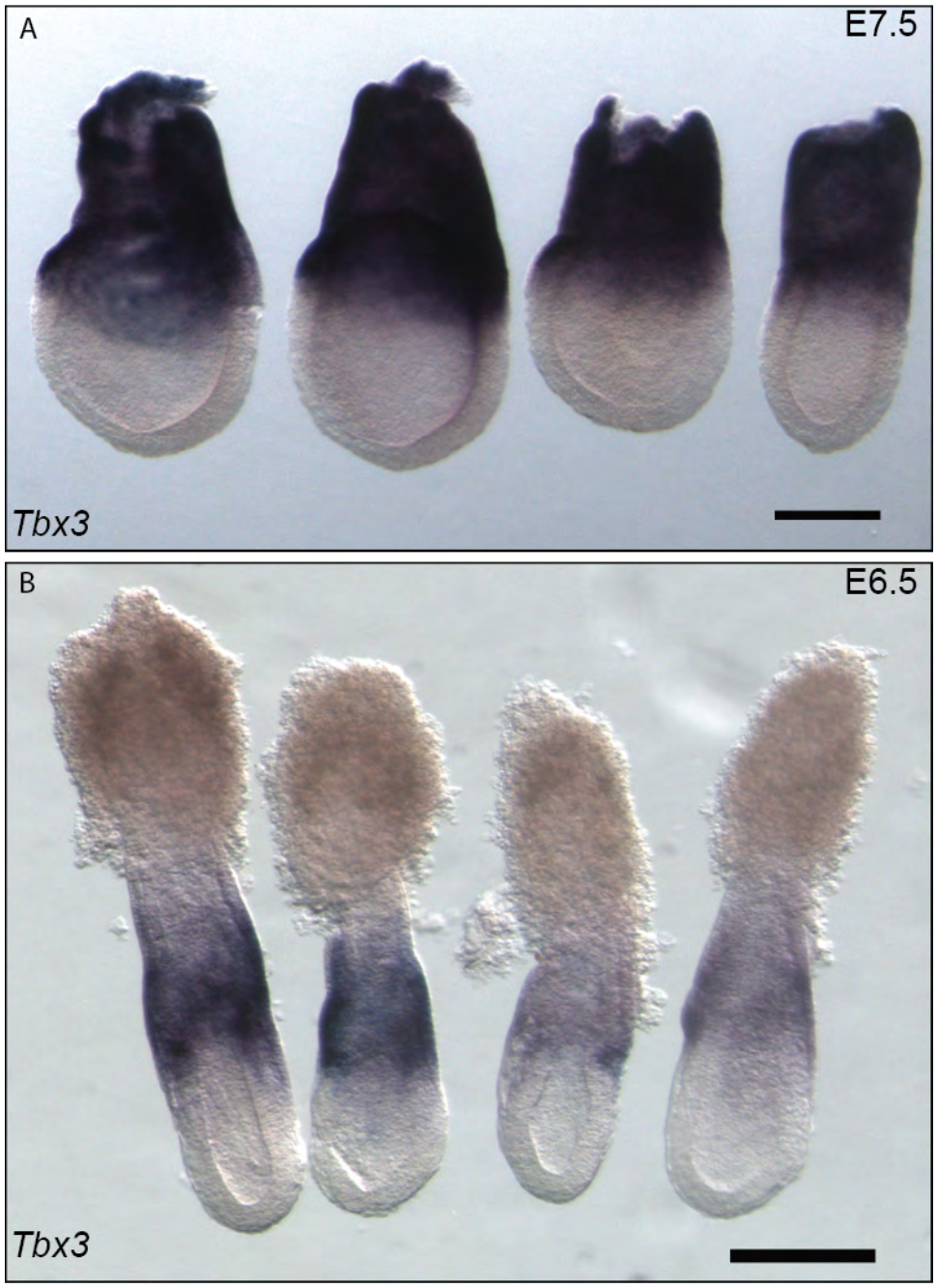

Figure A2.1. Whole mount *in situ* hybridization analysis of *Tbx3* expression in early post-implantation mouse embryos. A. In E7.5 embryos, *Tbx3* mRNA is exclusively present in the extra-embryonic visceral endoderm. **B**. The expression of Tbx3 is already restricted to the extra-embryonic ectoderm in E6.5 embryos. Scale bars: 200 μm.

Figure. A2.2

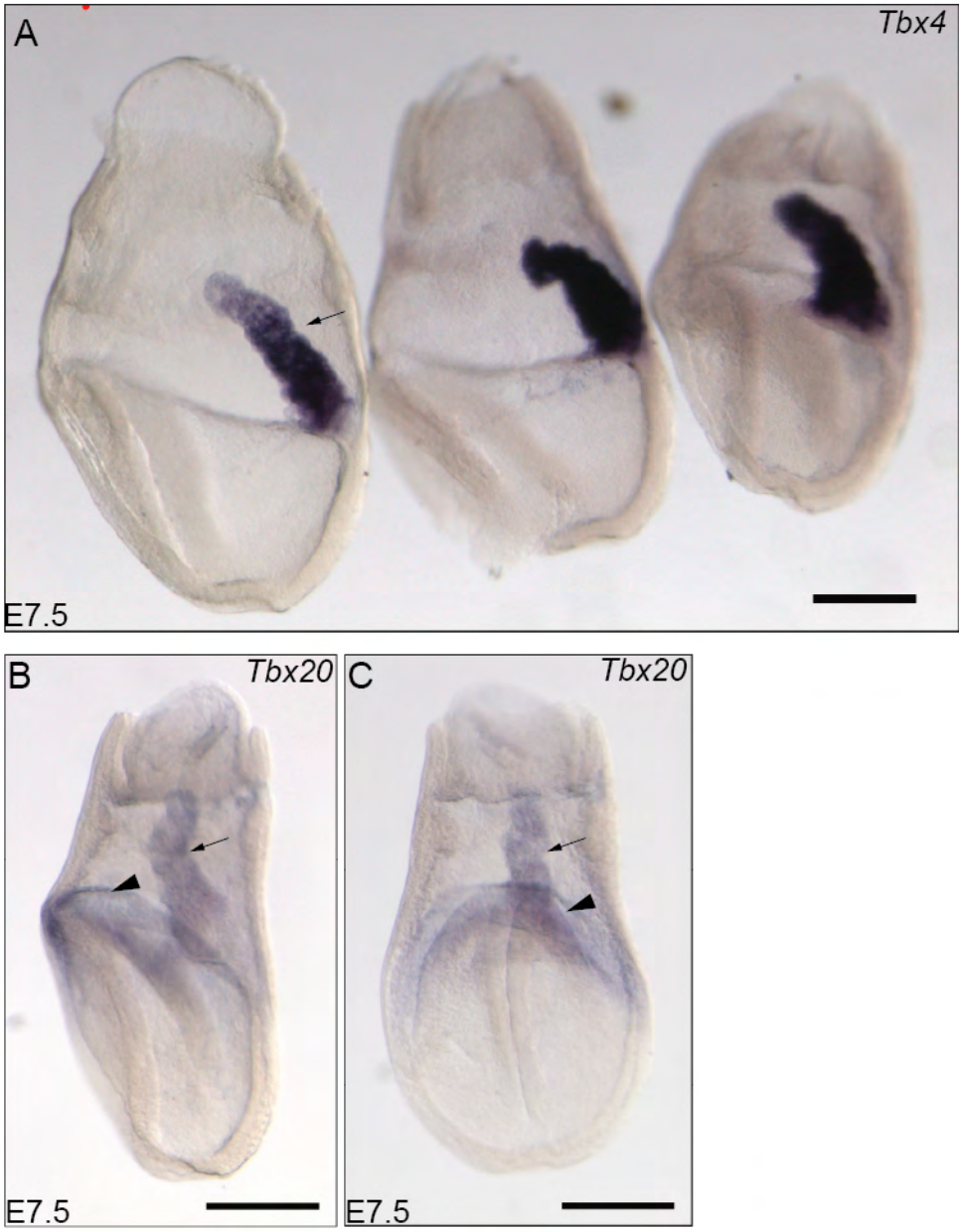

Figure A2.2. Whole mount *in situ* hybridization analysis of the expression of *Tbx4* and *Tbx20*. A. E7.5 embryos are assayed for *Tbx4* expression. *Tbx4* mRNA is exclusively present in the developing allantois (arrow). **B**. Analysis of the expression of *Tbx20* in E7.5 embryos. *Tbx20* mRNA is present in the heart crescent (arrowheads) and in the allantois (arrows). Scale bars: 100 μm.

BIBLIOGRAPHY

Acampora, D., Mazan, S., Lallemand, Y., Avantaggiato, V., Maury, M., Simeone, A. and Brulet, P. (1995) 'Forebrain and midbrain regions are deleted in Otx2-/- mutants due to a defective anterior neuroectoderm specification during gastrulation', *Development* 121(10): 3279-90.

Al-Mohanna, M. A., Manogaran, P. S., Al-Mukhalafi, Z., K, A. A.-H. and Aboussekhra, A. (2004) 'The tumor suppressor p16(INK4a) gene is a regulator of apoptosis induced by ultraviolet light and cisplatin', *Oncogene* 23(1): 201-12.

Arai, A., Yamamoto, K. and Toyama, J. (1997) 'Murine cardiac progenitor cells require visceral embryonic endoderm and primitive streak for terminal differentiation', *Dev Dyn* 210(3): 344-53.

Arnold, S. J. and Robertson, E. J. (2009) 'Making a commitment: cell lineage allocation and axis patterning in the early mouse embryo', *Nat Rev Mol Cell Biol* 10(2): 91-103.

Assemat, E., Vinot, S., Gofflot, F., Linsel-Nitschke, P., Illien, F., Chatelet, F., Verroust, P., Louvet-Vallee, S., Rinninger, F. and Kozyraki, R. (2005) 'Expression and role of cubilin in the internalization of nutrients during the peri-implantation development of the rodent embryo', *Biol Reprod* 72(5): 1079-86.

Bachvarova, R. F., Skromne, I. and Stern, C. D. (1998) 'Induction of primitive streak and Hensen's node by the posterior marginal zone in the early chick embryo', *Development* 125(17): 3521-34.

Baker, D. J., Wijshake, T., Tchkonia, T., LeBrasseur, N. K., Childs, B. G., van de Sluis, B., Kirkland, J. L. and van Deursen, J. M. (2011) 'Clearance of p16Ink4a-positive senescent cells delays ageing-associated disorders', *Nature* 479(7372): 232-6.

Bally-Cuif, L. and Boncinelli, E. (1997) 'Transcription factors and head formation in vertebrates', *Bioessays* 19(2): 127-35.

Bandyopadhyay, A., Yadav, P. S. and Prashar, P. (2013) 'BMP signaling in development and diseases: a pharmacological perspective', *Biochem Pharmacol* 85(7): 857-64.

Barbacci, E., Reber, M., Ott, M. O., Breillat, C., Huetz, F. and Cereghini, S. (1999) 'Variant hepatocyte nuclear factor 1 is required for visceral endoderm specification', *Development* 126(21): 4795-805.

Barrow, J. R. (2006) 'Wnt/PCP signaling: a veritable polar star in establishing patterns of polarity in embryonic tissues', *Semin Cell Dev Biol* 17(2): 185-93.

Barrow, J. R., Howell, W. D., Rule, M., Hayashi, S., Thomas, K. R., Capecchi, M. R. and McMahon, A. P. (2007) 'Wnt3 signaling in the epiblast is required for proper orientation of the anteroposterior axis', *Dev Biol* 312(1): 312-20.

Beddington, R. S. and Robertson, E. J. (1998) 'Anterior patterning in mouse', *Trends Genet* 14(7): 277-84.

Beddington, R. S. and Robertson, E. J. (1999) 'Axis development and early asymmetry in mammals', *Cell* 96(2): 195-209.

Belaoussoff, M., Farrington, S. M. and Baron, M. H. (1998) 'Hematopoietic induction and respecification of A-P identity by visceral endoderm signaling in the mouse embryo', *Development* 125(24): 5009-18.

Ben-Haim, N., Lu, C., Guzman-Ayala, M., Pescatore, L., Mesnard, D., Bischofberger, M., Naef, F., Robertson, E. J. and Constam, D. B. (2006) 'The nodal precursor acting via activin receptors induces mesoderm by maintaining a source of its convertases and BMP4', *Dev Cell* 11(3): 313-23.

Ben-Porath, I. and Weinberg, R. A. (2005) 'The signals and pathways activating cellular senescence', *Int J Biochem Cell Biol* 37(5): 961-76.

Bernard, O., Ripoche, M. A. and Bennett, D. (1977) 'Distribution of maternal immunoglobulins in the mouse uterus and embryo in the days after implantation', *J Exp Med* 145(1): 58-75.

Bianco, C., Strizzi, L., Rehman, A., Normanno, N., Wechselberger, C., Sun, Y., Khan, N., Hirota, M., Adkins, H., Williams, K. et al. (2003) 'A Nodal- and ALK4-independent signaling pathway activated by Cripto-1 through Glypican-1 and c-Src', *Cancer Res* 63(6): 1192-7.

Biben, C., Stanley, E., Fabri, L., Kotecha, S., Rhinn, M., Drinkwater, C., Lah, M., Wang, C. C., Nash, A., Hilton, D. et al. (1998) 'Murine cerberus homologue mCer-1: a candidate anterior patterning molecule', *Dev Biol* 194(2): 135-51.

Bielinska, M., Narita, N. and Wilson, D. B. (1999) 'Distinct roles for visceral endoderm during embryonic mouse development', *Int J Dev Biol* 43(3): 183-205.

Boucher, D. M. and Pedersen, R. A. (1996) 'Induction and differentiation of extra-embryonic mesoderm in the mouse', *Reprod Fertil Dev* 8(4): 765-77.

Bowman, P. D., Meek, R. L. and Daniel, C. W. (1975) 'Aging of human fibroblasts in vitro. Correlations between DNA synthetic ability and cell size', *Exp Cell Res* 93(1): 184-90.

Brennan, J., Lu, C. C., Norris, D. P., Rodriguez, T. A., Beddington, R. S. and Robertson, E. J. (2001) 'Nodal signalling in the epiblast patterns the early mouse embryo', *Nature* 411(6840): 965-9.

Campisi, J. (2001) 'Cellular senescence as a tumor-suppressor mechanism', *Trends Cell Biol* 11(11): S27-31.

Campisi, J. and d'Adda di Fagagna, F. (2007) 'Cellular senescence: when bad things happen to good cells', *Nat Rev Mol Cell Biol* 8(9): 729-40.

Chen, W. S., Manova, K., Weinstein, D. C., Duncan, S. A., Plump, A. S., Prezioso, V. R., Bachvarova, R. F. and Darnell, J. E., Jr. (1994) 'Disruption of the HNF-4 gene, expressed in visceral endoderm, leads to cell death in embryonic ectoderm and impaired gastrulation of mouse embryos', *Genes Dev* 8(20): 2466-77.

Chenn, A. and Walsh, C. A. (2002) 'Regulation of cerebral cortical size by control of cell cycle exit in neural precursors', *Science* 297(5580): 365-9.

Chien, A. J., Conrad, W. H. and Moon, R. T. (2009) 'A Wnt survival guide: from flies to human disease', *J Invest Dermatol* 129(7): 1614-27.

Chu, J., Ding, J., Jeays-Ward, K., Price, S. M., Placzek, M. and Shen, M. M. (2005) 'Non-cell-autonomous role for Cripto in axial midline formation during vertebrate embryogenesis', *Development* 132(24): 5539-51.

Clements, W. K., Ong, K. G. and Traver, D. (2009) 'Zebrafish wnt3 is expressed in developing neural tissue', *Dev Dyn* 238(7): 1788-95.

Conlon, F. L., Barth, K. S. and Robertson, E. J. (1991) 'A novel retrovirally induced embryonic lethal mutation in the mouse: assessment of the developmental fate of embryonic stem cells homozygous for the 413.d proviral integration', *Development* 111(4): 969-81.

Conlon, F. L., Lyons, K. M., Takaesu, N., Barth, K. S., Kispert, A., Herrmann, B. and Robertson, E. J. (1994) 'A primary requirement for nodal in the formation and maintenance of the primitive streak in the mouse', *Development* 120(7): 1919-28.

Conlon, F. L. a. B., R. (1995) 'Mouse Gastrulation from a Frog's Prospective. ', *Seminars in Developmental Biology.* 6(4): 249-256.

Costantini, F. and Lacy, E. (1981) 'Introduction of a rabbit beta-globin gene into the mouse germ line', *Nature* 294(5836): 92-4.

Coucouvanis, E. and Martin, G. R. (1995) 'Signals for death and survival: a two-step mechanism for cavitation in the vertebrate embryo', *Cell* 83(2): 279-87.

D'Andrea, D., Liguori, G. L., Le Good, J. A., Lonardo, E., Andersson, O., Constam, D. B., Persico, M. G. and Minchiotti, G. (2008) 'Cripto promotes A-P

axis specification independently of its stimulatory effect on Nodal autoinduction', *J Cell Biol* 180(3): 597-605.

De Robertis, E. M., Larrain, J., Oelgeschlager, M. and Wessely, O. (2000) 'The establishment of Spemann's organizer and patterning of the vertebrate embryo', *Nat Rev Genet* 1(3): 171-81.

Debacq-Chainiaux, F., Erusalimsky, J. D., Campisi, J. and Toussaint, O. (2009) 'Protocols to detect senescence-associated beta-galactosidase (SA-betagal) activity, a biomarker of senescent cells in culture and in vivo', *Nat Protoc* 4(12): 1798-806.

Di Leonardo, A., Linke, S. P., Clarkin, K. and Wahl, G. M. (1994) 'DNA damage triggers a prolonged p53-dependent G1 arrest and long-term induction of Cip1 in normal human fibroblasts', *Genes Dev* 8(21): 2540-51.

Dimri, G. P., Lee, X., Basile, G., Acosta, M., Scott, G., Roskelley, C., Medrano, E. E., Linskens, M., Rubelj, I., Pereira-Smith, O. et al. (1995) 'A biomarker that identifies senescent human cells in culture and in aging skin in vivo', *Proc Natl Acad Sci U S A* 92(20): 9363-7.

Ding, J., Yang, L., Yan, Y. T., Chen, A., Desai, N., Wynshaw-Boris, A. and Shen, M. M. (1998) 'Cripto is required for correct orientation of the anterior-posterior axis in the mouse embryo', *Nature* 395(6703): 702-7.

Ding, S., Wu, X., Li, G., Han, M., Zhuang, Y. and Xu, T. (2005) 'Efficient transposition of the piggyBac (PB) transposon in mammalian cells and mice', *Cell* 122(3): 473-83.

Dobrovolskaia-Zavadskaia, N. (1927) 'Sur la mortification spontan´ee de la queue chez la
souris nouveau-n´ee et sur l'existence d'un caract`ere (facteur) h´er´editaire "non viable".', *C. R. Acad. Sci. Biol.* 97: 114-16.

Donnison, M., Beaton, A., Davey, H. W., Broadhurst, R., L'Huillier, P. and Pfeffer, P. L. (2005) 'Loss of the extraembryonic ectoderm in Elf5 mutants leads to defects in embryonic patterning', *Development* 132(10): 2299-308.

Dorey, K. and Amaya, E. (2010) 'FGF signalling: diverse roles during early vertebrate embryogenesis', *Development* 137(22): 3731-42.

Downs, K. M. and Davies, T. (1993) 'Staging of gastrulating mouse embryos by morphological landmarks in the dissecting microscope', *Development* 118(4): 1255-66.

Dutko, J. A. and Mullins, M. C. (2011) 'SnapShot: BMP signaling in development', *Cell* 145(4): 636, 636 e1-2.

Dziadek, M. (1978) 'Modulation of alphafetoprotein synthesis in the early postimplantation mouse embryo', *J Embryol Exp Morphol* 46: 135-46.

Dziadek, M. and Adamson, E. (1978) 'Localization and synthesis of alphafoetoprotein in post-implantation mouse embryos', *J Embryol Exp Morphol* 43: 289-313.

Dziadek, M. A. and Andrews, G. K. (1983) 'Tissue specificity of alpha-fetoprotein messenger RNA expression during mouse embryogenesis', *EMBO J* 2(4): 549-54.

Dzierzak, E. and Medvinsky, A. (1995) 'Mouse embryonic hematopoiesis', *Trends Genet* 11(9): 359-66.

Erusalimsky, J. D. and Kurz, D. J. (2005) 'Cellular senescence in vivo: its relevance in ageing and cardiovascular disease', *Exp Gerontol* 40(8-9): 634-42.

Espinosa, J. M., Verdun, R. E. and Emerson, B. M. (2003) 'p53 functions through stress- and promoter-specific recruitment of transcription initiation components before and after DNA damage', *Mol Cell* 12(4): 1015-27.

Exalto, N. (1995) 'Early human nutrition', *Eur J Obstet Gynecol Reprod Biol* 61(1): 3-6.

Farnebo, M., Bykov, V. J. and Wiman, K. G. (2010) 'The p53 tumor suppressor: a master regulator of diverse cellular processes and therapeutic target in cancer', *Biochem Biophys Res Commun* 396(1): 85-9.

Ferkowicz, M. J. and Yoder, M. C. (2005) 'Blood island formation: longstanding observations and modern interpretations', *Exp Hematol* 33(9): 1041-7.

Foley, A. C., Korol, O., Timmer, A. M. and Mercola, M. (2007) 'Multiple functions of Cerberus cooperate to induce heart downstream of Nodal', *Dev Biol* 303(1): 57-65.

Freeman, S. J. (1990) 'Functions of extraembryonic membranes. In *Postimplantation Mammalian Embryos: A Practical Approach.* (eds. A.J. Copp and D.L. Cockroft)', *New York: Oxford University Press*: pp.249-265.

Fujiwara, T., Dehart, D. B., Sulik, K. K. and Hogan, B. L. (2002) 'Distinct requirements for extra-embryonic and embryonic bone morphogenetic protein 4

in the formation of the node and primitive streak and coordination of left-right asymmetry in the mouse', *Development* 129(20): 4685-96.

Gardner, R. L. (1983) 'Origin and differentiation of extraembryonic tissues in the mouse', *Int Rev Exp Pathol* 24: 63-133.

Garriock, R. J., Warkman, A. S., Meadows, S. M., D'Agostino, S. and Krieg, P. A. (2007) 'Census of vertebrate Wnt genes: isolation and developmental expression of Xenopus Wnt2, Wnt3, Wnt9a, Wnt9b, Wnt10a, and Wnt16', *Dev Dyn* 236(5): 1249-58.

Gartel, A. L. and Tyner, A. L. (2002) 'The role of the cyclin-dependent kinase inhibitor p21 in apoptosis', *Mol Cancer Ther* 1(8): 639-49.

Gerhart, J. (1999) 'Pieter Nieuwkoop's contributions to the understanding of meso-endoderm induction and neural induction in chordate development', *Int J Dev Biol* 43(7): 605-13.

Gil, J. and Peters, G. (2006) 'Regulation of the INK4b-ARF-INK4a tumour suppressor locus: all for one or one for all', *Nat Rev Mol Cell Biol* 7(9): 667-77.

Gilbert, S. F. (2000) 'Developmental Biology. 6th edition.', *Early Development in Fish*.

Gire, V., Roux, P., Wynford-Thomas, D., Brondello, J. M. and Dulic, V. (2004) 'DNA damage checkpoint kinase Chk2 triggers replicative senescence', *EMBO J* 23(13): 2554-63.

Going, J. J., Stuart, R. C., Downie, M., Fletcher-Monaghan, A. J. and Keith, W. N. (2002) ''Senescence-associated' beta-galactosidase activity in the upper gastrointestinal tract', *J Pathol* 196(4): 394-400.

Gospodarowicz, D. and Moran, J. S. (1975) 'Mitogenic effect of fibroblast growth factor on early passage cultures of human and murine fibroblasts', *J Cell Biol* 66(2): 451-7.

Granier, C., Gurchenkov, V., Perea-Gomez, A., Camus, A., Ott, S., Papanayotou, C., Iranzo, J., Moreau, A., Reid, J., Koentges, G. et al. (2011) 'Nodal cis-regulatory elements reveal epiblast and primitive endoderm heterogeneity in the peri-implantation mouse embryo', *Dev Biol* 349(2): 350-62.

Griffin, K. J., Amacher, S. L., Kimmel, C. B. and Kimelman, D. (1998) 'Molecular identification of spadetail: regulation of zebrafish trunk and tail mesoderm formation by T-box genes', *Development* 125(17): 3379-88.

Harland, R. and Gerhart, J. (1997) 'Formation and function of Spemann's organizer', *Annu Rev Cell Dev Biol* 13: 611-67.

Hayflick, L. (1965) 'The Limited in Vitro Lifetime of Human Diploid Cell Strains', *Exp Cell Res* 37: 614-36.

Hayflick, L. and Moorhead, P. S. (1961) 'The serial cultivation of human diploid cell strains', *Exp Cell Res* 25: 585-621.

Heasman, J. (2006) 'Patterning the early Xenopus embryo', *Development* 133(7): 1205-17.

Hemann, M. T., Hackett, J., A, I. J. and Greider, C. W. (2000) 'Telomere length, telomere-binding proteins, and DNA damage signaling', *Cold Spring Harb Symp Quant Biol* 65: 275-9.

Herbig, U., Jobling, W. A., Chen, B. P., Chen, D. J. and Sedivy, J. M. (2004) 'Telomere shortening triggers senescence of human cells through a pathway involving ATM, p53, and p21(CIP1), but not p16(INK4a)', *Mol Cell* 14(4): 501-13.

Hirst, C. E., Ng, E. S., Azzola, L., Voss, A. K., Thomas, T., Stanley, E. G. and Elefanty, A. G. (2006) 'Transcriptional profiling of mouse and human ES cells identifies SLAIN1, a novel stem cell gene', *Dev Biol* 293(1): 90-103.

Hogan, B., Beddington, R., Costantini, F., and Lacy, E. (1994) 'Manipulating the Mouse Embryo: A laboratory Manual. ', *Cold Spring Harbor, NY: Cold Spring Harbor Press*.

Hohn, A., Jung, T., Grimm, S. and Grune, T. (2010) 'Lipofuscin-bound iron is a major intracellular source of oxidants: role in senescent cells', *Free Radic Biol Med* 48(8): 1100-8.

Huelsken, J., Vogel, R., Brinkmann, V., Erdmann, B., Birchmeier, C. and Birchmeier, W. (2000) 'Requirement for beta-catenin in anterior-posterior axis formation in mice', *J Cell Biol* 148(3): 567-78.

Huxham, I. M. and Beck, F. (1985) 'Maternal transferrin uptake by and transfer across the visceral yolk sac of the early postimplantation rat conceptus in vitro', *Dev Biol* 110(1): 75-83.

Ichimura, T., Hatae, T., Sakurai, T. and Ishida, T. (1994) 'Three-dimensional architecture of the tubular endocytic apparatus and paramembranous networks of the endoplasmic reticulum in the rat visceral yolk-sac endoderm', *Cell Tissue Res* 278(2): 353-61.

Ishikawa, T. O., Tamai, Y., Li, Q., Oshima, M. and Taketo, M. M. (2003) 'Requirement for tumor suppressor Apc in the morphogenesis of anterior and ventral mouse embryo', *Dev Biol* 253(2): 230-46.

Jackson, J. G. and Pereira-Smith, O. M. (2006) 'p53 is preferentially recruited to the promoters of growth arrest genes p21 and GADD45 during replicative senescence of normal human fibroblasts', *Cancer Res* 66(17): 8356-60.

Jackson, S. A., Schiesser, J., Stanley, E. G. and Elefanty, A. G. (2010) 'Differentiating embryonic stem cells pass through 'temporal windows' that mark responsiveness to exogenous and paracrine mesendoderm inducing signals', *PLoS One* 5(5): e10706.

Johnson, M. H. and Ziomek, C. A. (1981) 'The foundation of two distinct cell lineages within the mouse morula', *Cell* 24(1): 71-80.

Jun, J. I. and Lau, L. F. (2010) 'The matricellular protein CCN1 induces fibroblast senescence and restricts fibrosis in cutaneous wound healing', *Nat Cell Biol* 12(7): 676-85.

Kawamura, N., Sun-Wada, G. H., Aoyama, M., Harada, A., Takasuga, S., Sasaki, T. and Wada, Y. (2012) 'Delivery of endosomes to lysosomes via

microautophagy in the visceral endoderm of mouse embryos', *Nat Commun* 3: 1071.

Kawano, Y. and Kypta, R. (2003) 'Secreted antagonists of the Wnt signalling pathway', *J Cell Sci* 116(Pt 13): 2627-34.

Keller, G. M. (1995) 'In vitro differentiation of embryonic stem cells', *Curr Opin Cell Biol* 7(6): 862-9.

Kelly, O. G., Pinson, K. I. and Skarnes, W. C. (2004) 'The Wnt co-receptors Lrp5 and Lrp6 are essential for gastrulation in mice', *Development* 131(12): 2803-15.

Kemp, C. (2007) 'the roles of wnt signaling in early mouse development and embryonic stem cells', *Functional Development and Embryology* 1(1): 1-13.

Kemp, C., Willems, E., Abdo, S., Lambiv, L. and Leyns, L. (2005) 'Expression of all Wnt genes and their secreted antagonists during mouse blastocyst and postimplantation development', *Dev Dyn* 233(3): 1064-75.

Kimura, C., Shen, M. M., Takeda, N., Aizawa, S. and Matsuo, I. (2001) 'Complementary functions of Otx2 and Cripto in initial patterning of mouse epiblast', *Dev Biol* 235(1): 12-32.

Kimura-Yoshida, C., Nakano, H., Okamura, D., Nakao, K., Yonemura, S., Belo, J. A., Aizawa, S., Matsui, Y. and Matsuo, I. (2005) 'Canonical Wnt signaling and its antagonist regulate anterior-posterior axis polarization by guiding cell migration in mouse visceral endoderm', *Dev Cell* 9(5): 639-50.

Kirkwood, T. B. and Austad, S. N. (2000) 'Why do we age?', *Nature* 408(6809): 233-8.

Kispert, A. and Hermann, B. G. (1993) 'The Brachyury gene encodes a novel DNA binding protein', *EMBO J* 12(12): 4898-9.

Kochav, S. and Eyal-Giladi, H. (1971) 'Bilateral symmetry in chick embryo determination by gravity', *Science* 171(3975): 1027-9.

Konishi, T., Takeyasu, A., Natsume, T., Furusawa, Y. and Hieda, K. (2011) 'Visualization of heavy ion tracks by labeling 3'-OH termini of induced DNA strand breaks', *J Radiat Res* 52(4): 433-40.

Krizhanovsky, V., Yon, M., Dickins, R. A., Hearn, S., Simon, J., Miething, C., Yee, H., Zender, L. and Lowe, S. W. (2008) 'Senescence of activated stellate cells limits liver fibrosis', *Cell* 134(4): 657-67.

Kuhl, M. (2002) 'Non-canonical Wnt signaling in Xenopus: regulation of axis formation and gastrulation', *Semin Cell Dev Biol* 13(3): 243-9.

Kurz, D. J., Decary, S., Hong, Y. and Erusalimsky, J. D. (2000) 'Senescence-associated (beta)-galactosidase reflects an increase in lysosomal mass during replicative ageing of human endothelial cells', *J Cell Sci* 113 (Pt 20): 3613-22.

Kwon, G. S., Fraser, S. T., Eakin, G. S., Mangano, M., Isern, J., Sahr, K. E., Hadjantonakis, A. K. and Baron, M. H. (2006) 'Tg(Afp-GFP) expression marks primitive and definitive endoderm lineages during mouse development', *Dev Dyn* 235(9): 2549-58.

Kwon, G. S. and Hadjantonakis, A. K. (2009) 'Transthyretin mouse transgenes direct RFP expression or Cre-mediated recombination throughout the visceral endoderm', *Genesis* 47(7): 447-55.

Kwon, G. S., Viotti, M. and Hadjantonakis, A. K. (2008) 'The endoderm of the mouse embryo arises by dynamic widespread intercalation of embryonic and extraembryonic lineages', *Dev Cell* 15(4): 509-20.

Lawson, K. A. and Pedersen, R. A. (1987) 'Cell fate, morphogenetic movement and population kinetics of embryonic endoderm at the time of germ layer formation in the mouse', *Development* 101(3): 627-52.

Lee, B. Y., Han, J. A., Im, J. S., Morrone, A., Johung, K., Goodwin, E. C., Kleijer, W. J., DiMaio, D. and Hwang, E. S. (2006) 'Senescence-associated beta-galactosidase is lysosomal beta-galactosidase', *Aging Cell* 5(2): 187-95.

Leonardi, E., Girlando, S., Serio, G., Mauri, F. A., Perrone, G., Scampini, S., Dalla Palma, P. and Barbareschi, M. (1992) 'PCNA and Ki67 expression in breast carcinoma: correlations with clinical and biological variables', *J Clin Pathol* 45(5): 416-9.

Leyns, L., Bouwmeester, T., Kim, S. H., Piccolo, S. and De Robertis, E. M. (1997) 'Frzb-1 is a secreted antagonist of Wnt signaling expressed in the Spemann organizer', *Cell* 88(6): 747-56.

Liu, H., Fergusson, M. M., Castilho, R. M., Liu, J., Cao, L., Chen, J., Malide, D., Rovira, II, Schimel, D., Kuo, C. J. et al. (2007) 'Augmented Wnt signaling in a mammalian model of accelerated aging', *Science* 317(5839): 803-6.

Liu, P., Wakamiya, M., Shea, M. J., Albrecht, U., Behringer, R. R. and Bradley, A. (1999) 'Requirement for Wnt3 in vertebrate axis formation', *Nat Genet* 22(4): 361-5.

Logan, C. Y. and Nusse, R. (2004) 'The Wnt signaling pathway in development and disease', *Annu Rev Cell Dev Biol* 20: 781-810.

Lu, F. I., Thisse, C. and Thisse, B. (2011) 'Identification and mechanism of regulation of the zebrafish dorsal determinant', *Proc Natl Acad Sci U S A* 108(38): 15876-80.

Macleod, K. F., Sherry, N., Hannon, G., Beach, D., Tokino, T., Kinzler, K., Vogelstein, B. and Jacks, T. (1995) 'p53-dependent and independent expression of p21 during cell growth, differentiation, and DNA damage', *Genes Dev* 9(8): 935-44.

Majumdar, A., Vainio, S., Kispert, A., McMahon, J. and McMahon, A. P. (2003) 'Wnt11 and Ret/Gdnf pathways cooperate in regulating ureteric branching during metanephric kidney development', *Development* 130(14): 3175-85.

Maretto, S., Cordenonsi, M., Dupont, S., Braghetta, P., Broccoli, V., Hassan, A. B., Volpin, D., Bressan, G. M. and Piccolo, S. (2003) 'Mapping Wnt/beta-catenin signaling during mouse development and in colorectal tumors', *Proc Natl Acad Sci U S A* 100(6): 3299-304.

Martens, U. M., Chavez, E. A., Poon, S. S., Schmoor, C. and Lansdorp, P. M. (2000) 'Accumulation of short telomeres in human fibroblasts prior to replicative senescence', *Exp Cell Res* 256(1): 291-9.

Martinez, D. E. (1998) 'Mortality patterns suggest lack of senescence in hydra', *Exp Gerontol* 33(3): 217-25.

Marvin, M. J., Di Rocco, G., Gardiner, A., Bush, S. M. and Lassar, A. B. (2001) 'Inhibition of Wnt activity induces heart formation from posterior mesoderm', *Genes Dev* 15(3): 316-27.

Meehan, R. R., Barlow, D. P., Hill, R. E., Hogan, B. L. and Hastie, N. D. (1984) 'Pattern of serum protein gene expression in mouse visceral yolk sac and foetal liver', *EMBO J* 3(8): 1881-5.

Meek, R. L., Bowman, P. D. and Daniel, C. W. (1977) 'Establishment of mouse embryo cells in vitro. Relationship of DNA synthesis, senescence and malignant transformation', *Exp Cell Res* 107(2): 277-84.

Melk, A., Kittikowit, W., Sandhu, I., Halloran, K. M., Grimm, P., Schmidt, B. M. and Halloran, P. F. (2003) 'Cell senescence in rat kidneys in vivo increases with growth and age despite lack of telomere shortening', *Kidney Int* 63(6): 2134-43.

Mijaljica, D., Prescott, M. and Devenish, R. J. (2011) 'Microautophagy in mammalian cells: revisiting a 40-year-old conundrum', *Autophagy* 7(7): 673-82.

Mishima, K., Handa, J. T., Aotaki-Keen, A., Lutty, G. A., Morse, L. S. and Hjelmeland, L. M. (1999) 'Senescence-associated beta-galactosidase histochemistry for the primate eye', *Invest Ophthalmol Vis Sci* 40(7): 1590-3.

Mishina, Y., Suzuki, A., Ueno, N. and Behringer, R. R. (1995) 'Bmpr encodes a type I bone morphogenetic protein receptor that is essential for gastrulation during mouse embryogenesis', *Genes Dev* 9(24): 3027-37.

Mohamed, O. A., Clarke, H. J. and Dufort, D. (2004) 'Beta-catenin signaling marks the prospective site of primitive streak formation in the mouse embryo', *Dev Dyn* 231(2): 416-24.

Morrisey, E. E., Tang, Z., Sigrist, K., Lu, M. M., Jiang, F., Ip, H. S. and Parmacek, M. S. (1998) 'GATA6 regulates HNF4 and is required for differentiation of visceral endoderm in the mouse embryo', *Genes Dev* 12(22): 3579-90.

Mukhopadhyay, M., Shtrom, S., Rodriguez-Esteban, C., Chen, L., Tsukui, T., Gomer, L., Dorward, D. W., Glinka, A., Grinberg, A., Huang, S. P. et al. (2001) 'Dickkopf1 is required for embryonic head induction and limb morphogenesis in the mouse', *Dev Cell* 1(3): 423-34.

Munoz-Espin, D., Canamero, M., Maraver, A., Gomez-Lopez, G., Contreras, J., Murillo-Cuesta, S., Rodriguez-Baeza, A., Varela-Nieto, I., Ruberte, J., Collado, M. et al. (2013) 'Programmed cell senescence during mammalian embryonic development', *Cell* 155(5): 1104-18.

Nacher, V., Carretero, A., Navarro, M., Armengol, C., Llombart, C., Rodriguez, A., Herrero-Fresneda, I., Ayuso, E. and Ruberte, J. (2006) 'The quail mesonephros: a new model for renal senescence?', *J Vasc Res* 43(6): 581-6.

Naiche, L. A., Harrelson, Z., Kelly, R. G. and Papaioannou, V. E. (2005) 'T-box genes in vertebrate development', *Annu Rev Genet* 39: 219-39.

Naiche, L. A. and Papaioannou, V. E. (2003) 'Loss of Tbx4 blocks hindlimb development and affects vascularization and fusion of the allantois', *Development* 130(12): 2681-93.

Nielsen, G. P., Stemmer-Rachamimov, A. O., Shaw, J., Roy, J. E., Koh, J. and Louis, D. N. (1999) 'Immunohistochemical survey of p16INK4A expression in normal human adult and infant tissues', *Lab Invest* 79(9): 1137-43.

Niemann, S., Zhao, C., Pascu, F., Stahl, U., Aulepp, U., Niswander, L., Weber, J. L. and Muller, U. (2004) 'Homozygous WNT3 mutation causes tetra-amelia in a large consanguineous family', *Am J Hum Genet* 74(3): 558-63.

Norris, D. P. and Robertson, E. J. (1999) 'Asymmetric and node-specific nodal expression patterns are controlled by two distinct cis-acting regulatory elements', *Genes Dev* 13(12): 1575-88.

Nusse, R. and Varmus, H. E. (1982) 'Many tumors induced by the mouse mammary tumor virus contain a provirus integrated in the same region of the host genome', *Cell* 31(1): 99-109.

Ogryzko, V. V., Hirai, T. H., Russanova, V. R., Barbie, D. A. and Howard, B. H. (1996) 'Human fibroblast commitment to a senescence-like state in response to histone deacetylase inhibitors is cell cycle dependent', *Mol Cell Biol* 16(9): 5210-8.

Oulad-Abdelghani, M., Chazaud, C., Bouillet, P., Mattei, M. G., Dolle, P. and Chambon, P. (1998) 'Stra3/lefty, a retinoic acid-inducible novel member of the transforming growth factor-beta superfamily', *Int J Dev Biol* 42(1): 23-32.

Papaioannou, V. E. (1999) 'The ascendency of developmental genetics, or how the T complex educated a generation of developmental biologists', *Genetics* 151(2): 421-5.

Papapetrou, C., Edwards, Y. H. and Sowden, J. C. (1997) 'The T transcription factor functions as a dimer and exhibits a common human polymorphism Gly-177-Asp in the conserved DNA-binding domain', *FEBS Lett* 409(2): 201-6.

Parrinello, S., Samper, E., Krtolica, A., Goldstein, J., Melov, S. and Campisi, J. (2003) 'Oxygen sensitivity severely limits the replicative lifespan of murine fibroblasts', *Nat Cell Biol* 5(8): 741-7.

Pearce, J. J. and Evans, M. J. (1999) 'Mml, a mouse Mix-like gene expressed in the primitive streak', *Mech Dev* 87(1-2): 189-92.

Pendergrass, W. R., Lane, M. A., Bodkin, N. L., Hansen, B. C., Ingram, D. K., Roth, G. S., Yi, L., Bin, H. and Wolf, N. S. (1999) 'Cellular proliferation potential during aging and caloric restriction in rhesus monkeys (Macaca mulatta)', *J Cell Physiol* 180(1): 123-30.

Perea-Gomez, A., Camus, A., Moreau, A., Grieve, K., Moneron, G., Dubois, A., Cibert, C. and Collignon, J. (2004) 'Initiation of gastrulation in the mouse embryo is preceded by an apparent shift in the orientation of the anterior-posterior axis', *Curr Biol* 14(3): 197-207.

Perea-Gomez, A., Lawson, K. A., Rhinn, M., Zakin, L., Brulet, P., Mazan, S. and Ang, S. L. (2001) 'Otx2 is required for visceral endoderm movement and for the restriction of posterior signals in the epiblast of the mouse embryo', *Development* 128(5): 753-65.

Perea-Gomez, A., Vella, F. D., Shawlot, W., Oulad-Abdelghani, M., Chazaud, C., Meno, C., Pfister, V., Chen, L., Robertson, E., Hamada, H. et al. (2002) 'Nodal

antagonists in the anterior visceral endoderm prevent the formation of multiple primitive streaks', *Dev Cell* 3(5): 745-56.

Pereira, P. N., Dobreva, M. P., Graham, L., Huylebroeck, D., Lawson, K. A. and Zwijsen, A. N. (2011) 'Amnion formation in the mouse embryo: the single amniochorionic fold model', *BMC Dev Biol* 11: 48.

Persico, M. G., Liguori, G. L., Parisi, S., D'Andrea, D., Salomon, D. S. and Minchiotti, G. (2001) 'Cripto in tumors and embryo development', *Biochim Biophys Acta* 1552(2): 87-93.

Pfister, S., Steiner, K. A. and Tam, P. P. (2007) 'Gene expression pattern and progression of embryogenesis in the immediate post-implantation period of mouse development', *Gene Expr Patterns* 7(5): 558-73.

Popperl, H., Schmidt, C., Wilson, V., Hume, C. R., Dodd, J., Krumlauf, R. and Beddington, R. S. (1997) 'Misexpression of Cwnt8C in the mouse induces an ectopic embryonic axis and causes a truncation of the anterior neuroectoderm', *Development* 124(15): 2997-3005.

Rhinn, M., Dierich, A., Shawlot, W., Behringer, R. R., Le Meur, M. and Ang, S. L. (1998) 'Sequential roles for Otx2 in visceral endoderm and neuroectoderm for forebrain and midbrain induction and specification', *Development* 125(5): 845-56.

Rijsewijk, F., Schuermann, M., Wagenaar, E., Parren, P., Weigel, D. and Nusse, R. (1987) 'The Drosophila homolog of the mouse mammary oncogene int-1 is identical to the segment polarity gene wingless', *Cell* 50(4): 649-57.

Rivera-Perez, J. A. (2007) 'Axial specification in mice: ten years of advances and controversies', *J Cell Physiol* 213(3): 654-60.

Rivera-Perez, J. A., Jones, V. and Tam, P. P. (2010) 'Culture of whole mouse embryos at early postimplantation to organogenesis stages: developmental staging and methods', *Methods Enzymol* 476: 185-203.

Rivera-Perez, J. A., Mager, J. and Magnuson, T. (2003) 'Dynamic morphogenetic events characterize the mouse visceral endoderm', *Dev Biol* 261(2): 470-87.

Rivera-Perez, J. A. and Magnuson, T. (2005) 'Primitive streak formation in mice is preceded by localized activation of Brachyury and Wnt3', *Dev Biol* 288(2): 363-71.

Robb, L., Hartley, L., Begley, C. G., Brodnicki, T. C., Copeland, N. G., Gilbert, D. J., Jenkins, N. A. and Elefanty, A. G. (2000) 'Cloning, expression analysis, and chromosomal localization of murine and human homologues of a Xenopus mix gene', *Dev Dyn* 219(4): 497-504.

Robertson, E. J., Norris, D. P., Brennan, J. and Bikoff, E. K. (2003) 'Control of early anterior-posterior patterning in the mouse embryo by TGF-beta signalling', *Philos Trans R Soc Lond B Biol Sci* 358(1436): 1351-7.

Rodier, F. and Campisi, J. (2011) 'Four faces of cellular senescence', *J Cell Biol* 192(4): 547-56.

Rossant, J. (1986) 'Development of extraembryonic lineages in the mouse embryo. In Experimental approaches to mammalian embryonic development. (eds. J.Rossant and R.A. Pedersen)', *Cambridge University Press*: pp. 97-119.

Schier, A. F. (2003) 'Nodal signaling in vertebrate development', *Annu Rev Cell Dev Biol* 19: 589-621.

Schier, A. F. (2009) 'Nodal morphogens', *Cold Spring Harb Perspect Biol* 1(5): a003459.

Schier, A. F., Neuhauss, S. C., Helde, K. A., Talbot, W. S. and Driever, W. (1997) 'The one-eyed pinhead gene functions in mesoderm and endoderm formation in zebrafish and interacts with no tail', *Development* 124(2): 327-42.

Schier, A. F. and Shen, M. M. (2000) 'Nodal signalling in vertebrate development', *Nature* 403(6768): 385-9.

Schmidt, W. (1992) 'The amniotic fluid compartment: the fetal habitat', *Adv Anat Embryol Cell Biol* 127: 1-100.

Schneider, E. L., Mitsui, Y., Au, K. S. and Shorr, S. S. (1977) 'Tissue-specific differences in cultured human diploid fibroblasts', *Exp Cell Res* 108(1): 1-6.

Schneider, V. A. and Mercola, M. (2001) 'Wnt antagonism initiates cardiogenesis in Xenopus laevis', *Genes Dev* 15(3): 304-15.

Schultz, R. M. (2002) 'The molecular foundations of the maternal to zygotic transition in the preimplantation embryo', *Hum Reprod Update* 8(4): 323-31.

Serrano, M., Lin, A. W., McCurrach, M. E., Beach, D. and Lowe, S. W. (1997) 'Oncogenic ras provokes premature cell senescence associated with accumulation of p53 and p16INK4a', *Cell* 88(5): 593-602.

Shay, J. W. and Roninson, I. B. (2004) 'Hallmarks of senescence in carcinogenesis and cancer therapy', *Oncogene* 23(16): 2919-33.

Shen, M. M. and Schier, A. F. (2000) 'The EGF-CFC gene family in vertebrate development', *Trends Genet* 16(7): 303-9.

Sigal, S. H., Rajvanshi, P., Gorla, G. R., Sokhi, R. P., Saxena, R., Gebhard, D. R., Jr., Reid, L. M. and Gupta, S. (1999) 'Partial hepatectomy-induced polyploidy attenuates hepatocyte replication and activates cell aging events', *Am J Physiol* 276(5 Pt 1): G1260-72.

Simons, J. W. (1967) 'The use of frequency distributions of cell diameters to characterize cell populations in tissue culture', *Exp Cell Res* 45(2): 336-50.

Skreb, N., Solter, D. and Damjanov, I. (1991) 'Developmental biology of the murine egg cylinder', *Int J Dev Biol* 35(3): 161-76.

Skromne, I. and Stern, C. D. (2001) 'Interactions between Wnt and Vg1 signalling pathways initiate primitive streak formation in the chick embryo', *Development* 128(15): 2915-27.

Slack, J. (1991) 'From egg to embryo: Regional specification in early development'.

Slack, J. M. W. (2013) 'Essential Developmental Biology (3rd Edition)', *WILEY-BLACKWELL*.

Smith, J. R. and Pereira-Smith, O. M. (1996) 'Replicative senescence: implications for in vivo aging and tumor suppression', *Science* 273(5271): 63-7.

Snow, M. H. (1977) 'Gastrulation in the mouse: Growth and regionalization of the epiblast.', *J Embryol Exp Morphol.* 1977(42): 293-303.

Snow, M. H. and Bennett, D. (1978) 'Gastrulation in the mouse: assessment of cell populations in the epiblast of tw18/tw18 embryos', *J Embryol Exp Morphol* 47: 39-52.

Solnica-Krezel, L. and Sepich, D. S. (2012) 'Gastrulation: making and shaping germ layers', *Annu Rev Cell Dev Biol* 28: 687-717.

Srinivas, S., Rodriguez, T., Clements, M., Smith, J. C. and Beddington, R. S. (2004) 'Active cell migration drives the unilateral movements of the anterior visceral endoderm', *Development* 131(5): 1157-64.

Stanford, W. L., Cohn, J. B. and Cordes, S. P. (2001) 'Gene-trap mutagenesis: past, present and beyond', *Nat Rev Genet* 2(10): 756-68.

Stennard, F. A., Costa, M. W., Lai, D., Biben, C., Furtado, M. B., Solloway, M. J., McCulley, D. J., Leimena, C., Preis, J. I., Dunwoodie, S. L. et al. (2005) 'Murine T-box transcription factor Tbx20 acts as a repressor during heart development, and is essential for adult heart integrity, function and adaptation', *Development* 132(10): 2451-62.

Stern, C. D. (2004) 'Gastrulation: From Cells to Embryos.', *Cold Spring Harbor, NY: Cold Spring Harbor Press*.

Storer, M., Mas, A., Robert-Moreno, A., Pecoraro, M., Ortells, M. C., Di Giacomo, V., Yosef, R., Pilpel, N., Krizhanovsky, V., Sharpe, J. et al. (2013) 'Senescence is a developmental mechanism that contributes to embryonic growth and patterning', *Cell* 155(5): 1119-30.

Stuckey, D. W., Clements, M., Di-Gregorio, A., Senner, C. E., Le Tissier, P., Srinivas, S. and Rodriguez, T. A. (2011) 'Coordination of cell proliferation and anterior-posterior axis establishment in the mouse embryo', *Development* 138(8): 1521-30.

Sumanas, S., Strege, P., Heasman, J. and Ekker, S. C. (2000) 'The putative wnt receptor Xenopus frizzled-7 functions upstream of beta-catenin in vertebrate dorsoventral mesoderm patterning', *Development* 127(9): 1981-90.

Sun, X., Meyers, E. N., Lewandoski, M. and Martin, G. R. (1999) 'Targeted disruption of Fgf8 causes failure of cell migration in the gastrulating mouse embryo', *Genes Dev* 13(14): 1834-46.

Sundararajan, S., Wakamiya, M., Behringer, R. R. and Rivera-Perez, J. A. (2012) 'A fast and sensitive alternative for beta-galactosidase detection in mouse embryos', *Development* 139(23): 4484-90.

Tam, P. P. and Behringer, R. R. (1997) 'Mouse gastrulation: the formation of a mammalian body plan', *Mech Dev* 68(1-2): 3-25.

Tam, P. P. and Loebel, D. A. (2007) 'Gene function in mouse embryogenesis: get set for gastrulation', *Nat Rev Genet* 8(5): 368-81.

Tam, P. P., Loebel, D. A. and Tanaka, S. S. (2006) 'Building the mouse gastrula: signals, asymmetry and lineages', *Curr Opin Genet Dev* 16(4): 419-25.

Tao, Q., Yokota, C., Puck, H., Kofron, M., Birsoy, B., Yan, D., Asashima, M., Wylie, C. C., Lin, X. and Heasman, J. (2005) 'Maternal wnt11 activates the

canonical wnt signaling pathway required for axis formation in Xenopus embryos', *Cell* 120(6): 857-71.

Thomas, P. and Beddington, R. (1996) 'Anterior primitive endoderm may be responsible for patterning the anterior neural plate in the mouse embryo', *Curr Biol* 6(11): 1487-96.

Thomas, P. Q., Brown, A. and Beddington, R. S. (1998) 'Hex: a homeobox gene revealing peri-implantation asymmetry in the mouse embryo and an early transient marker of endothelial cell precursors', *Development* 125(1): 85-94.

Tortelote, G. G., Hernandez-Hernandez, J. M., Quaresma, A. J., Nickerson, J. A., Imbalzano, A. N. and Rivera-Perez, J. A. (2013) 'Wnt3 function in the epiblast is required for the maintenance but not the initiation of gastrulation in mice', *Dev Biol* 374(1): 164-73.

van Amerongen, R. and Berns, A. (2006) 'Knockout mouse models to study Wnt signal transduction', *Trends Genet* 22(12): 678-89.

Varlet, I., Collignon, J. and Robertson, E. J. (1997) 'nodal expression in the primitive endoderm is required for specification of the anterior axis during mouse gastrulation', *Development* 124(5): 1033-44.

Viotti, M., Nowotschin, S. and Hadjantonakis, A. K. (2011) 'Afp::mCherry, a red fluorescent transgenic reporter of the mouse visceral endoderm', *Genesis* 49(3): 124-33.

von Zglinicki, T., Nilsson, E., Docke, W. D. and Brunk, U. T. (1995) 'Lipofuscin accumulation and ageing of fibroblasts', *Gerontology* 41 Suppl 2: 95-108.

Vonica, A. and Gumbiner, B. M. (2007) 'The Xenopus Nieuwkoop center and Spemann-Mangold organizer share molecular components and a requirement for maternal Wnt activity', *Dev Biol* 312(1): 90-102.

Wada, Y., Sun-Wada, G. H. and Kawamura, N. (2013) 'Microautophagy in the visceral endoderm is essential for mouse early development', *Autophagy* 9(2): 252-4.

Waldrip, W. R., Bikoff, E. K., Hoodless, P. A., Wrana, J. L. and Robertson, E. J. (1998) 'Smad2 signaling in extraembryonic tissues determines anterior-posterior polarity of the early mouse embryo', *Cell* 92(6): 797-808.

Wei, Y., Yu, L., Bowen, J., Gorovsky, M. A. and Allis, C. D. (1999) 'Phosphorylation of histone H3 is required for proper chromosome condensation and segregation', *Cell* 97(1): 99-109.

Winnier, G., Blessing, M., Labosky, P. A. and Hogan, B. L. (1995) 'Bone morphogenetic protein-4 is required for mesoderm formation and patterning in the mouse', *Genes Dev* 9(17): 2105-16.

Wodarz, A. and Nusse, R. (1998) 'Mechanisms of Wnt signaling in development', *Annu Rev Cell Dev Biol* 14: 59-88.

Wolpert, L. (2002) 'Book: Principles of Development second edition'.

Yamamoto, M., Saijoh, Y., Perea-Gomez, A., Shawlot, W., Behringer, R. R., Ang, S. L., Hamada, H. and Meno, C. (2004) 'Nodal antagonists regulate formation of the anteroposterior axis of the mouse embryo', *Nature* 428(6981): 387-92.

Yan, Y. T., Gritsman, K., Ding, J., Burdine, R. D., Corrales, J. D., Price, S. M., Talbot, W. S., Schier, A. F. and Shen, M. M. (1999) 'Conserved requirement for EGF-CFC genes in vertebrate left-right axis formation', *Genes Dev* 13(19): 2527-37.

Yan, Y. T., Liu, J. J., Luo, Y., E, C., Haltiwanger, R. S., Abate-Shen, C. and Shen, M. M. (2002) 'Dual roles of Cripto as a ligand and coreceptor in the nodal signaling pathway', *Mol Cell Biol* 22(13): 4439-49.

Yegorov, Y. E., Akimov, S. S., Hass, R., Zelenin, A. V. and Prudovsky, I. A. (1998) 'Endogenous beta-galactosidase activity in continuously nonproliferating cells', *Exp Cell Res* 243(1): 207-11.

Zeng, L., Fagotto, F., Zhang, T., Hsu, W., Vasicek, T. J., Perry, W. L., 3rd, Lee, J. J., Tilghman, S. M., Gumbiner, B. M. and Costantini, F. (1997) 'The mouse Fused locus encodes Axin, an inhibitor of the Wnt signaling pathway that regulates embryonic axis formation', *Cell* 90(1): 181-92.

Zhang, H. (2007) 'Molecular signaling and genetic pathways of senescence: Its role in tumorigenesis and aging', *J Cell Physiol* 210(3): 567-74.

Zhou, X., Sasaki, H., Lowe, L., Hogan, B. L. and Kuehn, M. R. (1993) 'Nodal is a novel TGF-beta-like gene expressed in the mouse node during gastrulation', *Nature* 361(6412): 543-7.

Zohn, I. E. and Sarkar, A. A. (2010) 'The visceral yolk sac endoderm provides for absorption of nutrients to the embryo during neurulation', *Birth Defects Res A Clin Mol Teratol* 88(8): 593-600.

Zon, L. I. (1995) 'Developmental biology of hematopoiesis', *Blood* 86(8): 2876-91.